A THEORETICAL APPROACH TO CALCULATE THE ANAEROBIC VOLUME FRACTION IN AERATED SOIL IN VIEW OF DENITRIFICATION

A COMPUTER SIMULATION STUDY

Autor : P.A. Leffelaar
Supervision : J. Goudriaan, H. van Keulen

REPORT no. 9, 1977
Dept. of Theoretical Production Ecology
Agricultural University
WAGENINGEN - THE NETHERLANDS

A THEORETICAL APPROACH TO CALCULATE THE ANAEROBIC VOLUME FRACTION IN AERATED SOIL IN VIEW OF DENITRIFICATION

A COMPUTER SIMULATION STUDY

Author : P.A. Leffelaar
Supervision : J. Goudriaan, H. van Keulen

REPORT no. 9, 1977
Dept. of Theoretical Production Ecology
Agricultural University
WAGENINGEN - THE NETHERLANDS

Preface

The interest I took in nitrogen behavior in soil urged me in April 1977 to have a discussion with Hans van Veen. In his Ph.D. thesis, he outlined a quantitative approach to the process of denitrification and in particular to the anaerobic soil conditions necessary to the onset of it.
Though the way anoxity is approached here is quite different as compared to his approach, the basic idea is kindly acknowledged.

Further, it would have been difficult to work without the stimulating help of Jan Goudriaan and Herman van Keulen. They both added to the quality of the work presented.

I also want to thank all people who were involved in discussions concerning this investigation and those who facilitated the time I spent in the department.

The help of Mr. G.C. Beekhof for drawing the figures and Mrs. J. van Dijk for typing the manuscript, are kindly acknowledged.

Summary

Factors affecting anaerobiosis in a loosely packed top soil in view of denitrification have been evaluated by considering an ideal soil composed of spherical aggregates.

A computer program was developed in which an analytical solution for the degree of anaerobiosis in aggregates, oxygen flow through the inter-aggregate pore space, and water flow in the soil were integrated.

Results of this computer model show that respiratory activity, the distribution of the respiratory activity over the aggregates, the diffusion coefficient of oxygen within a sphere, and the depth of the ground water table are of crucial importance in determining anaerobiosis in this topsoil. Water consumption rate by roots, critical oxygen concentration at which effectively anaerobic soil conditions prevail, and rain duration, intensity and distribution in time have less impact on this parameter.

Due to lack of data no model calibration and validation could be performed in this study.

Contents

1. Introduction

1.1. General

"Denitrification appears to be the least understood of all the N-transformation processes", Tanji & Gupta (1977).

Denitrification or nitrate dissimilation denotes the microbial process by which under very low partial oxygen pressures nitrates or nitrites are reduced to gaseous compounds, usually nitrous oxide (N_2O) and dinitrogen (N_2). Like most processes taking place in an environment where biological and physico-chemical reactions interact, the rate of denitrification is affected by many variables such as, the genera of microorganisms, availability of nitrates, amount and quality of easily decomposable organic matter, partial oxygen pressure, soil acidity and temperature (Allison et al., 1960; Flühler et al., 1976a; 1976b; Focht, 1974; Mc Garity, 1961; van Kessel, 1976; Stanford et al., 1975a; 1975b; Woldendorp, 1963).
Many of these parameters are very difficult to measure, supporting the view expressed by Tanji & Gupta.

Denitrification is an important process. From the point of view of environmental quality a favourable one, because it unloads waste water from the ballast of nitrates (van Kessel, 1976). For agriculture denitrification means a waste of money and labour, as nitrates are lost from the cultivated soil.
Expressed as a percentage of the total nitrogen application 25-35%, Walker (1956), up to 40-60%, Lemon (1977), of nitrates are reported to be transformed into gaseous compounds. However, whether or not denitrification alone is responsible for these large losses is still to be elucidated.

Up till now only a few serious attempts to model this microbial transformation process were reported. Hagin & Amberger (1974) took into account rate constants depending on temperature, available organic matter, acidity and partial oxygen pressure. They did, however, not specify the location of the denitrification process in soil except that it should take place in the water filled pore space.
The model of van Veen (1977) described denitrification with respect to local partial oxygen pressure. In a soil volume of 1 cm^3, with known moisture characteristics and pore geometry, it predicts where and when anoxic conditions will occur, at a certain degree of water saturation, around a pore.

1.2. Aims of investigation

From the above considerations it becomes clear that anaerobic conditions should prevail in a potentially denitrifying soil. Therefore, the work will be confined to this physical soil condition.
A serious attempt will be made to give a theoretical basis for calculating anaerobic conditions in an idealized soil system. A basic assumption is that in non-water-saturated soils local sites may occur, which are anaerobic due to structural properties. Sometimes this assumption is called the microsite concept, after Currie (1961a) and Greenwood (1961).

The approach will be to outline a mathematical formulation of anaerobiosis and to link this with other processes in soils such as water flow and oxygen diffusion in the soil profile as a whole. Values for parameters will be collected from literature or estimated.

The purpose of this modelling is twofold. First it enables to gain insight in the gaps in existing knowledge. Secondly, a model may give insight in the relative importance of the variables used: sensitivity analysis. Sensitivity analysis is a method to investigate to which parameters the model is sensitive. As a consequence these results point out which further investigations should have priority.

Further, it is aimed at calculating the right order of magnitude of the anaerobic soil volume. However, in view of the many simplifications to be made to describe the system, and the scarce literature data available, this is probably a goal which first needs more investigation.

The computer program will be written in CSMP III, and run on a DEC 10 computer.

2. Literature review

Mc. Garity (1961) investigated factors affecting denitrification in soils under anaerobic laboratory conditions. Soil samples of a red-brown earth (fine sandy loam to loam) and a black earth (clay loam) were collected and their aggregates studied. The major conclusions of his work were that neither lack of organic carbon nor lack of organisms would be factors limiting denitrification in these soils: denitrification occurred in all aggregates collected from the soil profiles up to a depth of 1.20 m. Combining this with the possible presence of nitrates and anaerobiosis in the field situation, volatilization takes place. It seems likely to locate anaerobiosis within soil aggregates. In this context Currie (1961a) and Greenwood (1961) described the aeration within spherical soil crumbs. Currie (1961a) stated that because soil microorganisms and plant roots require intimate contact with the soil particles for satisfactory uptake of nutrients and water, they are predominantly found in the finer pores of the soil within the crumb pores. Respiration tends to take place therefore within the crumbs rather than between them.
Flühler et al. (1976b) considered this approach a key for eliminating many misinterpretations of soil aeration measurements. A schematic representation of this concept is given in Fig. 1, which shows that the sphere of interest, in this case the anaerobic microsite exists next to aerobic pores (inter-crumb pores). In evaluating the significance of spatial resolution of aeration sensors, they start from the basic assumption, that in soils built up of structural units, two pore phases can be distinguished: intra-crumb pores and inter-crumb pores, corresponding approximately to the familiar capillary and non-capillary pores, respectively. At soil moisture suctions of 100 mbar, the larger inter-crumb pores are involved in the exchange of gases between soil and atmosphere, because they are air-filled. They supply oxygen to roots and microorganisms. Intra-crumb pores however will be partially water-filled, thus decreasing the diffusion rate of oxygen into the aggregates. Hence, it seems of importance to distinguish between the two pore phases. How this could be done will be dealt with in the chapter concerning model evaluation. It suffices here to state that this soil "constant" is difficult to determine, considering for instance swelling and shrinking associated with variations in water content, and the complex nature of water films covering an irregular surface.

In contrast to pore phase distribution more is known about aggregate size--distributions in field soils. Gardner (1956) found that the majority of size--distributions (weight-fractions obtained by sieving, mainly American soils) of

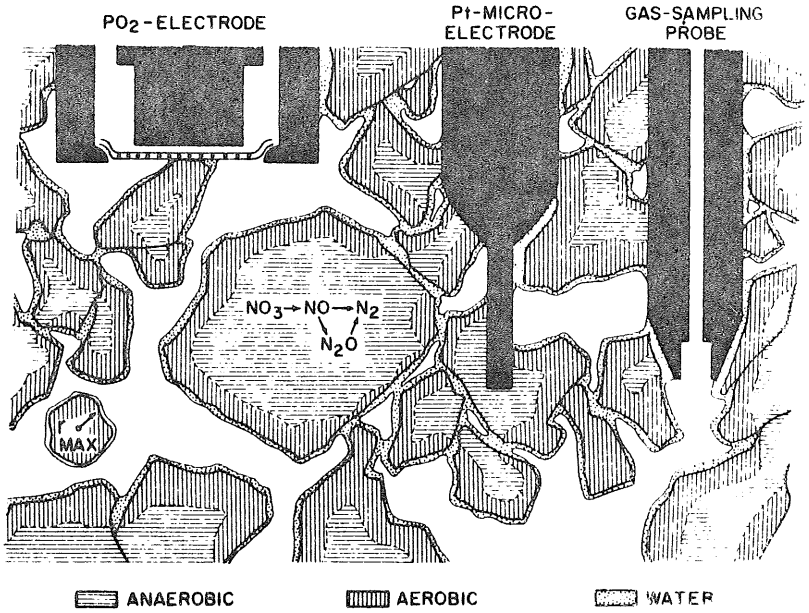

Figure 1. Schematic of an aggregated soil with different aeration sensors inserted. After Flühler et al. (1976b).

more than 200 samples, showed logarithmic-normal distributions, or nearly so. Combining the results of Gardner (1956) and Currie (1961a), Smith (1977) attempted to give formula's by which anaerobiosis can be calculated. However, the question how log-normally distributed crumbs are arranged in a three dimensional soil system, was not included. This geometry seems of major importance to the present author. Obviously, one arrives at the starting point again.
A simplification had to be made.

In a mathematical approach soil crumbs could be considered as spherical elements, Currie (1961a). This assumption was also the basis for building a model constructed of equal sized spherical rigid aggregates.
Assuming these aggregates to be non-porous, a certain inter-aggregate porosity would result. On the other hand, any porosity assigned to the aggregates could be called an intra-aggregate porosity or simply crumb-porosity. Thus, such a model enables one to include the two pore phases, to make exact calculations about the geometry of the system and to derive such properties as water content versus suction.
This approach to model building is not new. Slichter (1899) was one of the first scientists to perform purely theoretical calculations about the flow of water through porous soils or rocks. For the purpose of constructing his formula, a study was made of the pores of an ideal spherical-grained soil, arranged in the most compact manner possible; the hexagonal or rhomboidal sphere packing or simply close sphere packing.
In 1921, Wilsdon published a paper titled "Studies in soil moisture", where the hydrostatic pressure of "free" water in the soil was treated. "Free" water was defined as the water held at the points of contact between equal sized spheres. The volume of water of these pendular rings was related to the moisture suction and presented as a soil moisture suction curve. Unfortunately, Wilsdon did not consider the pendular water rings in their spatial relations to adjacent wedges, which resulted in a maximum moisture content exceeding the porosity of the rhomboidal system, as was pointed out by Keen (1924). Further, soil cohesion as developed by capillary forces was studied by Haines (1925a, 1925b,1927, 1930), and Fisher (1926). Smith et al. (1931) and van Brakel (1975) devoted papers to the capillary rise, whereas Sewell & Watson (1965) discussed hysteresis in the moisture characteristics of ideal bodies.
A basic property of the ideal systems quoted, is the absence of pores within the spherical particles.

It seems time for the introduction of this complicating factor and to link this ideal aggregate system with the microsite concept for anaerobiosis.

3. Theory

Before giving details on the geometry of the ideal system, the basic assumptions underlying the approach will be elucidated.
For a single sphere, the oxygen status will be governed by its radius, the external oxygen concentration, the diffusion coefficient in the interior, the solubility of oxygen in water, the oxygen consumption rate, and the water content.
For a certain sphere in the ideal soil system oxygen diffusion through the inter-crumb pores will be hampered by the solid phase and the water-filled pores. As a result, the external oxygen concentration will be governed by the macro diffusion process.
Because the diffusion coefficient of oxygen in water is about 10.000 times smaller than in free air, the diffusion rate of oxygen from a macro-pore into a sphere will decline when water partially covers the sphere as can be the case at the points of contact. The water covered or air exposed area of a sphere will therefore be considered.

In the following theoretical treatment the physical properties of the system will be derived.
At first the inter-aggregate properties are considered. Subsequently, the calculation procedure of the anaerobic volume of a sphere according to Currie (1961a), will be given.

Whenever too much detail could be annoying, reference is made to the relevant appendix.

3.1 Geometry of the rhomboidal ideal soil

A rhomboidal, hexagonal or closest packing is a way of arranging equidimensional spheres in space so that the available space is filled as efficiently as possible. Such an arrangement is achieved when each sphere is in actual contact with the maximum number of like spheres. This means that each sphere has six nearest neighbors in a closest-packed layer and twelve nearest neighbors in a three dimensional closest packing. Figure 2 shows a layer of spheres arranged in a hexagonal way. The area of the hexagonal is comprised of six triangles, resulting in a surface area of $6 \frac{1}{2} 2 R \sqrt{3} R = 6 \sqrt{3} R^2$. The (two-dimensional) efficiency with which the available space in this layer is utilized is obtained

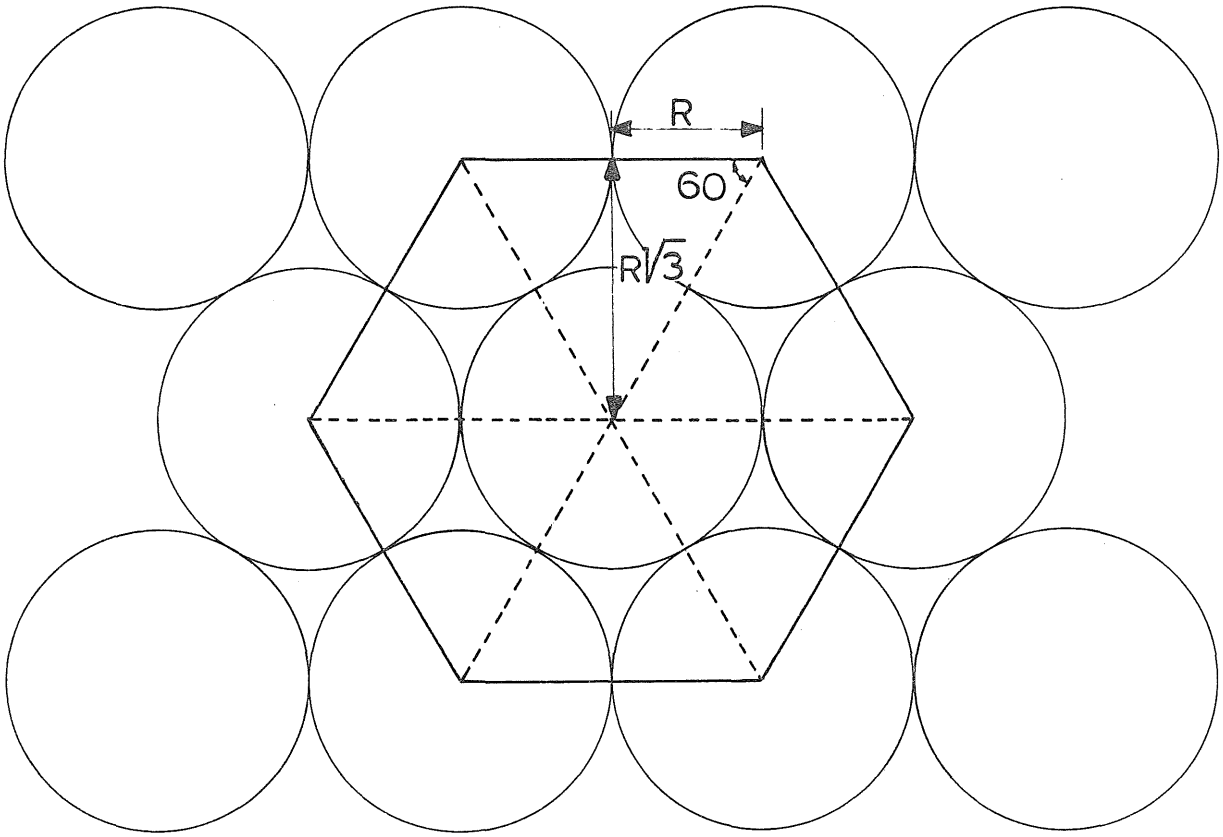

Figure 2. A closest-packed layer of spheres.

by dividing the area of the circles enclosed by the hexagonal by its area. Thus, this efficiency results in $\{(6 \frac{1}{3} + 1) \pi R^2 / 6 \sqrt{3} R^2\} 100\% = 90.69\%$.
The remaining space is the porosity or void fraction, amounting to 9.31%.
In Fig. 3 it is readily seen that, if the spheres in a hexagonal closest-packed layer are all moved from their original sites A to new sites B or C, other hexagonal closest-packed layers result. It should be obvious that, in the stacking of layers to form a closest-packing, a hexagonal closest-packed layer can occupy only the sites A, B or C. Figure 4, showing the simple two-layer sequence ...A B A B... is adopted for further investigation.

A similar calculation as for a single layer may be made to obtain the space efficiency and porosity or void fraction of a closest packing. Consider Fig. 5, where a unit cell of the sequence A B A is shown, thick dots indicating the sphere centers. To calculate the space efficiency, the number of spheres effectively occupying the body E... F- G...L has to be known and of course the volume of that body. As the surface area of the base is already known ($6 \sqrt{3} R^2$), the height of the unit cell is to be calculated to find this volume. This figure is composed of the height of the two dashed tetrahedrons, one with its apex pointing down and the other with its apex pointing up.
From simple geometry the height of a tetrahedron is derived as $2 \sqrt{2/3}$ R. Hence, the volume of the unit cell is $2 (2 \sqrt{2/3} R) 6 \sqrt{3} R^2 = 24 \sqrt{2} R^3$. The number of spheres in this volume is $(1 + 6 \frac{1}{3}) \frac{1}{2}$ for both the bottom and top layers, while the middle layer is effectively fully enclosed, yielding 3 spheres, the total being thus 6. The space efficiency therefore equals $\{6 \frac{4}{3} \pi R^3 / 24 \sqrt{2} R^3\}$ 100% = 74.0480%. The complementary porosity or void fraction therefore amounts to 25.9520%.

3.1.1 The voids in the rhomboidal packing

Two kinds of voids can be distinguished in a closest packing. If the triangular void in a closest-packed layer has a sphere directly over it, a void results with four spheres arount it, as shown in Fig. 6A. The four spheres are arranged on the corners of a tetrahedron (Fig. 6B), and such a void is called a tetrahedral void. On the other hand, if a triangular void pointing up in one closest-packed layer is covered by a triangular void pointing down in an adjacent layer, then a void surrounded by six spheres results (Fig. 7A). These six spheres are arranged on the corners of an octahedron (Fig. 7B), and such a void is called an octahedral void. Carefull examination of Fig. 3 learns that these

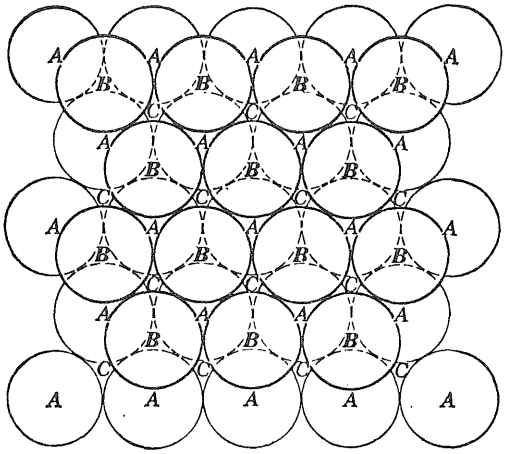

Figure 3.

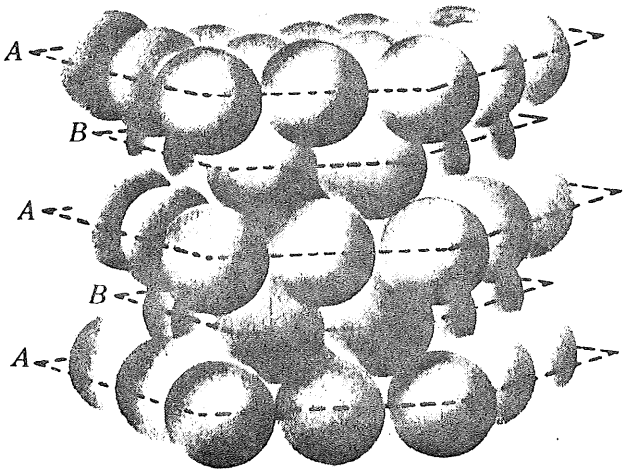

Figure 4.

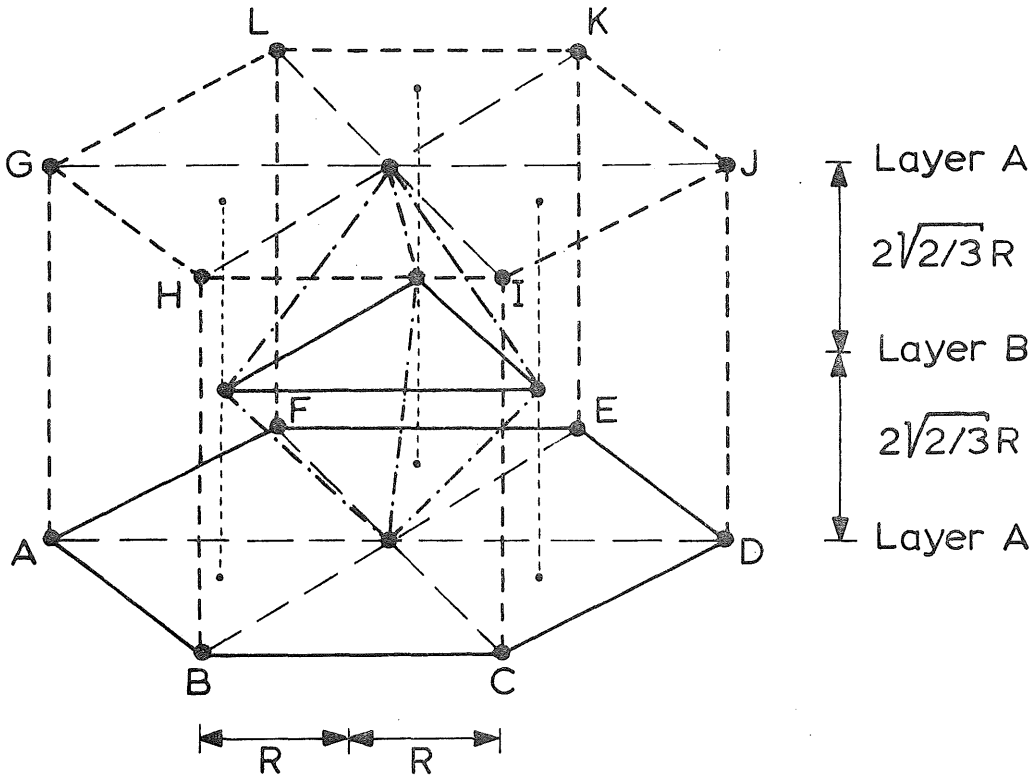

Figure 5. The unit rhomboidal cell.

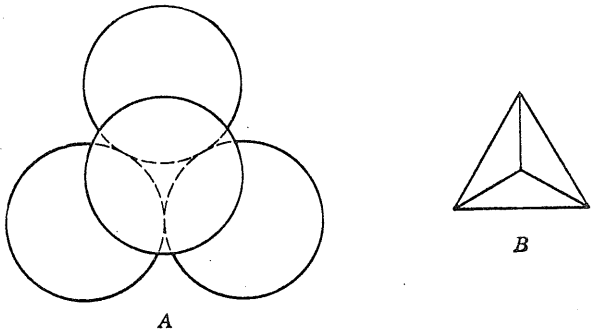

Figure 6.

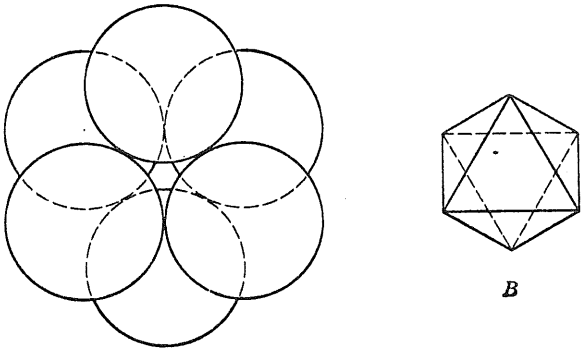

Figure 7.

are the only kinds of voids that can occur in a closest packing.

The number of voids surrounding any sphere in a closest packing may be readily determined. A sphere in a hexagonal closest-packed layer A is surrounded by six triangular voids of two kinds, B and C. When the next closest-packed layer above is added, a B layer, then the three B voids become tetrahedral voids and the three C voids become octahedral voids. Similarly, the closest-packed layer below the A layer leads to three tetrahedral and three octahedral voids. Furthermore, the particular sphere in layer A being considered itself covers a triangular void in the closest-packed layer above and in the layer below the sphere. Thus two more tetrahedral voids surround the sphere. This results in 2 3 = 6 octahedral voids and 2 3 + 1 + 1 = 8 tetrahedral voids surrounding the sphere. Since the total number of spheres and voids in a closest packing is very large it is only possible to determine the average number of voids of each kind belonging to a sphere. Each octahedral void is surrounded by 6 spheres and each sphere is surrounded by 6 octahedral voids. The number of octahedral voids belonging to one sphere is given by the ratio

$$\frac{\text{Number of octahedral voids around a sphere}}{\text{Number of spheres around void}} = \frac{6}{6} = 1$$

Each tetrahedral void is surrounded by 4 spheres and each sphere is surrounded by 8 voids. The number of tetrahedral voids belonging to one sphere is given by the ratio

$$\frac{\text{Number of tetrahedral voids around sphere}}{\text{Number of spheres around void}} = \frac{8}{4} = 2$$

The number of octahedral voids in a unit cell of a closest packing, therefore, is equal to 6, and the number of tetrahedral voids in the cell, is equal to 12.

3.1.2 Inscribed spheres inside the voids

Since the porosity of the unit cell of the rhomboidal packing seems rather high to represent the inter-aggregate porosity of a loosely structured field soil, the inscribed spheres in the tetrahedral voids and the octahedral voids are calculated. When these spheres are inserted the inter-aggregate porosity will decrease, while the water holding capacity is increased as will be shown later.

The inscribed spheres in both kinds of voids are located in the center of gravity of the tetrahedron and octahedron, respectively. From geometry (see Fig. 8) it is calculated that $R_4 = R\sqrt{\frac{2}{3}}\ (\frac{3}{2} - \sqrt{\frac{3}{2}}) = 0.2247\ R$, where R_4 represents the radius of the inscribed sphere in a tetrahedral void. For the inscribed sphere in a octahedral void (see Fig. 9) this radius is calculated as $R_8 = R\ (\sqrt{2} - 1) = 0.4142\ R$, where the index 8 refers to an octahedral void.

The porosity of the unit cell of the rhomboidal cell with 12 inscribed spheres in the tetrahedral voids and 6 inscribed spheres in the octahedral voids is calculated as follows:

$$(1-\{(R^3 + 2\ (R\sqrt{\tfrac{2}{3}}\ (\tfrac{3}{2}-\sqrt{\tfrac{3}{2}}))^3 + (R(\sqrt{2}-1))^3)\ 6\ \pi\ \tfrac{4}{3}\}\ /\ 24\sqrt{2}R^3)100\% = 19.0083\%$$

The efficiency with which the available space in the unit cell is utilised is 80.9917%, and this may also be called the solid phase of the system.

The system designed so far, is used in further discussions. For a very detailed description of this system, reference is made to Slichter (1899) and Azároff (1960

3.2 Moisture characteristics of the system

3.2.1 Calculation of the pendular water ring volume

In the ideal soil the water will be present as annuli of wedge-shaped cross-section around the points of contact of the spheres (pendular rings). This conception of moisture distribution was introduced as early as 1897 by Briggs.

Figure 10 shows such a pendular water ring. The formula to calculate the volume of water at given soil-moisture suctions was derived by Wilsdon (1921), for equal sized spheres in a rhomboidal structure. However, the system under consideration contains spheres of smaller sizes in the voids, thus necessitating a new formula. In order to keep the mathematics involved as simple as possible this water volume was calculated as follows, (Fig. 11):

$$V_{p.r.} = V_c - (V_R + V_{R_x} + V_t) \qquad (1)$$

where $V_{p.r.}$ is the water volume of the pendular ring

V_c is the volume of a truncated cone

V_R is the volume of a spherical segment of one base of the big spheres

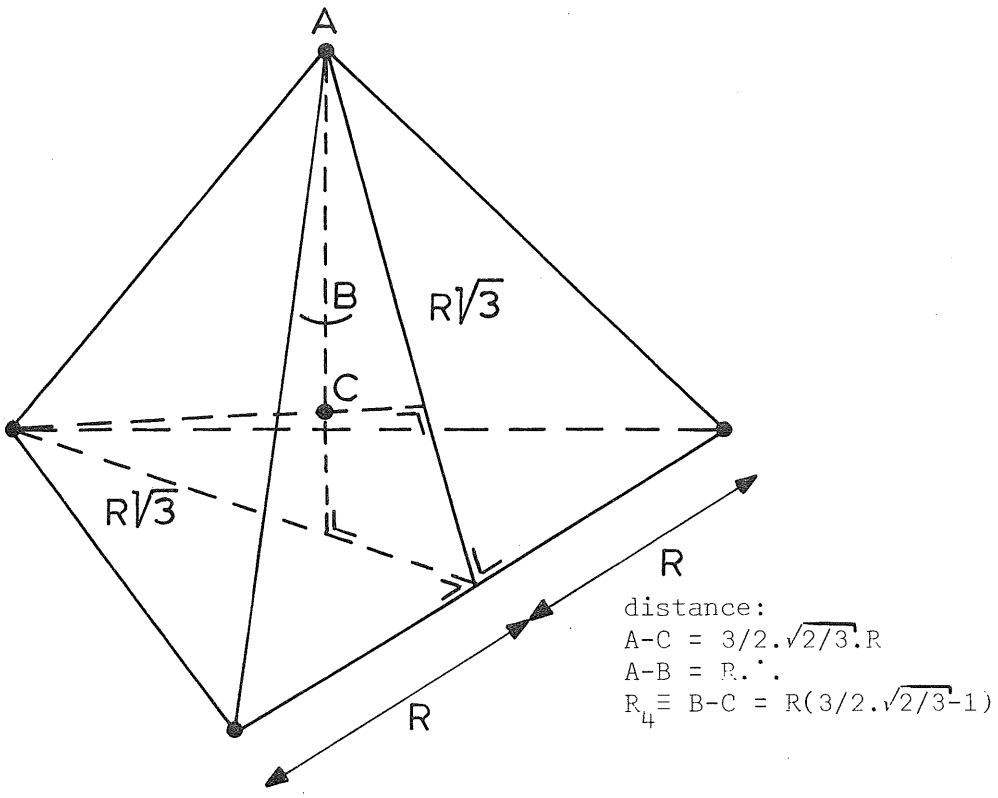

Figure 8. A tetrahedron with the center of gravity (C).

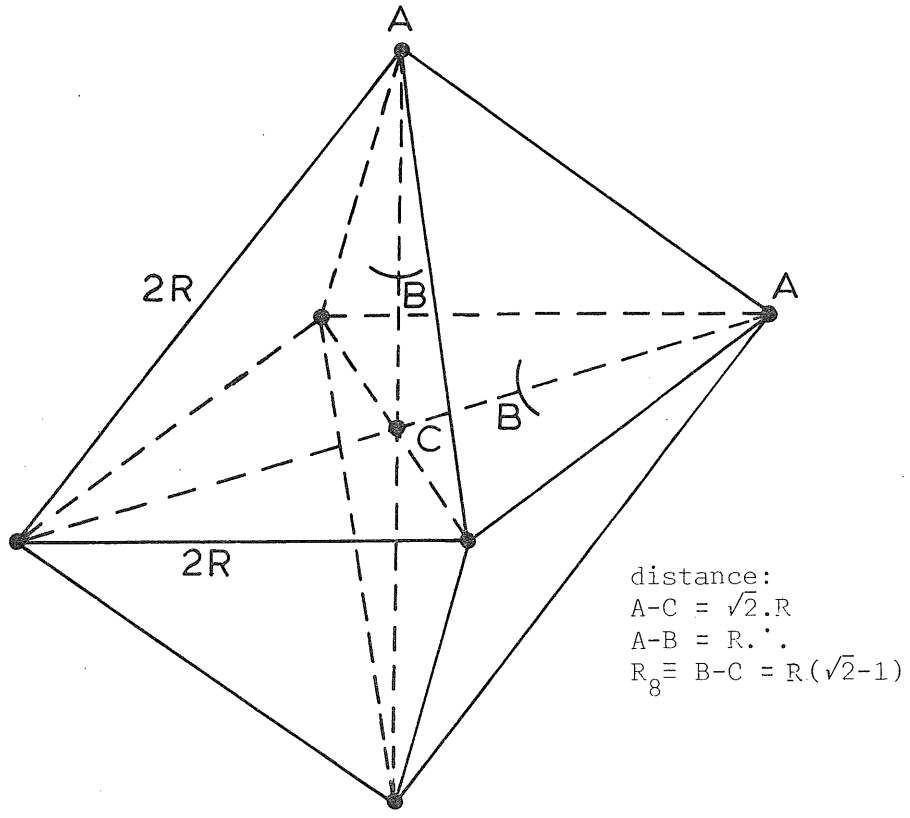

Figure 9. An octahedron with the center of gravity (C).

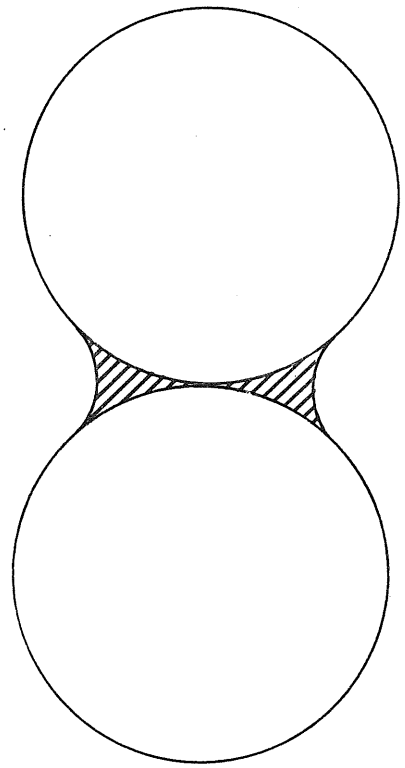

Figure 10. A pendular water ring.

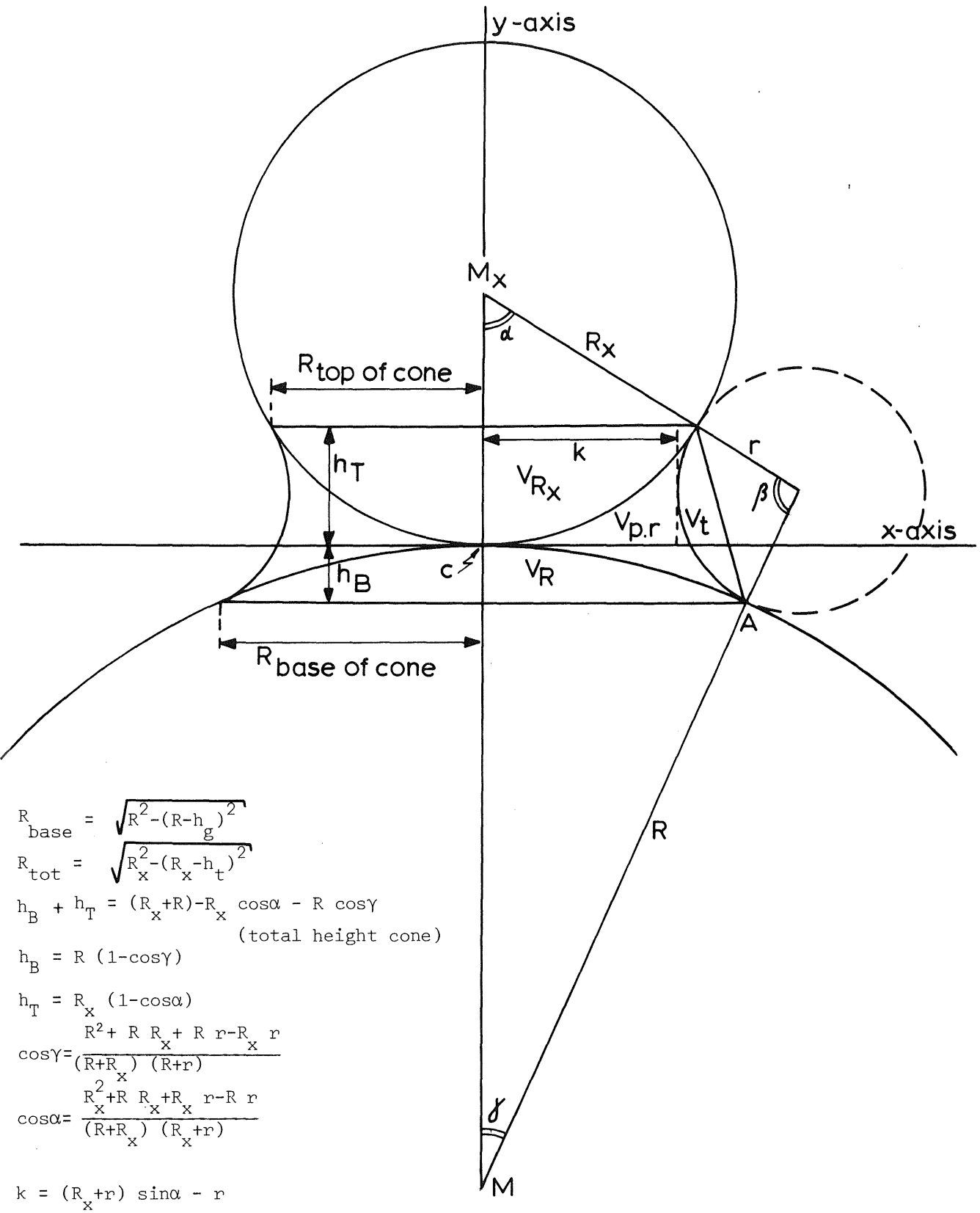

$$R_{base} = \sqrt{R^2-(R-h_g)^2}$$

$$R_{tot} = \sqrt{R_x^2-(R_x-h_t)^2}$$

$$h_B + h_T = (R_x+R)-R_x \cos\alpha - R \cos\gamma$$

(total height cone)

$$h_B = R\,(1-\cos\gamma)$$

$$h_T = R_x\,(1-\cos\alpha)$$

$$\cos\gamma = \frac{R^2+ R\,R_x+ R\,r-R_x\,r}{(R+R_x)\,(R+r)}$$

$$\cos\alpha = \frac{R_x^2+R\,R_x+R_x\,r-R\,r}{(R+R_x)\,(R_x+r)}$$

$$k = (R_x+r)\,\sin\alpha - r$$

Figure 11. General coordinate system to calculate pendular ring volume.

V_{R_x} is, when x = 4, the volume of a spherical segment of one base of the inscribed sphere in a tetrahedron, and when x = 8, it is this volume of the inscribed sphere in an octahedron.

V_t is a fraction of the volume of the torus included by the cone.

In Fig. 11 the geometry is shown and the important expressions to derive the formula's for the symbols in Eq. (1) are given. The volumes of Eq. (1) are fully derived in Appendix I, and the results are given as:

$$V_c=\frac{\pi}{3} R_x\{(1-\cos\alpha)+ R\ (1+\cos(\alpha+\beta))\}\{R^2\sin^2(\alpha+\beta) + R_x^2\ \sin^2\alpha + R_x\sin\alpha\ R\ \sin(\alpha+\beta)\} \tag{2}$$

$$V_R = \frac{\pi}{12} R^3\ (8 + 9\ \cos\ (\alpha+\beta)- \cos\ 3\ (\alpha+\beta)) \tag{3}$$

$$V_{R_x} = \frac{\pi}{12} R_x^3\ (\ 8 - 9\ \cos\alpha + \cos\ 3\ \alpha) \tag{4}$$

$$V_t=\pi\{r^2\sin\alpha(r+R_x)(\frac{2\pi\beta}{360} -\sin\beta)-\frac{4}{3}\ r^3\ \cos(\alpha+\tfrac{1}{2}\beta-90)\sin^3\tfrac{1}{2}\beta\} \tag{5}$$

where α and β refer to the angles in Fig. 11, and r is the radius of curvature of the air-water interface. All angles are expressed in degrees.

A number of assumptions had to be made in order to develop Eqs. (1) to (5). First, gravitational distortion was ignored, furthermore, the properties of both solid-fluid interface were considered uniform at all points in the region in which the meniscus meets the solid surface. It follows that the three phase line of contact is characterized by a uniform contact angle. Hence, the meniscus will take the form of a surface of revolution. The contact angle, defined as the angle between the tangent in the point of contact with the sphere, and the toroidal meniscus in that point, was taken as zero degrees. As the process of capillary condensation, which actually is dealt with here, takes place after the spheres have been covered with one or more absorbed layers, complete wetting (contact angle equals zero) is plausible, Kruyer (1958).

Exact data for the meniscus surface were calculated by Radushkevich (cf. Kruyer, 1958), who found it to be a nodoidal meniscus. Kruyer (1958) approximated these exact data, using a surface of a hyperboloid, which compared very well. These data in turn were compared with results taken from Carman (1953), who worked along the same lines as the present paper. From data given by Kruyer it was calculated that the toroidal approximation introduces a positive absolute error in the volumetric moisture content of 0.2066%, when the angle α amounts to 30^o (cf. Fig. 11),

which value corresponds to a relative error of 3.388%. On the other hand, using a correction on this volume as given by Fisher (1926), (see his Fig. 4, page 502), this error was calculated as 3.0%. These data represent the maximum possible error in a system of equidimentional spheres as will be pointed out in the next chapter. It is concluded therefore, that the toroidal approximation is sufficiently accurate for the present purpose.

In the special case where $\alpha = \gamma$, Eqs. (1) to (5) should give the same numerical results as the formula derived by Wilsdon (1921, p. 165); this was indeed the case. In addition, for this case where the truncated cone takes the form of a cylinder, the following formula, which expresses V uniquely in the radii of the big spheres and the curvature of the air-water interface, was derived.

$$V_{p.r.} = 2\pi r^2 \{ (\frac{R}{R+r})^3 (R+\frac{r}{3}) - (\sqrt{r^2+2Rr} (\arcsin \frac{R}{R+r} - \frac{R}{R+r} \sqrt{1-(\frac{R}{R+r})^2}) + - \frac{2}{3} r (\frac{R}{R+r})^3) \} \qquad (6)$$

Numerical results obtained with the Eqs. (1) to (6) will be given after soil moisture suction is dealt with.

3.2.2 Calculation of the maximum angle α

The angle α represents the distance in units of degrees between the point where the spheres touch (C in Fig. 11) and the point A where the liquid surface meets the sphere. Obviously, there is a limit to this angle when considering a pendular water ring in its spatial relations to adjacent rings. A consideration of one face of the regular tetrahedron, Fig. 12, will make this clear. In the plane of this face the cross-section of the spheres and pendular rings shows that the menisci of the latter will come into contact when the angle α is equal to 30%. At other points in the mass, the menisci will not yet be in contact at this angle.

For equidimensional sphere systems the moisture content calculations will break down above this angle of 30%, as the water starts to coalesce. The most marked effect will naturally occur where the air-spaces are narrowest, that is at the connecting waists or windows. In this stage the water rings are unstable and the change takes place spontaneously. Moreover, their volumes are no longer expressed by the simple relations given above, (Haines, 1927; Keen, 1924). More recently, van Brakel (1975) described capillary rise in a rhomboidal packing

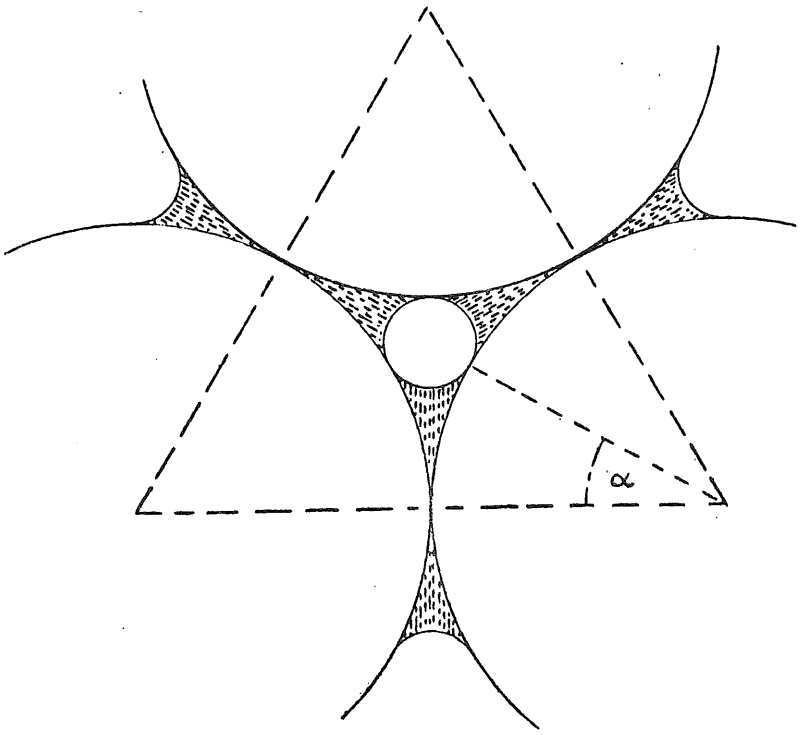

Figure 12. The maximum angle α at which pendular rings touch eachother.

by the subsequent closing of the tetrahedral and octahedral cavities, (pp. 120--121).

The system described, however, contains inscribed spheres as well. This property would smoothen the changes described above because of the variations in the size of particles, as suggested by Haines (1927). The process of capillary rize will start at an earlier stage, too.
From geometry, it was derived that the radius of a cylinder which would just pass a window is:

$$r_{max} = \frac{R + R_x - A}{R - R_x + A} \quad R_x \qquad (7)$$

where $A = \sqrt{2\ R_x\ R + R_x^2}$. The complete derivation of Eq. (7) is given in Appendix II. It should be noted that for $R_x = R$, the value of r is obtained for which coalescence just starts, i.e. $\alpha = 30^o$, namely $r = 0.1547\ R$.

3.2.3 The relation between suction and pendular ring volume

The relation between matrix suction (Sm) and surface tension (σ) may be described by the expression

$$Sm = \frac{\sigma}{\rho\ g} \left(\frac{1}{r_1} + \frac{1}{r_2}\right) \qquad (8)$$

where Sm is expressed in mbar or cm H_2O
σ is expressed as dynes $cm^{-1} \equiv g.\ cm.\ s^{-2}$
ρ is the density of water, taken as 1 $g.\ cm^{-3}$
g is the acceleration due to gravity, taken as 980 $cm.\ s^{-2}$
r_1, r_2 are the principal radii of curvature, expressed as cm.

The constant $(\sigma/\rho g)$ in Eq. (8) takes the value 0.0745 cm^{-2} at about 15^oC.
Eq. (8) simplifies to $Sm = 2\ \sigma/\rho g r$, when the radii would be of the same magnitude and curvature. This expression is often used in calculations where the soil body is thought to be build up of cylindrical tubes, (c.f. Rao et al., 1976). The radii in case of pendular water rings are of opposite sign and do not have the same numerical value. They are taken as:

$r_1 = r$ (cf. Fig. 11)

$$r_2 = -\{(R_x - r)\frac{2\sqrt{(R+R_x+r)\ R\ R_x\ r}}{R_x(R+R_x+r) + R\ r} - r\} \qquad (9)$$

Eq. (9) holds for both the asymmetrical spheres and the symmetrical ones, and represents the distance k in Fig. 11. For the symmetrical spheres, Eq. (10) was derived from Eq. (9) by substituting R for R_x:

$$r_2 = -\left(\sqrt{r^2 + 2\ R\ r} - r\right) \qquad (10)$$

The sign of r_2 is negative because the curvature is opposite to the one of r_1.

In a static system, the surface free energy of the air-water interface would be constant, which should be reflected by the radius of curvature (r_c). This is equal to the harmonic mean of the two principal radii of curvature r_1 and r_2,

$$\frac{2}{r_c} = \frac{1}{r_1} + \frac{1}{r_2} \qquad (11)$$

and should have a constant value at all points on the surface.
In case of a toroidal surface, this condition is not satisfied, because the first principal radius r_1 equals the radius of the circular arc, which is constant, whereas the second principal radius r_2 equals the distance from the axis of revolution measured along the normal and taken with a negative sign, $-r_2$, which varies from -R through -k to $-R_x$, Kruyer (1958). In this paper, the highest value occurring on the surface was used by calculating r_c from

$$\frac{2}{r_c} = \frac{1}{r_1} - \frac{1}{k} \qquad (12)$$

This was also done by Carman (1953). Kruyer, later on, commented that a better approximation would have been to take the mean radius of curvature on the torus. The implication of this approach is that at any given suction, the volume of water is slightly overestimated, as was shown already.

Obviously, at a certain suction, different radii of curvature belong to the inscribed spheres and the equidimensional spheres. Therefore, at the suctions demanded the radii should be calculated, which should be used in their turn to calculate the corresponding volume of water.

3.2.4 Calculation of moisture content

The moisture characteristic of a soil, and so of this hypothetical system, usually is given as suction (Sm) plotted against moisture content (θ_v) expressed as a percentage of the volume of soil. Hence, last but not least, an equation has to be advanced to calculate moisture content.
In chapter 3.1 it was shown that a unit cell contains 6 big spheres, 6 R_8-spheres, and 12 R_4-spheres.
The big spheres each have 12 points of contact among themselves. Each pendular water ring actually belongs to two spheres. This means that each sphere has 12 $\frac{1}{2}$ = 6 waterrings around it, and 6 6 = 36 waterrings are due to the big spheres.
The R_8-spheres each touch 6 big spheres, and will contribute 36 waterrings too.
The R_4-spheres each touch 4 big spheres, and will therefore contribute to the moisture content 4 12 = 48 pendular rings.
Depicting the pendular rings in case of the big spheres as $V_{p.r.}$, and the ones in case of the other spheres as $V_{p.r.8.}$ and $V_{p.r.4.}$, the following equation gives the moisture content in a hexagonal structure:

$$\theta_v(\%) = \frac{36\ V_{p.r.} + 36\ V_{p.r.8} + 48\ V_{p.r.4}}{24\ \sqrt{2}\ R^3}\ 100 \qquad (13)$$

3.2.5 The moisture characteristic

The moisture characteristic of the "soil" was calculated using Eqs. (1) to (13). Numerical results for R = 0.5 cm are presented in Table 1. This table shows the contribution of the independent pendular rings at certain suctions of the different spheres, as well as the complete system above a suction of about 1 mbar. Figure 13 shows the whole system graphically.
The moisture characteristic presented by Haines (1930) in his description of hysteresis effects appears similar to the one given.

3.3 The air-exposed area of the spheres in the rhombohedron

Diffusion of oxygen from inter-aggregate pores into the spheres, when they would be porous, will be hampered by the pendular water rings. The diffusion will be proportional to the air-exposed area, which is defined as the area complementary to the water-covered part of the sphere, and will be expressed as a

Table 1. The moisture-suction relationship of the rhomboidal system; R=0.5cm.

Sm(mbar)	$\theta_{v.p.r.}$	$\theta_{v.p.r.8}$	$\theta_{v.p.r.4}$	θ_{v} (%)
0.6106	6.3063	-	-	-
0.6368	6.0168	-	-	-
0.6985	5.4121	-	-	-
0.7701	4.8241	-	-	-
0.8540	4.2546	-	-	-
0.9538	3.7056	-	-	-
0.8067	4.5615	1.6645	-	-
0.9038	3.9656	1.4798	-	-
1.0471	3.2867	1.2613	-	-
1.2276	2.6623	1.0518	-	-
1.0174	3.4114	1.3022	0.6843	5.3979
1.4615	2.0944	0.8578	0.4784	3.4306
1.7762	1.5854	0.6664	0.3863	2.6380
2.2208	1.1382	0.4947	0.2971	1.9300
2.5	0.9502	0.4199	0.2735	1.6436
2.8950	0.7564	0.3409	0.2127	1.3100
4.0322	0.4445	0.2084	0.1357	0.7886
6.3393	0.2083	0.1022	0.0699	0.3804
10.0	0.0942	0.0479	0.0342	0.1762
13.3892	0.0559	0.0290	0.0211	0.1060
16.9525	0.0364	0.0192	0.0142	0.0698
22.9236	0.0209	0.0112	0.0084	0.0405
31.0	0.0119	0.0065	0.0049	0.0233
34.9418	0.0095	0.0052	0.0040	0.0187
71.2916	0.0025	0.0014	0.0011	0.0049
100.0	$1.2846.10^{-3}$	$7.2033.10^{-4}$	$5.7286.10^{-4}$	$2.5778.10^{-3}$
200.0	$3.3478.10^{-4}$	$1.9017.10^{-4}$	$1.5344.10^{-4}$	$6.7839.10^{-4}$
500.0	$5.5571.10^{-5}$	$3.1937.10^{-5}$	$2.6118.10^{-5}$	$1.1363.10^{-4}$

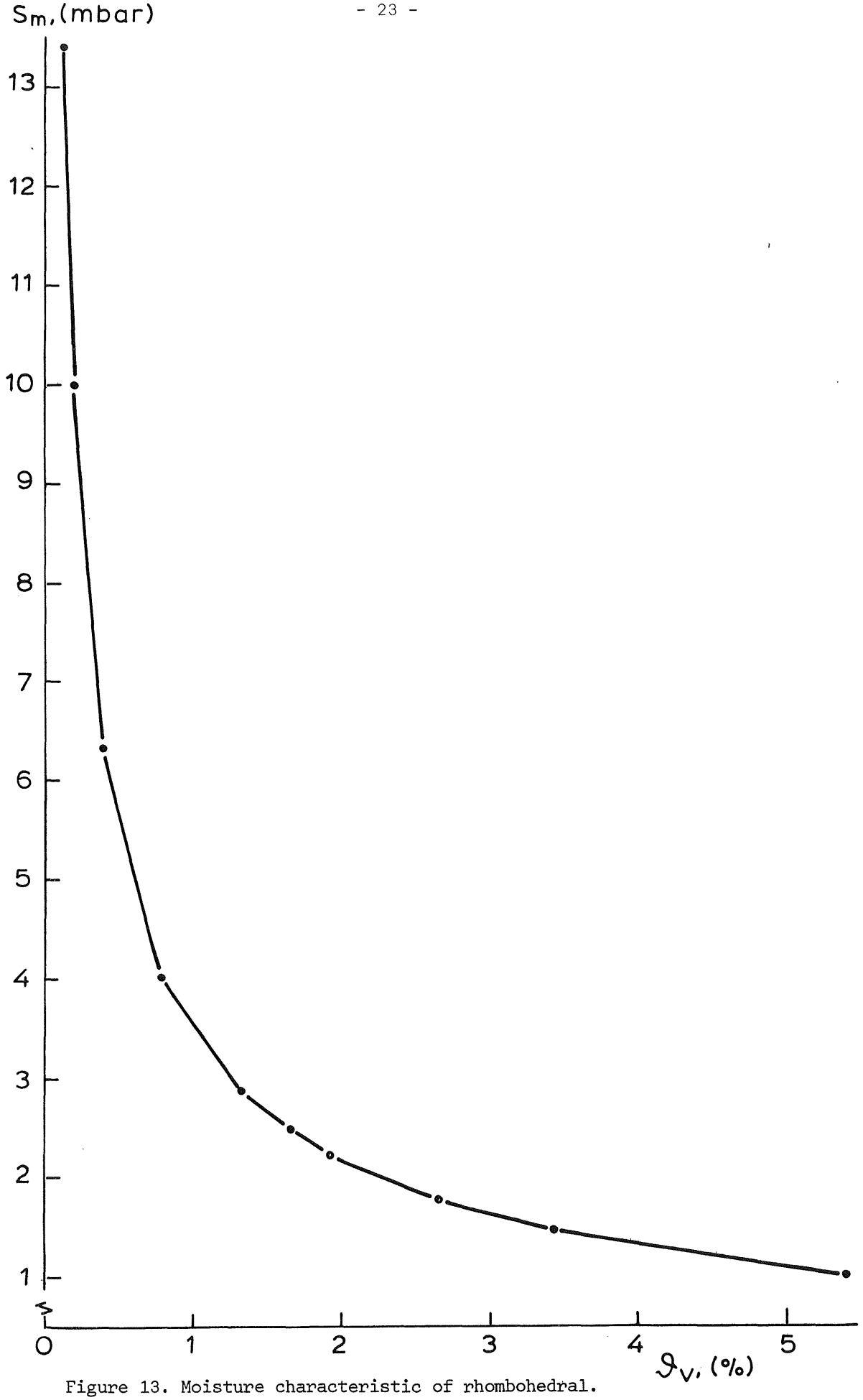

Figure 13. Moisture characteristic of rhombohedral.

percentage. The equations to calculate the air-exposed area were derived taking into account the geometrical properties of the pendular rings, as given in Fig. 11, and the number of points of contact per sphere.

The general expression for the air-exposed area, due to C waterrings is

$$\text{A.E.A. } (\%) = \{1 - C \tfrac{1}{2} \left(1 - \frac{(R_x (R_x + R) + r (R_x - R))}{(R_x + R) (R_x + r)} \right)\} 100 \qquad (14)$$

Equation (14) can be simplified for equidimensional spheres by substituting R for R_x and than yields

$$\text{A.E.A. } (\%) = \left(1 - C \tfrac{1}{2} \left(\frac{r}{R + r}\right)\right) \; 100 \qquad (15)$$

In determining the air-exposed area of the inscribed spheres, C takes the value of 4 or 6 for R_4- and R_8-spheres, respectively. The situation is more complicated for the big spheres. First the value C equals 12 in Eq. (15), and secondly there are $\frac{48}{6} = 8$ points of contact due to R_4-spheres, and $\frac{36}{6} = 6$ points of contact due to R_8-spheres. This means that on the average the big spheres have 12 + 8 + 6 = 26 points of contact each.
This more complex situation also implies the use of Eq. (14) twice with C = 8 and C = 6 respectively, and in combination with Eq. (15) these numbers apply to the big spheres. Appendix III gives the derivation of Eq. (14) in more detail. In Table 2 the numerical values of A.E.A. are given, whereas in Figs. 14 and 15, suction vs. A.E.A. and θ_v vs. A.E.A. are plotted, respectively, for the three sphere classes.

3.4 Calculation of the ratio D / D_o

The ratio D / D_o gives the diffusion coefficient of molecules in a porous system (D) as compared to the diffusion of the same medium (water or air) without any solid obstacle. Analytical solutions to the problem of soil aeration have been given by van Bavel (1951, 1952) and Taylor (1949). These authors, however, considered the soil to be uniform. Soil structure inevitably causus inhomogeneity in soils, a factor investigated by Bakker & Hidding (1970) and Currie (1960a, 1960b, 1961a, 1961b). Currie presented detailed results with respect to diffusion in systems having clear distinction between intra- and inter-aggregate pores, and carried out measurements in both dry and wet materials. Later on, Millington & Shearer (1971) advanced an equation to describe diffusion in such systems.

Table 2. Values of Sm and A.E.A. for the different sphere classes.

Sm(mbar)	A.E.A. (%)		
	big spheres	R_8-spheres	R_4-spheres
1.0174	17.7761	22.9635	15.4701
1.4615	36.7948	38.6666	29.6317
1.7762	45.5915	46.3199	37.0243
2.2208	54.4637	54.3029	45.1029
2.8950	63.4146	62.6375	53.9616
4.0322	72.4463	71.3473	63.7138
6.3393	81.5595	80.4583	74.4996
13.3892	90.7508	89.9988	86.5003
16.9525	92.5975	91.9611	89.0672
22.9236	94.4465	93.9422	91.6957
34.9418	96.2975	95.9421	94.3896
71.2916	98.1493	97.9613	97.1539
100.0	98.6716	98.5343	97.9473
200.0	99.3288	99.2577	98.9557
500.0	99.7291	99.6999	99.5763

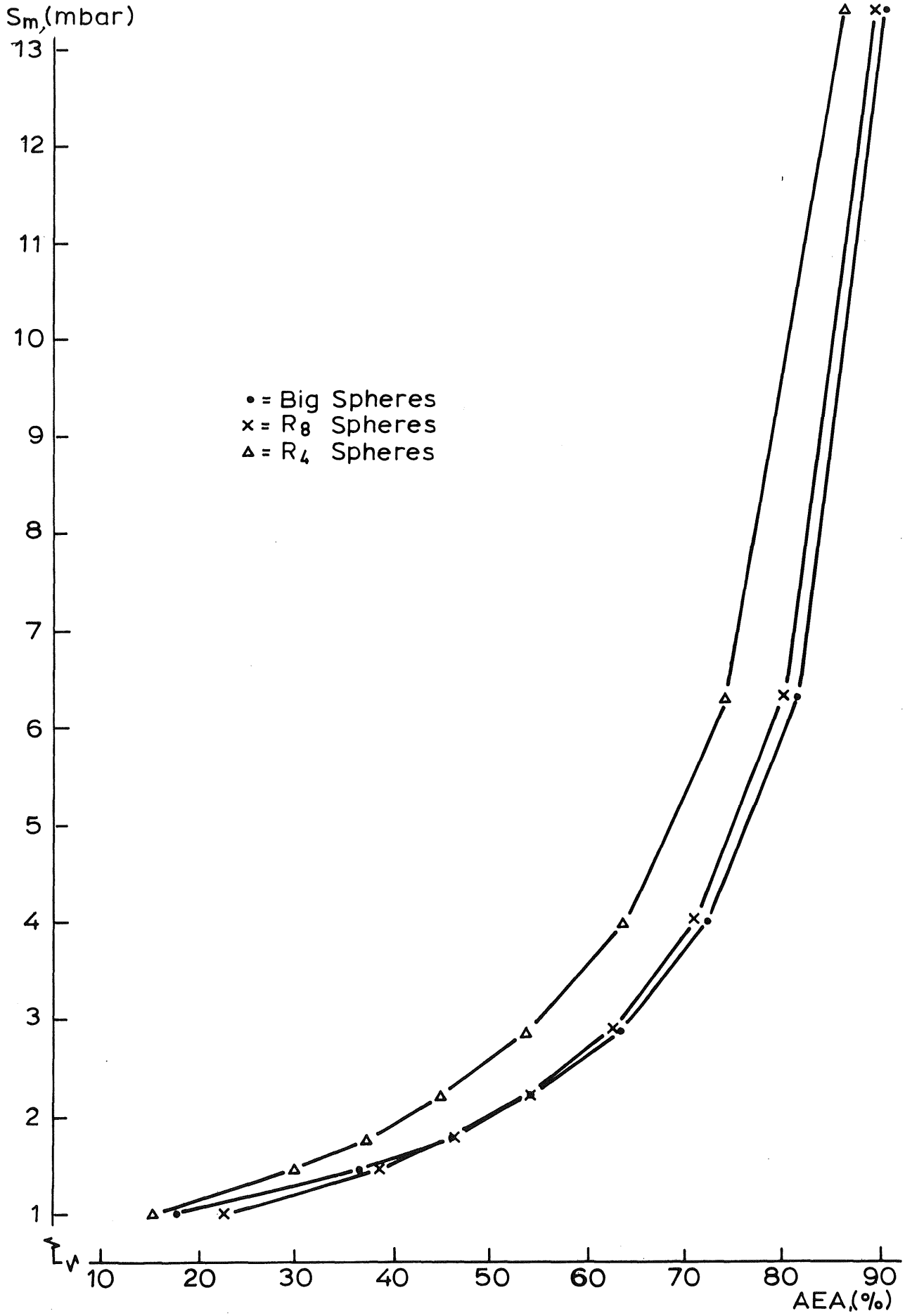

Figure 14. The relation between air exposed area of spheres and moisture suction.

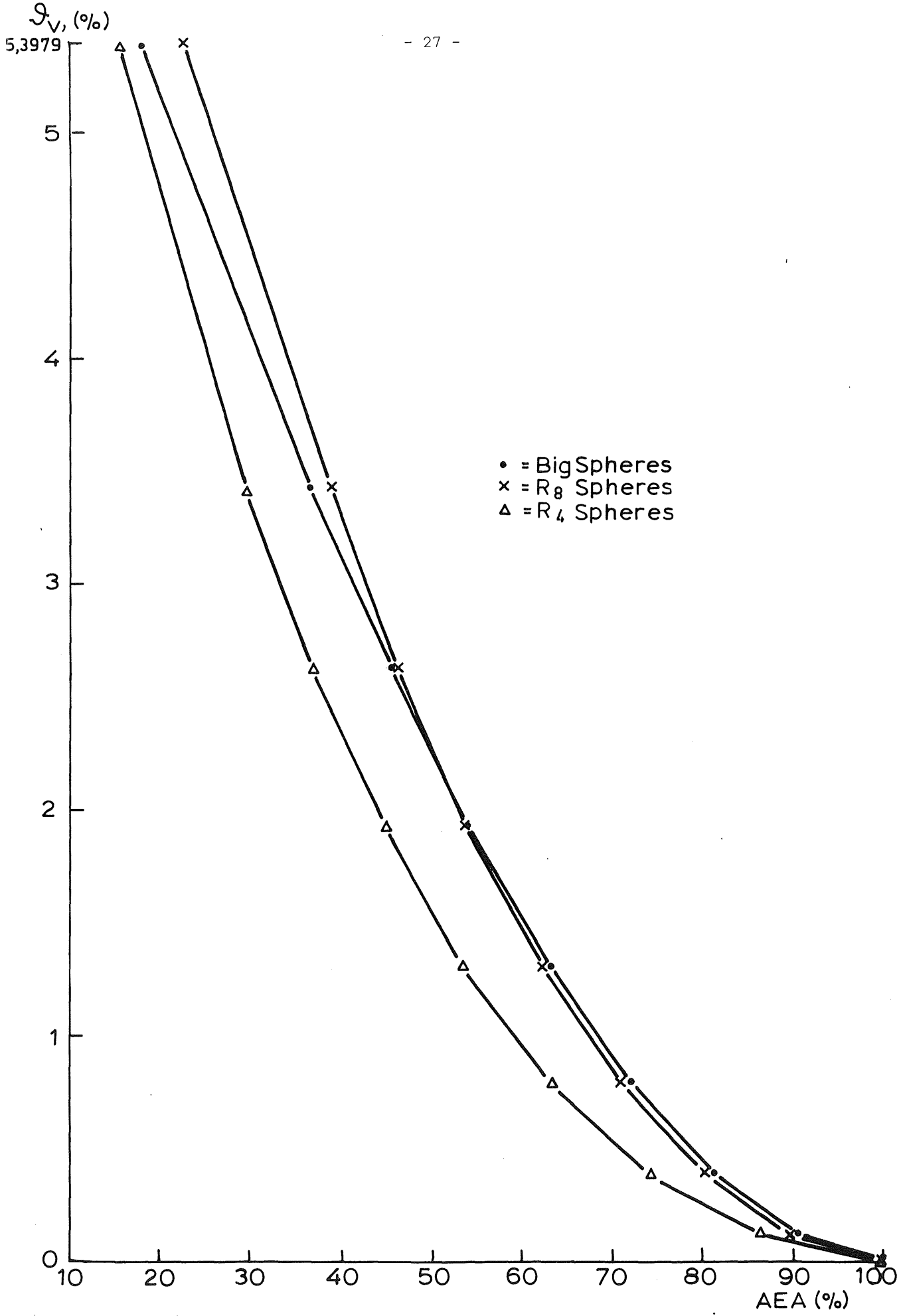

Figure 15. The relation between air exposed area of spheres and moisture content.

The agreement between their results and those of Currie was within about 30%. Therefore, although the calculations are somewhat cumbersome, use is made of their equation.

Their basic assumption was the analogy between the diffusion process through aggregates and inter-aggregate voids, and electrical resistances. The transition of gas flowing through an aggregate into the inter-aggregate void and further into another aggregate, situated below the first one, is represented by two resistances in series. Furthermore, there is a parallel flow path through the continuous inter-aggregate voids, the diffusion through which is simply added to the former result.

The equation of Millington & Shearer is given as:

$$D / D_o = \frac{(1-S_{WA})^2 \, (A-\theta_A/A+S)^{2n}(1-P^{2x}) \, ((P-\theta_P)-(P-\theta_P)^{2x_1})}{(1-S_{WA})^2 \, (A-\theta_A/A+S)^{2n} \, (1-P^{2x})+((P-\theta_P)-(P-\theta_P)^{2x_1})} + (1-S_{WP})^2(P-\theta_P)^{2x_1} \qquad (16)$$

where $S_{WA} = \theta_A / A$, fractional liquid saturation in the aggregate pore space

$S_{WP} = \theta_P / P$, fractional liquid saturation in the inter-aggregate pore space

θ_A is the volume of water per unit bed volume contained in the aggregate pore space

θ_P is the volume of water per unit bed volume contained in the inter-aggregate pore space

A is the aggregate porosity, fraction

P is the inter-aggregate porosity, fraction

S is the solid phase, fraction

n, x, and x_1 are obtained by an iterative procedure.

The terms used in Eq. (16) have the following meaning:

$(1-S_{WP})^2$ is the probability of a continuous air-phase in the inter-aggregate pore space.

$(1-S_{WA})^2$ is the probability with reference to the intra-aggregate pores.

$(1-S_{WP})$ and $(1-S_{WA})$ represent the degree of air-saturation in the inter- and intra-aggregate pore space.

$(A-\theta_A)/(A+S)$ is the porosity of the aggregates in cm^3 per cm^3 of aggregate.

$((A-\theta_A)/(A+S))^{2n}$ is the effective pore area per unit area of aggregate.

P^{2x} is the effective area maintaining pore continuity in case of the inter-aggregate pores.

$(1-P^{2x})$ is the area occupied by aggregates.

$(P-\theta_p) - (P-\theta_p)^{2x}$ is the effective area of aggregates exposed to the inter--aggregate pore space.

As it is difficult to explain the equation in more detail without repeating the original paper, the reader is kindly referred to that paper.

When the moisture depletion inside and in between the aggregates is known as a function of suction, the air-filled pore space can be calculated for different suctions. These values in turn can be used to calculate the contribution of the intra- (1 st. term of Eq. (16)) and inter-aggregate pores (2 nd. term of Eq. (16)) to diffusion. These calculations were performed applying the hypothetical suction vs. moisture content curve to represent the inter-aggregate pores, and a suction vs. moisture content curve of a sandy loam soil to represent the intra-aggregate properties. This moisture characteristic was taken from work of Rijtema (1969), (soil no. 9), and the soil porosity amounts to 46.5%.
The total soil porosity amounts therefore to 46.5 + 19.01 = 65.51%. This number will be discussed in section 3.5.

Results of the calculations with Eq. (16) are presented in Table 3 and Fig. 16. It is seen that the ratio D / D_o is hardly influenced when the aggregate pores are filled with water (going from right to left in Fig. (16)). However, below the "point" where intra-aggregate pores start filling, e.g. $\varepsilon_g = \pm 0.216$ there is a substantional decrease in this ratio.
Millington & Shearer (1971) found reasonable agreement between the shape of the experimental and calculated curves assuming little or no overlap of pore size classes between the inter- and intra-aggregate void components. Also here the range of overlap is rather small $0.20 < \varepsilon_g < 0.238$, resulting in a similar curve.

A rough control to check whether the ratio D / D_o is in the expected order of magnitude could be made by comparing the range $(0.04 < D / D_o < 0.18)$ with data from Currie (1965): $0.025 < D / D_o < 0.156$ for eight soils with aggregate porosities in the range of 0.25 to 0.41.

3.5 The superposition of a moisture characteristic from literature and the rhombohedron

The soil moisture characteristics of the rhomboidal system, with R = 0.5, and that of the sandy loam soil from Rijtema (1969) were superimposed.
As a result the total system has a porosity of 65.51%, and the literature curve refers uniquely to the aggregated soil fraction. If the data obtained with this

Table 3. The relation between D / D_o, θ_v and ε_g for soil no. 9, Rijtema (1969), and the rhombohedron.

θ_v	ε_g	D / D_o		
		soil no 9	rhombohedron	total
0.0150	0.6401	$5.572.10^{-2}$	0.1241	0.1798
0.0610	0.5941	$5.229.10^{-2}$	0.1241	0.1764
0.0920	0.5631	$4.928.10^{-2}$	0.1241	0.1734
0.1420	0.5131	$4.290.10^{-2}$	0.1241	0.1670
0.1950	0.4601	$3.381.10^{-2}$	0.1241	0.1579
0.2600	0.3951	$2.020.10^{-2}$	0.1240	0.1442
0.3361	0.3190	$7.645.10^{-3}$	0.1240	0.1316
0.4101	0.2450	$5.000.10^{-4}$	0.1237	0.1242
0.4283	0.2268	$1.212.10^{-4}$	0.1233	0.1234
0.4393	0.2158	$5.560.10^{-5}$	0.1219	0.1220
0.4438	0.2113	$3.529.10^{-5}$	0.1205	0.1206
0.4541	0.2010	$9.089.10^{-6}$	0.1165	0.1165
0.4721	0.1830	$9.207.10^{-7}$	0.0979	0.0979
0.4790	0.1761	$4.232.10^{-7}$	0.0890	0.0890
0.4871	0.1680	$2.149.10^{-7}$	0.0781	0.0781
0.4958	0.1593	$1.198.10^{-7}$	0.0669	0.0669
0.5165	0.1386	$4.018.10^{-8}$	0.0441	0.0441

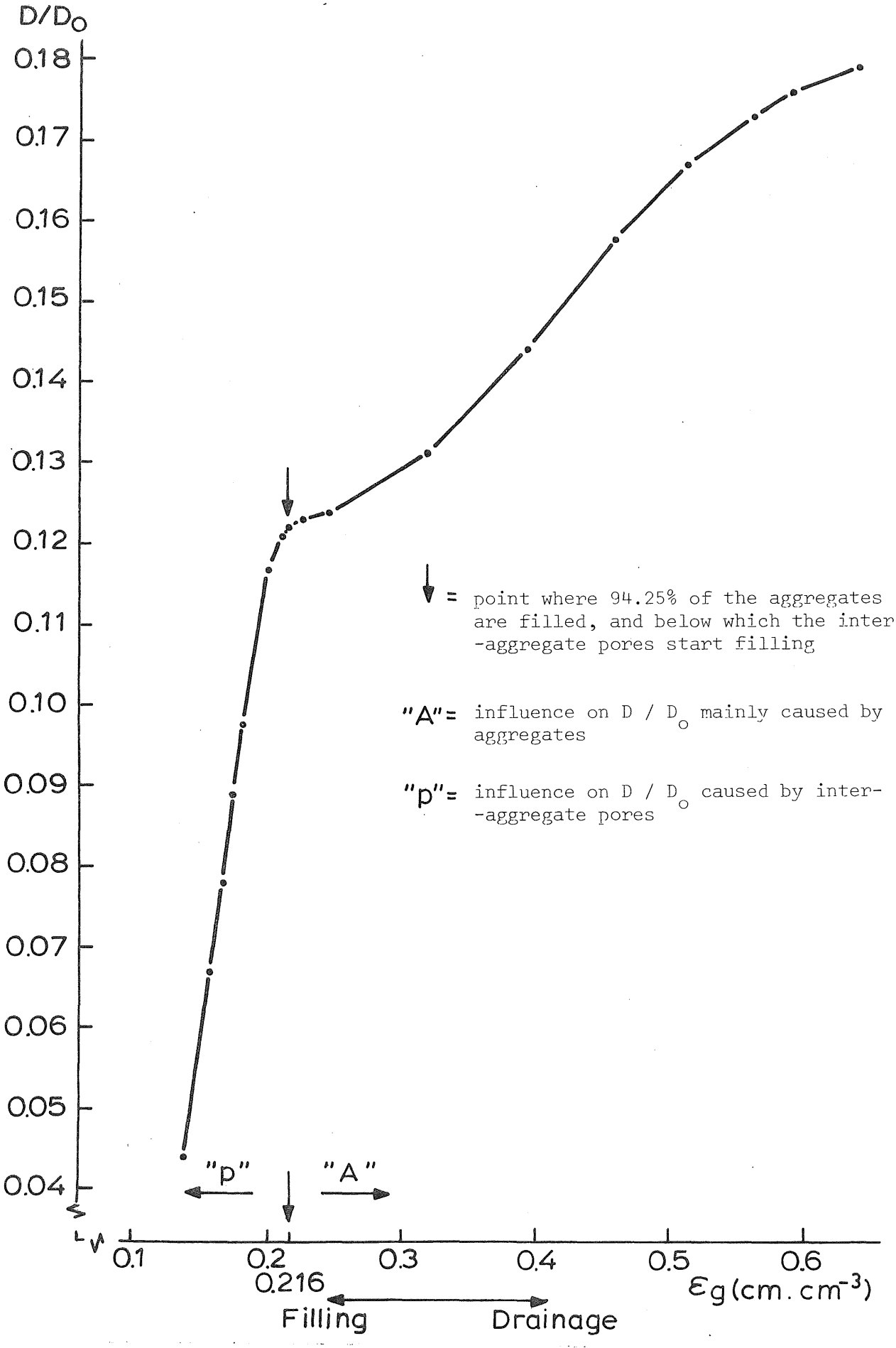

Figure 16. The relation between D / D_o and gas-filled porosity, ε_g.

system, would have to represent the properties of the sandy loam soil, serious criticism would be justified. The reasons for this approach are however:
Firstly, the ideal soil is though to be the best approximation to represent a tilled surface soil of say, 25 cm depth.
Secondly, for the aggregated part of the soil some assumption had to be made with respect to its moisture depletion with an increasing suction. A straight line with a certain slope could have been taken, but a better estimate is probably obtained by assigning data from literature to the aggregates.
The model designed, will have to be considered in the prospect of the importance of parameters which should be investigated in more detail experimentally. So, it will be used as a tool to design experiments in the field of soil physics and eventually in the field of microbiology.

The radius R was taken as 0.5 cm because this seems to be a fair estimate of the largest aggregates present in a soil.

A discussion on the use and accuracy of the soil moisture characteristic, as well as on the possibilities to determine roughly the intra- and inter-aggregate porosities will be given in a later section.

3.6 Diffusion within an aggregate

The work presented here leans upon a paper by Currie (1961a) titled: "Gaseous diffusion in the aeration of aggregated soils". The soil is thought to be made up of spherical aggregates, which are uniform with respect to their diffusion (D) and respiration (S) properties.

For an isotropic concentric shell of radius r, the diffusion equation may be written as

$$\varepsilon \frac{\partial (O_2)}{\partial t} = \frac{1}{r^2} \frac{\partial (O_2)}{\partial r} \left(D r^2 \frac{\partial (O_2)}{\partial r} \right) + S \qquad (17)$$

where ε is the aggregate porosity, $cm^3 . cm^{-3}$

(O_2) is the concentration of oxygen in the pores, $g\ O_2 . cm^{-3}$

D is the diffusion coeffient in the aggregates, $cm^2 . d^{-1}$

t is time, day

S is the respiratory activity, $g\ O_2\ cm^{-3} . d^{-1}$

In a soil at equilibrium with respect to its oxygen status, the term $\partial(O_2)/\partial t$ may be set at zero and Eq. (17) can be rewritten in the form:

$$\frac{d}{d\,r}\left(D\,r^2 \frac{d\,(O_2)}{d\,r} \right) = -\,S\,r^2 \qquad (18)$$

For a uniform crumb in which D and S are independent of r, this gives

$$D\,r^2 \frac{d\,(O_2)}{d\,r} = -\frac{S\,r^3}{3} + \text{constant} \qquad (19)$$

and if $d\,(O_2)/\,d\,r = 0$ at $r = 0$, then

$$D \frac{d\,(O_2)}{d\,r} = -\frac{S\,r}{3} \qquad (20)$$

Further integration gives

$$(O_2) = (O_2)_s + \frac{S}{6\,D}\,(a^2 - r^2) \qquad (21)$$

where $(O_2)_s$ is the concentration at the aggregate surface ($r = a$). For diffusion in the liquid phase in a saturated crumb, Eq. (21) becomes

$$(O_2)_l = K\,(O_2)_{sl} + \frac{S}{6\,D_l}\,(a^2 - r^2) \qquad (22)$$

where the index "l" means liquid

K is the solubility of oxygen in the liquid.

For the diffusion of oxygen, the deficit existing within a crumb can be written:

$$(O_2)_s - (O_2) = \frac{S}{6\,D}\,(a^2 - r^2) \qquad (23)$$

and the maximum deficit in the center is $S\,a^2/\,6\,D$, that is it is quadrupled when the crumb radius is doubled.

The ratio $((O_2)_s - (O_2))\,/\,(O_2)_s$ represents the oxygen deficit as a fraction of the physical maximum. It is obvious that when this ratio tends to be greater than unity, it points to the onset of anaerobic conditions within the aggregate. In that case oxygen consumption is inhibited, that is, the respiration ceases and the term S becomes zero.

The concentration gradients within the aggregate are modified to take into account this central anaerobic zone. If the critical concentration is reached within the aggregate at radius $r = b$, the new boundary conditions become: for all r, D is constant; for $0 \leqslant r < b$, $S = o$; for $b < r \leqslant a$, $S = \text{constant} \neq 0$; and at $r = a$, $(O_2) = (O_2)_s$. Then it follows from integration that for $b \leqslant r \leqslant a$:

$$(O_2) = (O_2)_s + \frac{S}{6\,D}\{(a^2 - r^2) - 2\,b^3(\frac{1}{r} - \frac{1}{a})\} \qquad (24)$$

and for $0 \leqslant r \leqslant b$

$$(O_2) = (O_2)_s + \frac{S\,a^2}{6\,D}\left(1 - 3\,\frac{b^2}{a^2} + 2\,\frac{b^3}{a^3}\right) \qquad (25)$$

The maximum radius at which a crumb is just fully aerobic is given by substituting $r = b = 0$ in Eq. (24) and is called its critical radius a_c where

$$((O_2)_s - (O_2))_c = \frac{S\,a_c^2}{6\,D} \qquad (26)$$

for dry aggregates. The right hand part of Eq. (26) becomes $S\,a_c^2 / 6\,D\,K$ for a wet aggregate.

For all $a > a_c$ and wet aggregates:

$$((O_2)_s - (O_2))_c = \frac{S\,a^2}{6\,D\,K}\left(1 - 3\,\frac{b^2}{a^2} + 2\,\frac{b^3}{a^3}\right) \qquad (27)$$

Equation (27) is used to calculate the fractional anaerobic volume in terms of the relative radius a / a_c. From Eqs. (26) and (27) follows

$$\left(\frac{a_c}{a}\right)^2 = 1 - 3\,\frac{b^2}{a^2} + 2\,\frac{b^3}{a^3} \qquad (28)$$

which equation is presented graphically in Fig. 17. If, for example, an aggregate has twice its critical radius, 30 percent of its bulk is anaerobic; at four times, this value is 60 percent. The data calculated are presented in Table 4, too.

Data obtained with Eq. (28) were calculated by an iterative procedure according to Newton (cf. Burington, 1973). An estimate of D / D_o for the aggregates was obtained by applying the first part of Eq. (16) for a completely dry aggregate. It amounts to 0.0566, a value which is very close to the one presented in Table 3 for $\theta_v = 0.015$. Currie (1961a) used a value of 0.05 for his calculations on anaerobiosis.

It should be realized that the parameters used to determine this ratio do not include the degree of cementation of the particles within an aggregate. This degree of cementation, however, along with the geometric construction of aggregates, should be a subject of investigation in the field of soil physics. The work presented by Currie (1965), dealing with complexity parameters of aggregates, and by Redlich (1940), Emerson (1955), Emerson (1959), and Emerson & Dettmann (1959),

Table 4. Values of the fractional anaerobic volume and the relative radius, according to Currie (1961a).

a / a_c	b^3 / a^3
radius relative to critical radius	anaerobic aggregate volume
0	0
1	0
1.1	0.0175
1.25	0.0675
1.50	0.1574
1.75	0.2375
2.0	0.3057
2.5	0.4125
3.0	0.5
3.5	0.5610
4.0	0.61
4.5	0.65
5.0	0.6805
5.5	0.707
6.0	0.73
6.5	0.7495
7.0	0.766
7.5	0.7825
8.0	0.795
8.5	0.807
9.0	0.816
9.5	0.826
10.0	0.8335
14.1421	0.8809
18.2574	0.9072
31.6228	0.9460

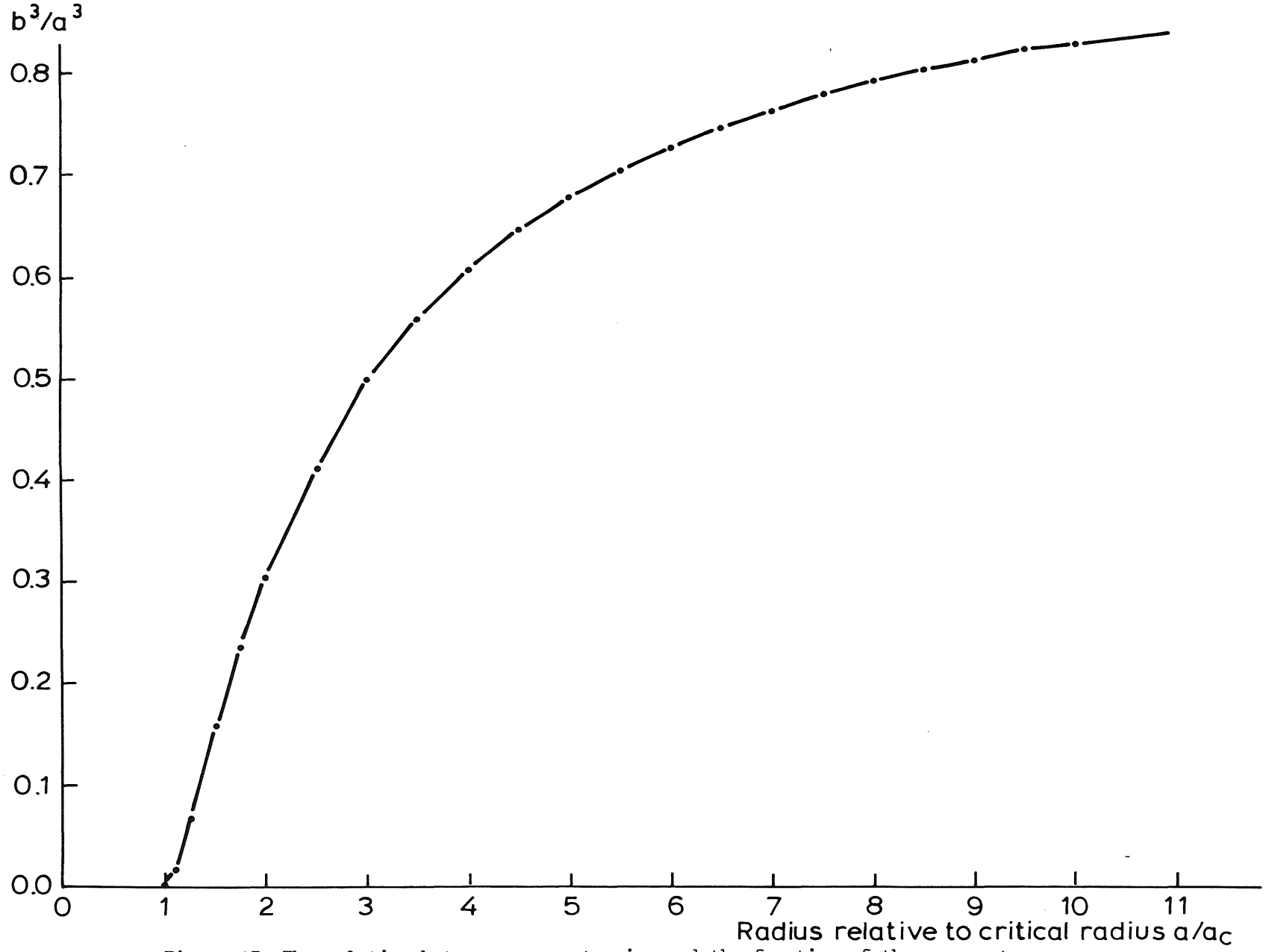

Figure 17. The relation between aggregate size and the fraction of the aggregate volume which is anaerobic. After Currie (1961a).

dealing with aggregate structures, can probably be a guideline in this direction.

3.7 An example of the calculation of anaerobiosis

The anaerobic fraction of an aggregate may be calculated for any place in the profile.
An aggregate will have a certain degree of moisture saturation, and a certain air-exposed area (A.E.A.). The distribution of water inside the aggregate is of prime importance. As a first approximation it is assumed that it is located in a concentric sphere within the aggregate. Knowing the water content, the porosity, and the radius of the aggregate, the radius (equivalent radius) of this water-filled sphere can be calculated. The sphere volume, V, equals $\frac{4}{3} \pi R^3$. Obviously, if $\theta_v = \varepsilon$, r_{eq} should equal R. For lower water contents a certain fraction of ε is assumed to be filled with water, e.g. $\frac{\theta_v}{\varepsilon}$. The equivalent volume amounts to:

$$V_{eq} = \frac{4}{3} \pi R^3 \frac{\theta_v}{\varepsilon} \tag{29}$$

V_{eq} can also be written as:

$$V_{eq} = \frac{4}{3} \pi r_{eq}^3 \tag{30}$$

Substituting Eq. (29) into (30) yields Eq. (31), which was used to calculate the equivalent radius of a certain water-filled portion of the sphere at moisture content θ_v and porosity ε:

$$r_{eq} = R \sqrt[3]{\frac{\theta_v}{\varepsilon}} \tag{31}$$

Taking the respiration rate, S, as $6.4645\ 10^{-5}$ g O_2. cm^{-3} aggregate $.d^{-1}$, which is equivalent to a respiration rate of 10 l $O_2.m^{-2}$. (0.25 m depth of soil)$^{-1}$. d^{-1} (Grable, 1966), the solubility of oxygen as $2.9796\ 10^{-2}$, the outside concentration of oxygen as $2.7487\ 10^{-4}$ $g.cm^{-3}$, equivalent to 21% O_2 in air, the diffusion coefficient in a water saturated sphere as $1.2715\ 10^{-1}$ $cm^2.d^{-1}$, the critical concentration at which effective anaerobic conditions occur as $2.24\ 10^{-8}$ g O_2. cm^{-3}, (van Veen, 1977), and a suction of 10, 25 and 100 mbar, respectively, the critical radius, a_c, and the fractional anaerobic volume can be calculated. The values are summarized in Table 5, for aggregate radii of 0.5 and

Table 5. Calculation of the anaerobic fraction of aggregates of different radii and at different suctions.

R, cm	0.5			1.0		
Sm, mbar	10	25	100	10	25	100
θ_v	0.4438	0.426	0.26	0.4438	0.426	0.26
A.E.A.	0.8785	0.9480	0.9867	0.8785	0.9480	0.9867
a_c^*, cm	0.4027	0.4183	0.4268	0.1425	0.1479	0.1509
r_{eq}, cm	0.4923	0.4856	0.4119	0.9846	0.9712	0.8238
r_{eq}/a_c	1.2225	1.1609	0.9651	6.9141	6.5668	5.4595
anaerobic sphere fraction fig (17).	0.0578	0.0377	-	0.762	0.750	0.703
anaerobic soil fraction, see Eq. (45), chapter 4.3.1	0.0428	0.0279	-	0.5642	0.5554	0.5206

* $a_c = \sqrt{\frac{6\ D\ AEA\ K\ ((O_2)_s-(O_2))}{S\ \frac{4}{3}\ \pi\ a^3}}$, which is Eq. (26)

rewritten for a wet aggregate.

1 cm, respectively.
These results show the importance of the sphere radius in calculating the anaerobic fraction of soil. It is also seen that even at a suction of 100 mbar, the fractional anaerobic soil volume amounts to 0.52, when R = 1 cm. More detail will be given later on in the discussion.

3.8 The hydraulic conductivity of the soil

The hydraulic conductivity of the soil was calculated on basis of the soil moisture characteristic given by Rijtema (1969), according to Eq. (1) of Green & Corey (1971), i.e. Eq. (32).

$$K(\theta)_i = \frac{K_s}{K_{sc}} \cdot \frac{86400\ \gamma^2}{\rho\ g\ \eta} \cdot \frac{\varepsilon^2}{n^2} \sum_{j=i}^{m} \left((2j + 1 - 2i)\ h_j^{-2} \right) \qquad (32)$$

$$i = 1, 2, \ldots, m$$

in which $K(\theta)_i$ is the calculated conductivity for a specified water content or pressure ($cm.d^{-1}$),

θ is the water content ($cm^3.cm^{-3}$),

i denotes the last water content class on the wet end, e.g., $i = 1$ identifies the pore class corresponding to the lowest water content for which conductivity is calculated,

K_s/K_{sc} is the matching factor (measured saturated conductivity/calculated saturated conductivity),

γ is the surface tension of water ($dynes.cm^{-1} = g.cm.s^{-2}$),

ρ is the density of water ($g.cm^{-3}$),

g is the gravitational constant ($cm.s^{-2}$),

η is the viscosity of water ($g.cm^{-1}.s^{-1}$),

ε is the porosity ($cm^3.cm^{-3}$),

n is the total number of pore classes between $\theta = 0$ and θ_s, the saturated water content,

h_j is the average pressure for a given class of water-filled pores (mbar).

Equation (32) actually is similar to Eq. (7) as presented in the paper of Marshall (1958), except that it contains a matching factor, (K_s/K_{sc}), by which one point of the curve is matched with the conductivity at saturation as determined in the field.

The influence of the inter-aggregate pores on the hydraulic conductivity in these calculations was ignored, this being the only deviation from the model. In Fig. 18 the calculated hydraulic conductivity is presented, details being given in Appendix IV.

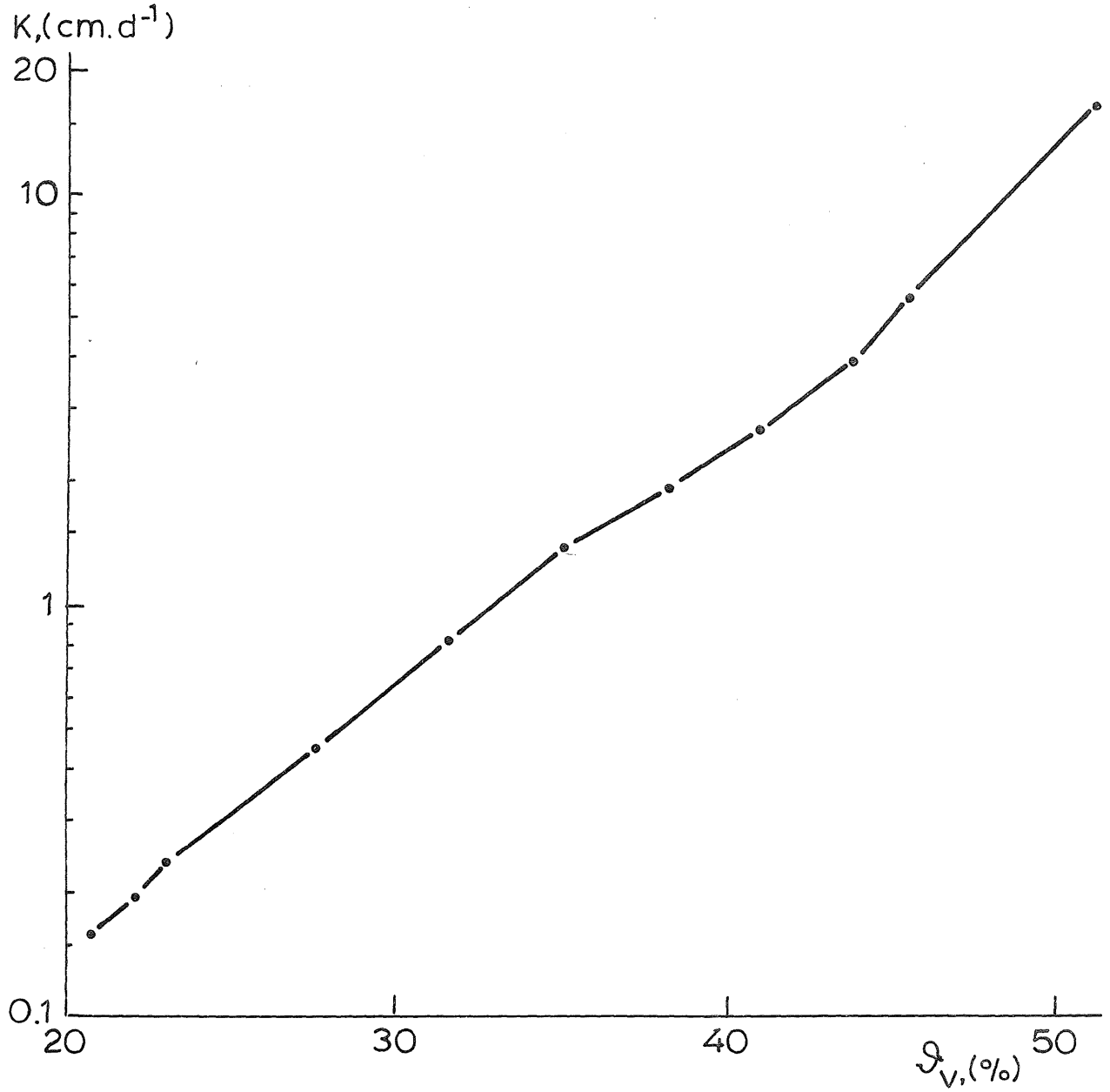

Figure 18. The relation between hydraulic conductivity and moisture content.

4. Program description

4.1 General

A model is a simplified representation of a system, with well defined boundaries. A model can be built if the structure of the system is sufficiently well known, so that the processes, playing a role in the system and their relations can be mathematically described.

In the state variable approach the rates of change are calculated from the state variables and driving variables and are mutually independent. This allows all rates of change to be calculated in any order at the same instant of time. After calculating all rates new values for the state variables are obtained by integrating the rates over a small time interval. In this way, a model operates in semi-parallel fashion, de Wit & Goudriaan (1974).
State variables are for instance the amount of water, and the amount of oxygen, whereas examples of rate variables are flow rates of water and oxygen.

The model presented here calculates the fraction of the (rhomboidal) soil system which becomes anaerobic under certain boundary conditions. The model is a formalization of the theory presented in chapter 3.
A full program listing is given in Appendix V. The CSMP-program can be split into three parts: the INITIAL section in which the problem is set up, the DYNAMIC section in which the time dependent calculations are carried out, and an OUTPUT section. The dynamic section is subdivided into four major parts; the subsection to calculate the anaerobic soil volume, the subsection water flow, the subsection oxygen flow macro system, and the subsection in which some integrals are defined. Each section will be described separately, and will include the assumptions underlying the model and the equations describing the processes. The numerical values of the parameters will be discussed in a following chapter. Functions will only be presented in full detail in Appendix V.

4.2 The initial part of the program

In the INITIAL section, which is calculated only once at the onset of the simulation, the invariable geometry of the system and the state of the system is calculated at time zero. The variables decrared in STORAGE are subscripted variable names for which memory space is reserved.

The numerical values can be calculated from the equations derived in the theory:

The thickness of a layer is taken as the height of a unit cell of the rhombohedron, which was derived in chapter 3.1 as $4\sqrt{\frac{2}{3}}$ R. Taking R1 = 0.5 this thickness (TCOM) is calculated as 1.633 cm.
Assuming no evaporation from the bare soil, and a water table of 100 cm depth, the equilibrium water content in each layer can easily be calculated from the moisture suction curve. All calculations are performed for the centers of the layers, DO-loop 3, and therefore the moisture suction in the first layer will be -(100-(1.633/2))= -99.1835 mbar, at which value a moisture content of 0.261883 belongs.

4.3 The dynamic part of the program

The DYNAMIC is repeatedly executed at each time interval. In this part of the program four subsections are distinguished. Each one is subdivided into a definition section (comments), followed by a section containing the equations, one defining the parameters, and one giving the functions.

4.3.1 Section to calculate the anaerobic soil volume

Usually, when solving a certain partial differential equation by a simulation procedure, the subject studied is divided into small increments of space and time. Then, the net flux over the layer boundaries of each space increment (layer thickness) is calculated in a certain time increment. In the section to calculate the anaerobic soil volume, the partial differential equation (Eq. 17) has been solved already analytically in chapter 3.6, under the assumption that at each moment equilibrium exists between the aggregate and its surroundings, ($\partial C/\partial t=0$). The program, therefore, calculates for each layer the water- and oxygen content, the critical radii of the aggregates at which anaerobic conditions occur, a_c, the equivalent radii, r_{eq}, pertaining to a certain moisture content, and the ratio, r_{eq}/a_c, which is used to read the fractional anaerobic aggregate volume from Fig. 17, whereafter the anaerobic soil fraction is obtained.

The relative content of water and oxygen ($cm^3.cm^{-3}$) in layer I, is calculated in DO-loop 6, by Eqs. (33) and (34):

```
WC(I)=AMW(I)/TCOM                                   (33)
CO(I)=AMO(I)/(TCOM*(PVOL-WC(I)))                    (34)
```

where AMW(I) and AMO(I) are the amounts of water in cm^3 and oxygen in grams in layer I, respectively. As the thickness of the layer, TCOM, equals 1.633 cm, and a unit surface area is considered, the numerical value of AMW(I) and AMO(I) is expressed per 1.633 cm^3. The oxygen concentration is based on the air-filled pore volume, (PVOL-WC(I)), because of the low solubility of oxygen in water.

In DO- loop 7 the calculation is started with the potential consumption rate of oxygen per layer:

CROC(I)=FRT*(COR+COM) (35)

The assumption was made that the roots are homogeneously distributed throughout the profile considered, implying that the fraction of roots in each layer, FRT, is inversely proportional to the number of layers, N(=15). The total consumption of oxygen, COT, is thought to be made up of the oxygen consumption by the roots, COR, and by the microorganisms, COM, in a ratio of 2:1 (Woldendorp, 1963, p. 37). COT is expressed in g O_2. cm^{-2}. $DEPTHT^{-1}$. d^{-1}, where DEPTHT denotes the total soil depth, which amounts to 15 1.633=24.495 cm.
In Eq. (36) the oxygen consumption per unit volume of aggregates, CROCVS, is calculated:

CROCVS(I)=CROC(I)*(VOLHEX/TOTVOL)/TCOM (36)

where CROC(I) is expressed in g O_2. 1.633 cm^{-3}. d^{-1}, and therefore is divided by TCOM to obtain the consumption per cm^3 of soil. The assumption was made that respiration takes place within the aggregates, where intimate contact exists between respiring tissue and soil particles. On the average, one cm^3 of soil contains 0.8099 cm^3 of aggregate. Therefore the right hand side of Eq. (36) should be multiplied by 0.8099^{-1}, which is the total volume of the rhombohedron or hexagonal, VOLHEX, divided by the total volume of aggregates, TOTVOL.
The actual consumption rate of oxygen in a layer is assumed to be proportional to the fractional aerobic volume of the soil:

CRO(I)=CROC(I)*(1.-FANVOL(I)) (37)

where FANVOL is the anaerobic volume fraction of the soil.
Numerical values of CRO(I) are used later on to calculate the net flow of oxygen. The air exposed area, AEAR, for each aggregate class was calculated in chapter 3.3, Table 2. The suction values were replaced by the corresponding volumetric

moisture contents and tabulated in the program. Equation (38) calculates the air exposed area by linear interpolation (code: AFGEN) at a given water content of the tabulated function, AEART.

```
AEAR(I)=AFGEN(AEART,WC(I))                                    (38)
```

As was already stated in chapter 3.3, the diffusion coefficient into the aggregate is assumed to be proportional to the air exposed area. This is expressed by:

```
DCALC(I)=DCSPH*AEAR(I)                                        (39)
```

where DCALC(I) is the calculated diffusion coefficient and DCSPH the diffusion coefficient of the sphere. This parameter is calculated by the method of Millington & Shearer (1971, chapter 3.4), which yields D/D_o. Combining this ratio with the literature value of the diffusion coefficient of oxygen in free water, D_o, gives the numerical value of D for diffusion in a water saturated aggregate. The next step in DO- loop 7 is the calculation of the actual consumption rate of oxygen in each aggregate class:

```
CROS(I)=CROCVS(I)*V*(1.-FVLAN(I))                             (40)
```

As before this consumption rate is inversely proportional to the fraction of the aggregate which is anaerobic, (1.-FVLAN(I)), and V is the volume of an aggregate, calculated in the INITIAL. All components are available now to calculate the critical radius for each aggregate class in a certain layer:

```
RCRIT(I)=SQRT(6.*DCALC(I)*(CO(I)-CCO)*SOLO/CROS(I))           (41)
```

where SQRT means square root, and CCO and SOLO denote the critical concentration of oxygen where effectively anaerobic conditions occur, and the relative solubility of oxygen in water, respectively. The latter variable has to be included to make the transition from oxygen in air to oxygen in water. SOLO is expressed in $(g\ O_2 .\ cm^{-3}\ H_2O)/(g\ O_2 .\ cm^{-3}$ air), and is thus dimensionless.

In DO- loop 8 first the equivalent radius, REQ(I), is calculated. In the tabulated function REQT, this radius is given as a fraction of an aggregate, with unit radius. Therefore, the value of REQ(I) has to be multiplied by the

actual radius of each aggregate to obtain the real equivalent radius. This multiplication is included in Eq. (42), which calculates the ratio of the equivalent radius and the critical radius.

```
RATIO(I)=REQ(I)*R/RCRIT(I)                                    (42)
```

The fractional anaerobic volume of an aggregate, FVLAN(I), is determined from the tabulated values of Fig. 17, in DO- loop 9. These values are generated by:

```
FVLAN(I)=AFGEN(VOLANT,RATIO(I))                               (43)
```

where VOLANT is the tabulated function referred to above.
The anaerobic volume of aggregates in a unit hexagonal cell is subsequently calculated:

```
VOLAN(I)=FVLAN(I)*6.*V                                        (44)
```

whereafter Eq. (45) expresses the total anaerobic volume of the aggregates (in cm^3) as a fraction of the soil volume, FANVOL, by dividing by VOLHEX:

```
FANVOL(I)=(VOLAN1(I)+VOLAN2(I)+VOLAN3(I))/VOLHEX              (45)
```

The latter procedure was also followed to calculate the anaerobic volume of soil in chapter 3.7, Table 5.

The reader might have noticed that when RATIO, Eq. (42) is to be calculated, RCRIT, Eq. (41), should be known. RCRIT is dependent on CROS, Eq. (40), which in turn can only be calculated when (1.-FVLAN) is known. As FVLAN can only be calculated when RATIO is known, an algebraic loop is introduced.
One way to tackle this problem is to design an iterative procedure in which RATIO and FVLAN are calculated several times within an increment of time, DELT, until a preset error criterion is met.
Another way to bypass the difficulty is to calculate RATIO at time T based on FVLAN of time T-DELT. The former procedure is physically sound. The latter method, which is followed here may give equally acurate results.
Whether the iterative method is more favourable with respect to cumputation time is not yet clear, as it was not tried.

4.3.2 The water flow section

Water flow through the soil is an important phenomenon as the oxygen situation in the soil is directly related to its moisture content. The submodel applied is based on a paper by van Keulen & van Beek (1971), and slightly modified for the present study.

In DO- loop 10 the suction in cm H_2O and the conductivity in cm. d^{-1} of the soil are read from tabulated functions with:

```
S(I)=-1.*AFGEN(SUTB,WC(I))                                    (46)
```

```
K(I)=AFGEN(KTB,WC(I))                                         (47)
```

These values are subsequently used to calculate the average conductivity, AVK(cm^2. d^{-1}), for the layers 2 to N, and the total potential, ST(mbar or cm H_2O), with:

```
AVK(I)=(K(I-1)+K(I))*.5                                       (48)
```

```
ST(I)=S(I)+(GRWTAB-DEPTH(I))                                  (49)
```

The total suction refers to the hydraulic potential, P^*, (Bolt et al., 1970) and is composed of the matric potential S(I), and the gravitational potential, (GRWTAB-DEPTH(I)), where GRWTAB represents the depth of the ground water table below the soil surface.

The flow rate of water from one soil layer to the adjacent one, is governed by the average conductivity of the soil for water flow, and the difference in water potential or the potential gradient existing between the centers of the two layers, according Darcy's law:

```
FLW(I)=AVK(I)*(ST(I-1)-ST(I))/TCOM                            (50)
```

The flow rates over the first and last boundary must be calculated separately, according to the imposed boundary conditions. The flow rate into the first layer, FLW(1), is determined by:

```
FLW(1)=FCNSW(THWL,AMIN1(MAXINF,RAIN),AMIN1(MAXINF,RAIN),
        AMIN1(MAXINF,RAIN+THWL/DELT))                              (51)
```

where FCNSW is a CSMP function switch, which takes the value of the second argument, if the first one < 0, the third one, if the first one = 0, and the fourth one if the first one > 0. AMIN1 is a functional statement, which takes as output the smallest of the two arguments.
THWL is the thickness of the water layer on top of the soil.
MAXINF is the maximum infiltration rate under the given conditions.
RAIN is the intensity of rain, dependent on time.

The thickness of the water layer on top of the soil is tracked in an integral at the end of the DYNAMIC.

```
THWL=INTGRL(0.,RAIN-FLW(1))                                        (52)
```

The maximum infiltration rate is calculated according to:

```
MAXINF=(K(1)+KSAT)*.5*(STSURF-ST(1))/(.5*TCOM)                     (53)
```

where KSAT is the saturated conductivity of the soil.
STSURF is calculated as the sum of a matric suction term at the soil surface, SSURF in mbar, a gravity potential term, GRWTAB, and the hydrostatic pressure of the water on top of the soil, THWL:

```
STSURF=SSURF+GRWTAB+THWL                                           (54)
```

It is assumed that when there is a layer of water on top of the soil, or when it is raining, there is always a thin saturated layer at the surface, which means that then SSURF is always zero.

Rainfall is introduced as a forcing function with:

```
RAIN=AFGEN(RAINTB,TIME)                                            (55)
```

The tabulated values of rain intensities were based on weather data of the years 1975 and 1976 in the Netherlands.

The flow rate over the last boundary is calculated by:

```
FLW(16)=(K(15)+KSAT)*.5*ST(15)/(GRWTAB-DEPTHT)                    (56)
```

Equation (56) calculates the average flow of water over the soil layer below the depth of interest, DEPTHT, which in this study equals 24.495 cm, to the ground water level.

The water consumption rate of a crop is calculated in DO- loop 13, by assuming a certain transpiration rate. Water uptake by the roots is assumed to be proportional to their relative abundance in the profile:

```
CRWC(I)=FRT*CWT                                                   (57)
```

where CWT is the total water consumption, expressed in cm^3 H_2O. cm^{-2}. $DEPTHT^{-1}$. d^{-1}.
Water uptake is not dependent on soil moisture suction, but is reduced by the fraction of the soil which is anaerobic, under the assumption that root activity ceases when oxygen shortage occurs.

```
CRW(I)=CRWC(I)*(1.-FANVOL(I))                                     (58)
```

The net flow rate into or out of each layer is calculated from the flow rates over the top and bottom boundaries of a layer, and the water extraction from that layer with:

```
NFLW(I)=FLW(I)-FLW(I+1)-CRW(I)                                    (59)
```

4.3.3 The oxygen flow macro system

The oxygen flow from one layer of the soil to another is referred to as the macro system, in contrast to the oxygen flow from the air-filled porosity of a soil layer into the aggregates.
The oxygen concentration in the air-filled soil pores in each layer is calculated in this submodel. The ratio of diffusion of oxygen in a porous system to

that in free air is obtained from a function, based on tabulated values of Fig. 16:

```
DEFAC(I)=AFGEN(DEFACT,(PVOL-WC(I)))                                    (60)
```

where DEFAC denotes the diffusion efficiency factor.
The effective diffusion coefficient, DEF, subsequently is calculated by:

```
DEF(I)=DZERO*DEFAC(I)                                                  (61)
```

where DZERO denotes D_o, or the diffusion of oxygen in free air.

The average diffusion coefficient over a boundary is calculated in DO-loop 15, for the layers 2 to N by Eq. (62), whereas the diffusional flow of oxygen is calculated similar to the water flow from the diffusivity and the gradient of oxygen concentration in the two adjacent layers:

```
ADEF(I)=(DEF(I)+DEF(I-1))*.5                                           (62)

DFLO(I)=ADEF(I)*(CO(I-1)-CO(I))/TCOM                                   (63)
```

The flow rates over the first and the last boundary again must be calculated separately. The flow rate into the first layer, DFLO(1), is defined as:

```
DFLO(1)=FCNSW(THWL,FLO,FLO,RDFLO)                                      (64)
```

FLO and RDFLO in Eq. (64) are defined by:

```
FLO=DEF(1)*(COUT-CO(1))/(.5*TCOM)                                      (65)

RDFLO=DZW*(COUT-CO(1))/(THWL+NOT(THWL))                                (66)
```

where COUT is the concentration of oxygen in free air.
DZW is the diffusion coefficient of oxygen in free water.
NOT(...) is a function to prevent zero division.
Equation (64) shows that the rate of oxygen diffusion into the profile is affected by the presence of a possible water layer on top of the soil. The presence of such a water layer will seriously impair oxygen diffusion as the diffusion

coefficient of oxygen in water is about 10^4 times smaller than that in free air.
The diffusional flow of oxygen over the last boundary is set to zero, as no roots are present below this depth. This condition is already stated in the INITIAL by: DFLO(16)=0..

In DO-loop 16 mass flow of oxygen due to changes in moisture content in the profile is calculated, under the assumption that air moves in and out of the profile fully complementary to the water:

```
MFLO(I)=NFLW(I)*CO(I)                                          (67)
```

The net flow of oxygen is finally calculated from the flow rates over the upper and lower boundaries of a layer, the oxygen consumption rate in a layer, and the mass flow of oxygen:

```
NFLO(I)=DFLO(I)-DFLO(I+1)-CRO(I)-MFLO(I)                       (68)
```

4.3.4 The integral section

Throughout the program so-called array-integrals are defined, indicated by the index (I).
In the integral section a few INTGRL statements are combined. Here, the amount of water per layer, AMW, the cumulative infiltration, CUMINF, the cumulative outflow of water, CUMOUT, the amount of oxygen per layer, AMO, the cumulative oxygen inflow, CUMCOX, and the thickness of the possible water layer, THWL, are taken care off by:

```
AMW=INTGRL(AMWI,NFLW,15)                                       (69)

CUMINF=INTGRL(0.,FLW(1))                                       (70)

CUMOUT=INTGRL(0.,FLW(16))                                      (71)

AMO=INTGRL(AMOI,NFLO,15)                                       (72)

CUMCOX=INTGRL(0.,DFLO(1))                                      (73)
```

```
THWL=INTGRL(0.,RAIN-FLW(1))                                    (52)
```

4.4 The output section

In the output section FORTRAN statements have been used to obtain printed output at each 0.01 day. The following variables are given per layer:

- the fractional anaerobic volume of soil, FANVOL, $cm^3.cm^{-3}$.
- the relative water content, WC, $cm^3.cm^{-3}$.
- the concentration of oxygen, CO, g $O_2.cm^{-3}$ air.
- the anaerobic volume of aggregates in a soil layer, VOLAN, cm^3.
- the ratio of the equivalent radius to critical radius for the largest aggregates, RATIO1.
- the consumption rate of water, CRW, cm^3 H_2O. $TCOM^{-1}$. d^{-1}.
- the consumption rate of oxygen, CRO, g $O_2.TCOM^{-1}$. d^{-1}.
- the mass flow of oxygen, MFLO, g $O_2.TCOM^{-1}$. d^{-1}.
- the soil moisture suction, S, cm H_2O or mbar.

In a CSMP PRINT statement the cumulative infiltration of water, the outflow of water at the bottom of layer 15, the total oxygen consumption, and the thickness of the water layer on top of the soil are asked for.

The integration method used is the rectilinear or Euler's method.

A finish condition was included to prevent the concentration of oxygen to drop below the concentration of oxygen where effectively anaerobic conditions occur. Further calculations would have been meaningless. This drop in oxygen concentration was thought to be possible when water would be present on top of the soil. This condition, however, has never occurred in the runs made with the model.

4.5 The parameters of the model

Nineteen parameter values are defined in the model. Fortunately not all of them are subject to variation, at least when temperature and barometric conditions are assumed to be constant. The numerical values of some important parameters will be discussed below.

Total oxygen consumption, COT

Grable (1966) reported values for oxygen consumption ranging from 5 to 10 l. m^{-2}. d^{-1}. Bakker & Hidding (1970) reported the highest value of Grable for only microorganisms ($\pm$ 8.9 l O_2 m^{-2}. 25 cm $depth^{-1}$. d^{-1}). Furthermore, Woldendorp (1963), showed that the ratio of respiratory activity of roots to microorganisms was about 2 to 1. This would imply that the highest reasonable estimate of oxygen consumption may be about 26.67 l O_2 m^{-2}. 25 cm $depth^{-1}$. d^{-1}. Assuming a dense system of grass roots in the upper 25 cm of soil, the oxygen consumption per day and per cm^2 may be calculated as 10 1.3089 10^{-4} = 1.3089 10^{-3} g O_2 for the lower limit and 26.67 1.3089 10^{-4} = 3.4904 10^{-3} g O_2 for the upper limit. The value of 1.3089 g O_2 per liter of pure oxygen follows from the identity that 24.448 l of gas = 1 mol = 32 gram at 25°C.

The diffusion coefficient of oxygen in an aggregate, DCSPH

Lemon & Wiegand (1962), give the diffusion coefficient for oxygen in free water as 2.6 10^{-5} $cm^2.s^{-1}$ at 25°C. In chapter 3.6 it was shown that the ratio of the diffusion coefficient in a porous medium to that in a medium without any solid obstacle, D / D_o, equals 0.0566 for a porosity of 0.465. Combining both figures and converting to days yields the diffusion coefficient of oxygen in a water saturated aggregate:

$$D = 0.0566\ 2.6\ 10^{-5}\ 86400 = 1.2715\ 10^{-1}\ cm^2.\ d^{-1}.$$

The relative solubility of oxygen in water, SOLO

Grable (1966) reported a value of 0.039 g O_2 l^{-1} water at 25°C and 1 bar pressure. Assuming 21% of oxygen to be present in air it follows that the concentration equals: 0.21 1.3089 10^{-3}= 2.7487 10^{-4} g O_2. cm^{-3} of air. The relative solubility is obtained by the ratio of the amount of oxygen in water to that in air and amounts to 0.039 10^{-3} / 1.3089 10^{-3} = 2.9796 10^{-2}.

The critical concentration of oxygen, CCO

Greenwood (1961) reported respiration to be inhibited at an oxygen concentration of about 7 10^{-7} Molar. Conversion of this value to g O_2.cm^{-3} of soil gives: 7 10^{-7} 32 10^{-3} = 2.24 10^{-8}, which figure was used by van Veen (1977).

This author, however, pointed out that there is a range of O_2-concentrations at which respiration of different microorganisms ceases rather than one single value. In view of this consideration, a run was made in which a higher critical oxygen concentration was taken (CCO = 2.24 10^{-7} g O_2. cm^{-3} of soil).

The depth of the ground water table, GRWTAB

The depth of the groundwater table in the model is either set at 100 cm or 50 cm below the soil surface. The initial equilibrium water contents, as given in TABLE RWC, were adjusted accordingly.

Total water consumption, CWT

The water consumption of a crop is given a small, 0.3, and a quite high value, 0.9 cm. d^{-1}. The high value may be found on a very bright summer day in the Netherlands.

Diffusion of oxygen in free air, DZERO

Grable (1966), reported a value of 0.226 cm^2. s^{-1} at 25°C. Conversion to the dimension cm^2. d^{-1} yields the value presented: 19526.

The oxygen concentration in free air, COUT, and the diffusion coefficient in free water are given during the calculations above, and are known therefore.

4.6 The time constant

The simplest way to find the correct time-interval of integration of a model is to run the model with values for DELT a factor two apart. A graph of a representative output variable at a given moment against the time interval used will show the region of instability of the system (de Wit & van Keulen, 1975). If reduction of the time interval by a factor two does not change the relevant results of the simulation more than a preset relative amount, it may be argued that a correct time-interval is reached (de Wit & Goudriaan, 1974). Figure 19 shows the influence of DELT on results of FANVOL, WC, and CO. The data for the water flow sub-model are very well described by both time intervals, which equal 8.64 and 17.28 seconds, respectively. The data, however, for the macro oxygen flow sub-model, start oscillating after 23 steps of integration (data not presented). The same picture is found for the variable

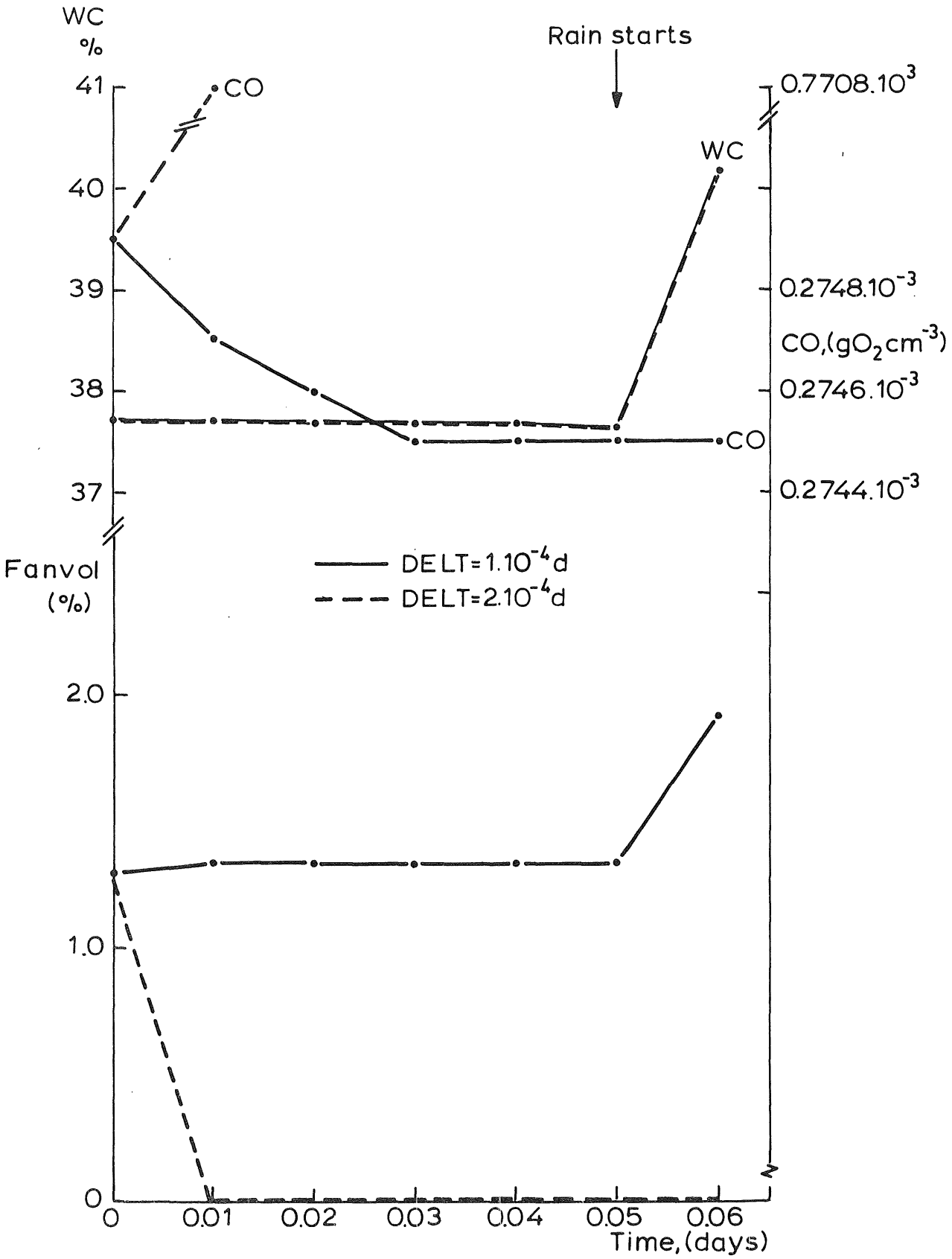

Figure 19. The influence of DELT on simulated results of FANVOL, WC, and CO.

FANVOL. This latter result is a consequence of the fact that CO starts to oscillate.

An estimate of the time constant (de Wit & Goudriaan, 1974), for the sub-model of oxygen flow, was obtained in a different way. Suppose the oxygen concentration to be CO(1) in the upper layer. The maximum amount of oxygen to be supplied to the first layer equals:

```
MAMO(1)=(COUT-CO(1))*(PVOL-WC(1))*TCOM                    (74)
```

The system will start oscillating if so much oxygen is supplied to the first compartment during the first time interval that its oxygen concentration increases beyond the outside concentration, COUT.
The flow rate at time zero into the first compartment equals:

```
FLO=DEF(1)*(COUT-CO(1))/(.5*TCOM)                         (65)
```

The time constant now is found by the inequality:

```
TMCNST*FLO<MAMO(1)                                        (75)
```

Rewriting gives:

$$TMCNST < \frac{0.5*TCOM^2*(PVOL-WC(1))}{DEF(1)} \qquad (76)$$

where DEF(1)=DZERO*DEFAC (61)

Equation (76) indeed has the right dimension of day.
At a water content of 0.261883, DEFAC is found from the FUNCTION DEFACT at a gas-filled porosity of 0.3932 as 0.1438. TMCNST can be calculated as:

$$TMCNST < 0.5*1.633^2*0.3932/19526*0.1438 = 1.867\ 10^{-4}\ \text{day}$$

In this perspective it is logical that an oscillation was found at a time-interval of $2\ 10^{-4}$ day, Fig. 19.

Following a similar procedure for the time constant of the water flow sub-model, de Wit & van Keulen (1975) derived the following equation:

$$TMCNST < \frac{TCOM^2}{D} \qquad (77)$$

where D is the diffusivity, calculated by dividing the hydraulic conductivity by the cotangent of the soil moisture characteristic, both at θ_v = 0.465 in the present case.

Then D is found as $16.5/2.4\ 10^{-3} = 6875\ cm^2.\ d^{-1}$, and the time-interval should be smaller than $1.633^2/6875 = 3.8788\ 10^{-4} \simeq 4\ 10^{-4}$ day. This value is seen to be a factor two higher as compared to the time-constant in case of the sub-model for oxygen flow, reason why this sub-model does not oscillate at a DELT of $2\ 10^4$ day, Fig. 19.

It is concluded that DELT = 10^{-4} day is a good choise for the time-interval of integration of the model.

5. Evaluation of the model

5.1 General

According to van Keulen (1974), proper evaluation of models should consist of two distinct phases: calibration and validation. In the calibration procedure, a set of data is used to calibrate, within reasonable limits, weak or unknown parameters or relations, to obtain the best overall agreement between simulated and observed results. For validation other completely independent sets of data must be used to show that the model yields correct results under different conditions.
Due to lack of data the model "ANAEROBIC SOIL VOLUME" will be hard to calibrate and validate.

Another evaluation technique is sensitivity analysis, which is most conveniently described as: a test on the relative influence of changes in input data and parameters on the relevant output of models (van Keulen, 1974).
Some simulation experiments are carried out in which a range of input data or parameter values and the output values are compared. This procedure is most helpful when it must be decided which subsystem should receive most attention; relations with the strongest impact on the final results should be studied with high priority, while those showing only little influence, may first be left alone.

5.2 Sensitivity analysis

The influence of the value of different parameters, as discussed in chapter 4.5, on the results of the simulations was tested by comparing the simulated results of the subsequent runs, in which one parameter or function was changed at a time, with those of the so-called basic run (Run no. 1). The schedule of reruns is presented in Table 6.
The results are given in Figs. 20 to 33, and will be discussed below.

5.2.1 General features

In Figs. 20-29 the fractional anaerobic volume of the soil (FANVOL), expressed as a percentage, is plotted against time for different values of the relevant parameters.
The graduated scales in all cases are the same, but the origin of the abscissa is sometimes shifted to higher values than zero. In each figure three soil

Table 6. The schedule of reruns.

RUN No. / PARAMETER	1	2	3	4	5	6	7	8	9	10	11	12
GRWTAB	100	100	50	100	100	100	100	100	100	100	100	100
RAIN INT/DUR	9/3	9/3	9/3	9/3	9/6	9/3	9/3	9/3	9/3	4.5/12	9/2-2-2	9/3
KTB	G&C[+]	G&C	G&C	S	G&C	G&C	G&C	G&C	G&C	G&C	G&C	G&C
CWT	0.3	0.3	0.3	0.3	0.3	0.3	0.3	0.9	0.3	0.3	0.3	0.3
COT*10^3	1.3089	3.4904	1.3089	1.3089	1.3089	1.3089	1.3089	1.3089	1.3089	1.3089	1.3089	1.3089[*]
CCO*10^8	2.24	2.24	2.24	2.24	2.24	22.4	2.24	2.24	2.24	2.24	2.24	2.24
DCSPH*10	1.2715	1.2715	1.2715	1.2715	1.2715	1.2715	0.63575	1.2715	1.2715	1.2715	1.2715	1.2715
DEFAC(1)	M&S	M&S	M&S	M&S	M&S	M&S	M&S	M&S	B&H	M&S	M&S	M&S

[+]G&C: according Green & Corey (1971); S: according Stroosnijder (1976); M&S: according Millington & Shearer (1971); B&H: according Bakker & Hidding (1970; $D / D_o = 2\ \varepsilon_g^3$).

[*]50% of aggregates respire, while total oxygen consumption equals the one in the basic run, no. 1.

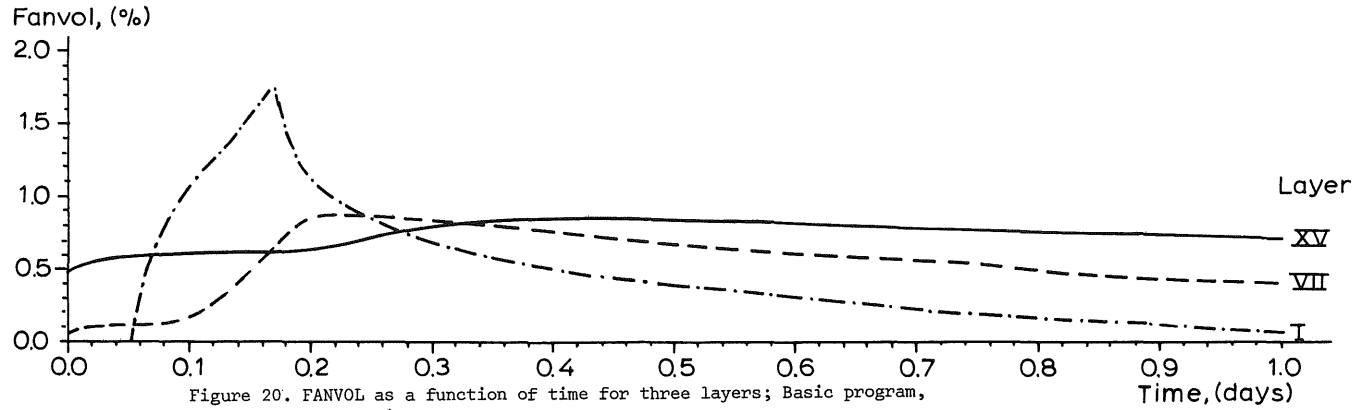

Figure 20. FANVOL as a function of time for three layers; Basic program, run no. 1.

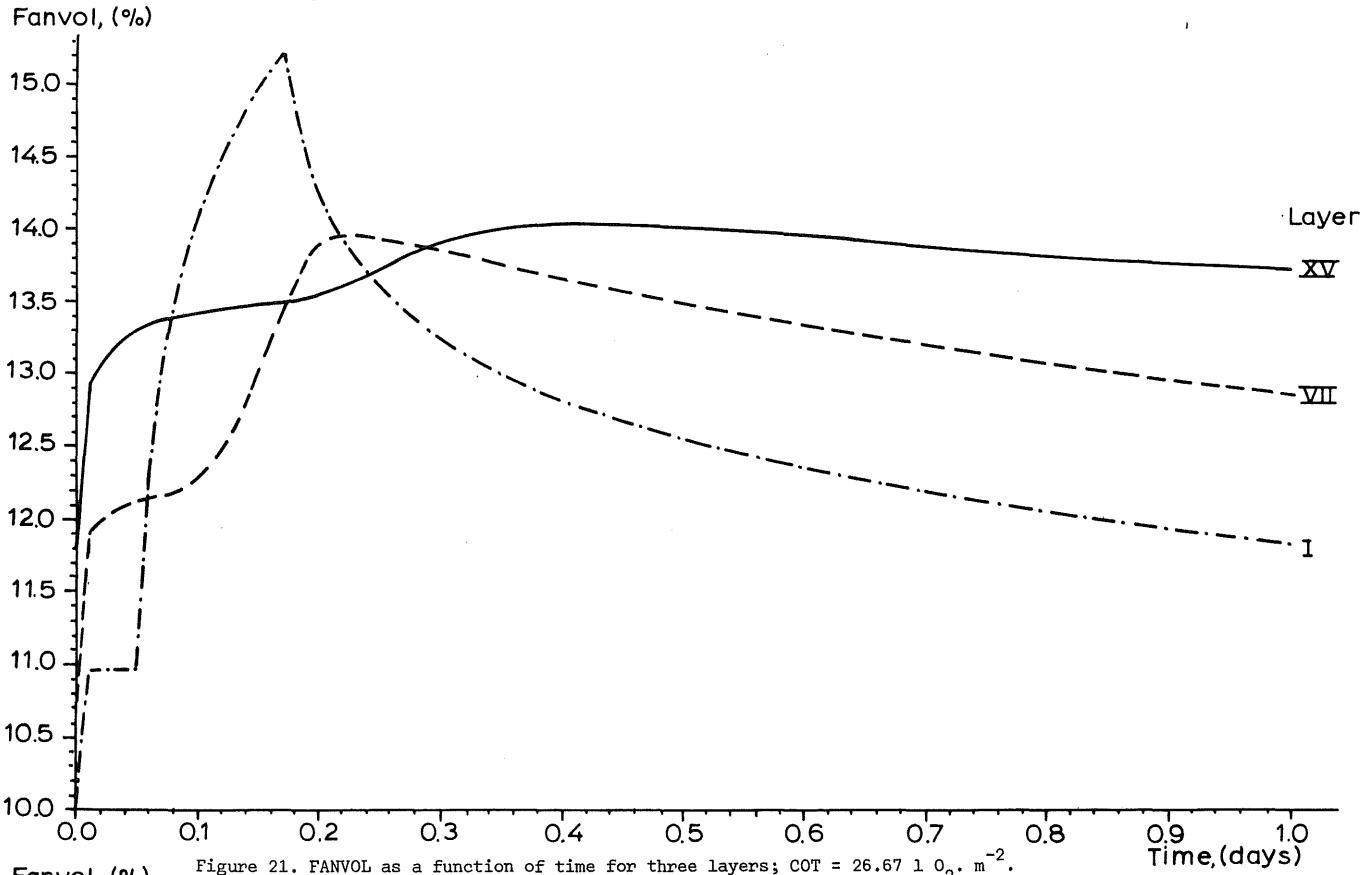

Figure 21. FANVOL as a function of time for three layers; COT = 26.67 l O_2. m^{-2}. $DEPTHT^{-1}$. d^{-1}, run no. 2.

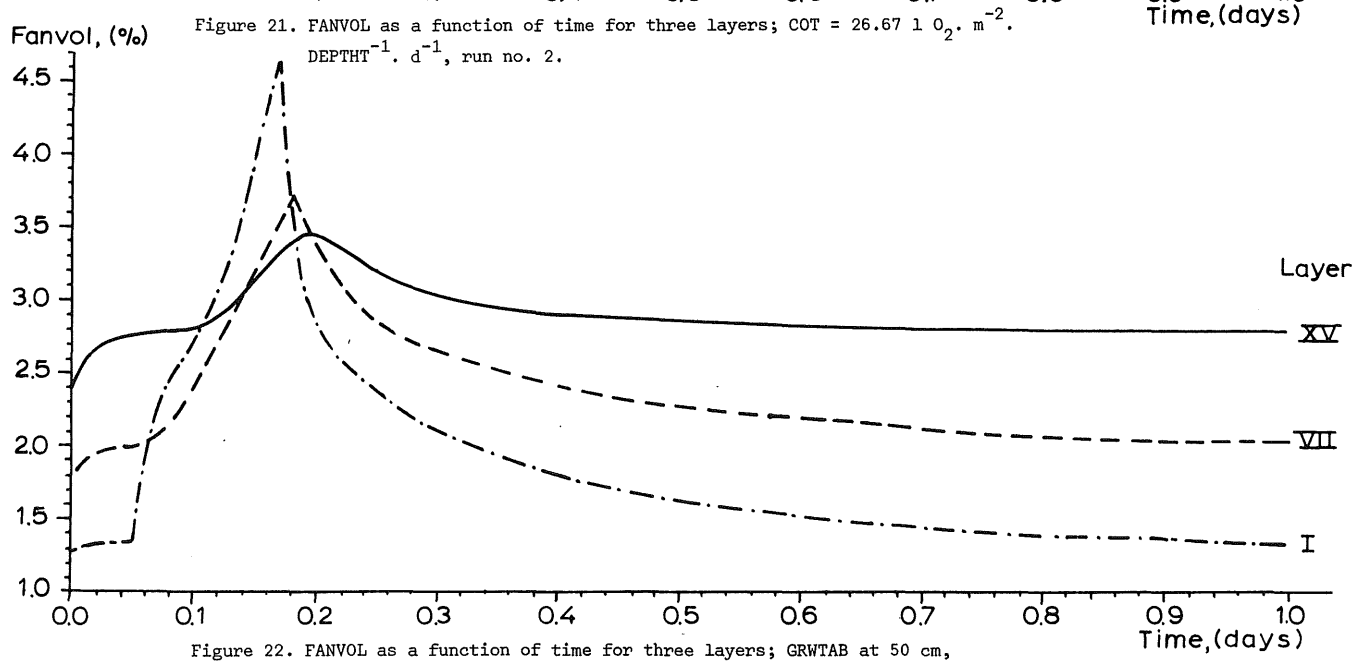

Figure 22. FANVOL as a function of time for three layers; GRWTAB at 50 cm, run no. 3.

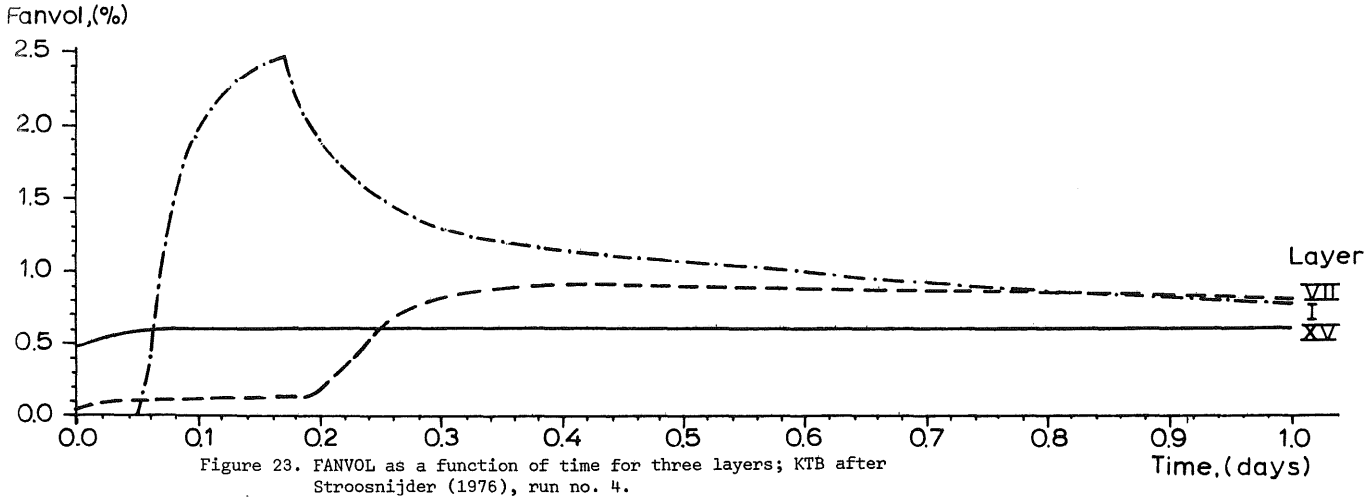

Figure 23. FANVOL as a function of time for three layers; KTB after Stroosnijder (1976), run no. 4.

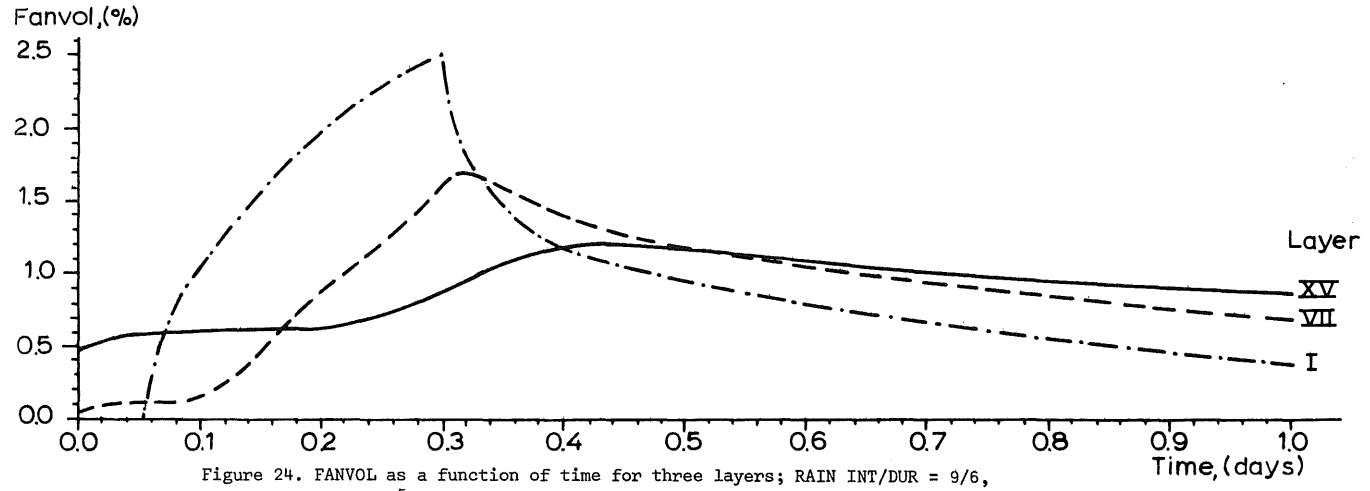

Figure 24. FANVOL as a function of time for three layers; RAIN INT/DUR = 9/6, run no. 5.

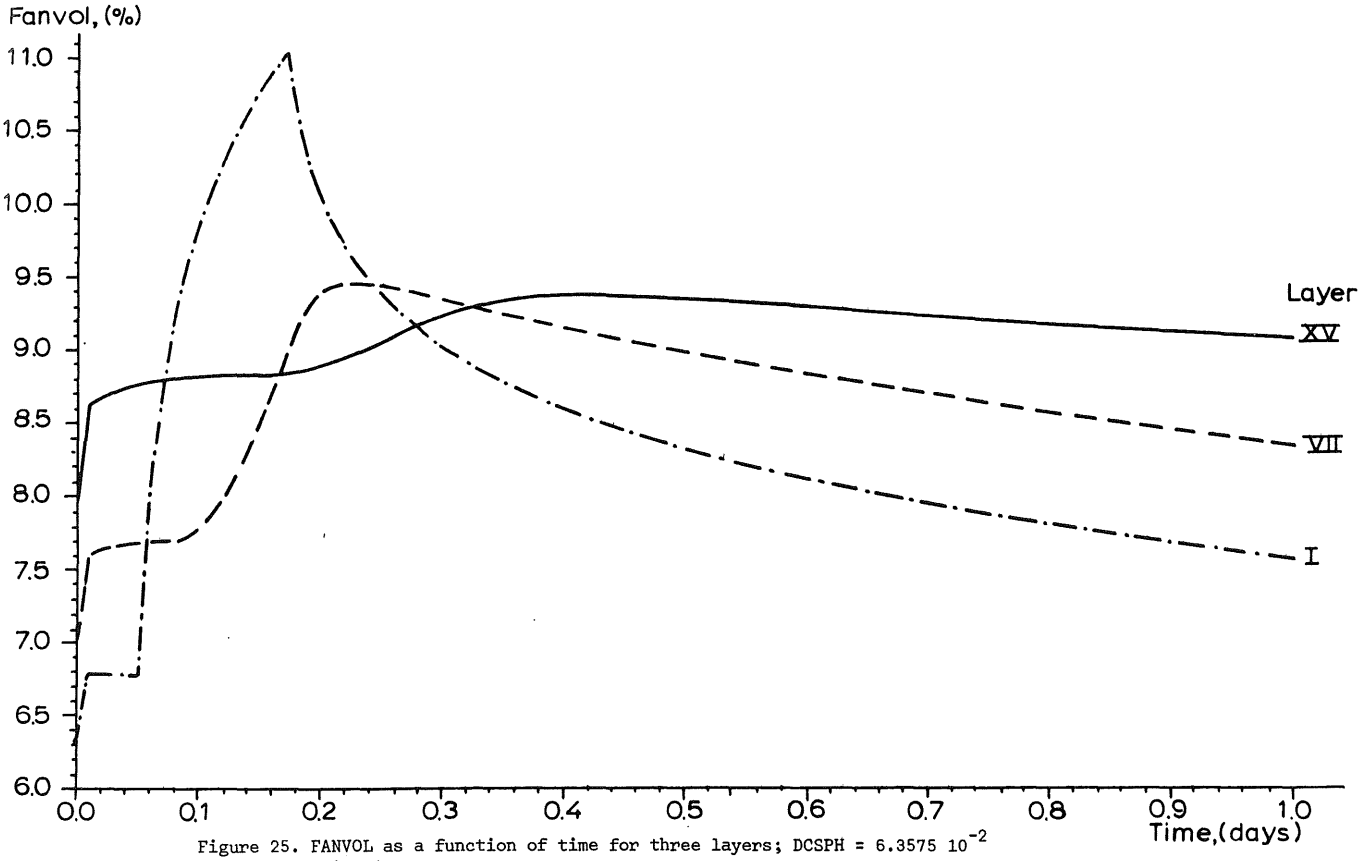

Figure 25. FANVOL as a function of time for three layers; DCSPH = 6.3575 10^{-2} $cm^2.d^{-1}$, run no. 7.

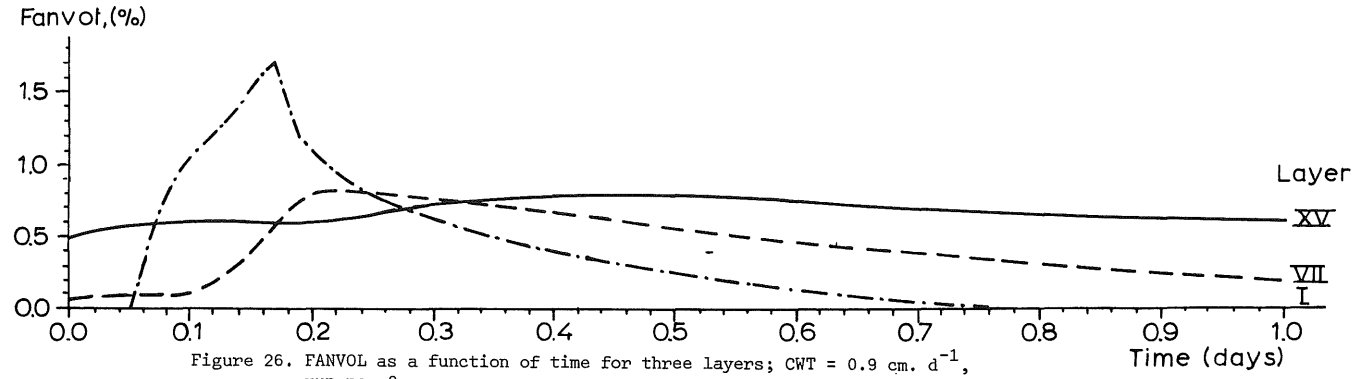

Figure 26. FANVOL as a function of time for three layers; CWT = 0.9 cm. d^{-1}, run no. 8.

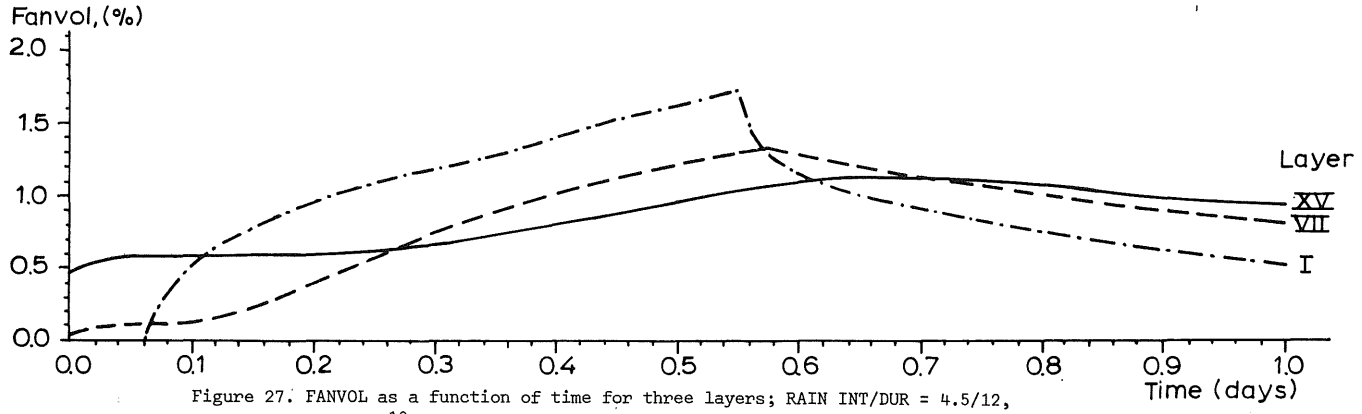

Figure 27. FANVOL as a function of time for three layers; RAIN INT/DUR = 4.5/12, run no. 10.

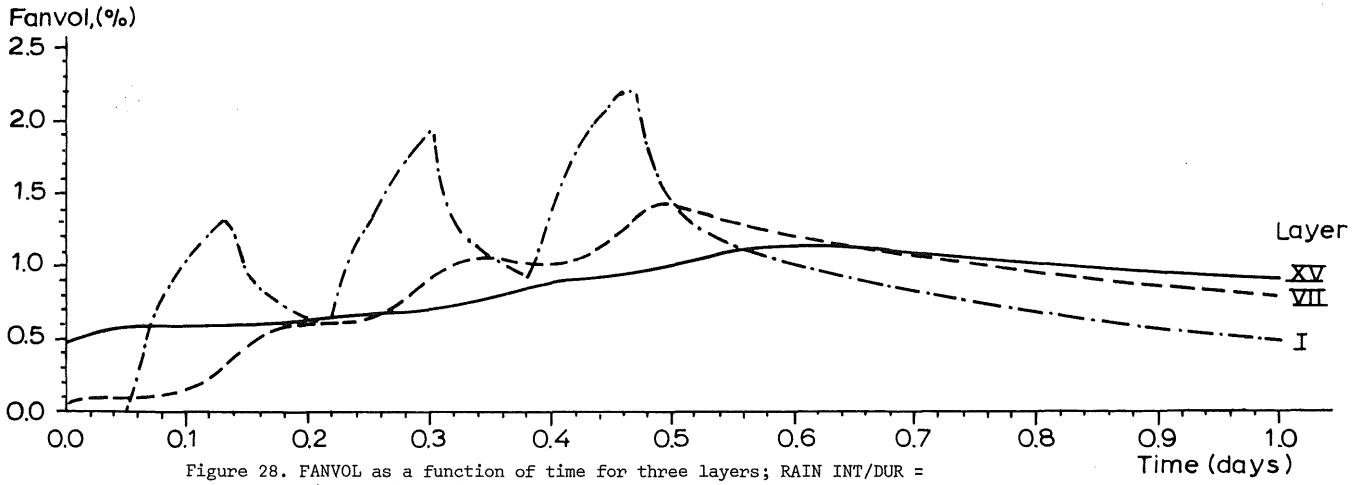

Figure 28. FANVOL as a function of time for three layers; RAIN INT/DUR = 9/2-2-2, intermittent, run no. 11.

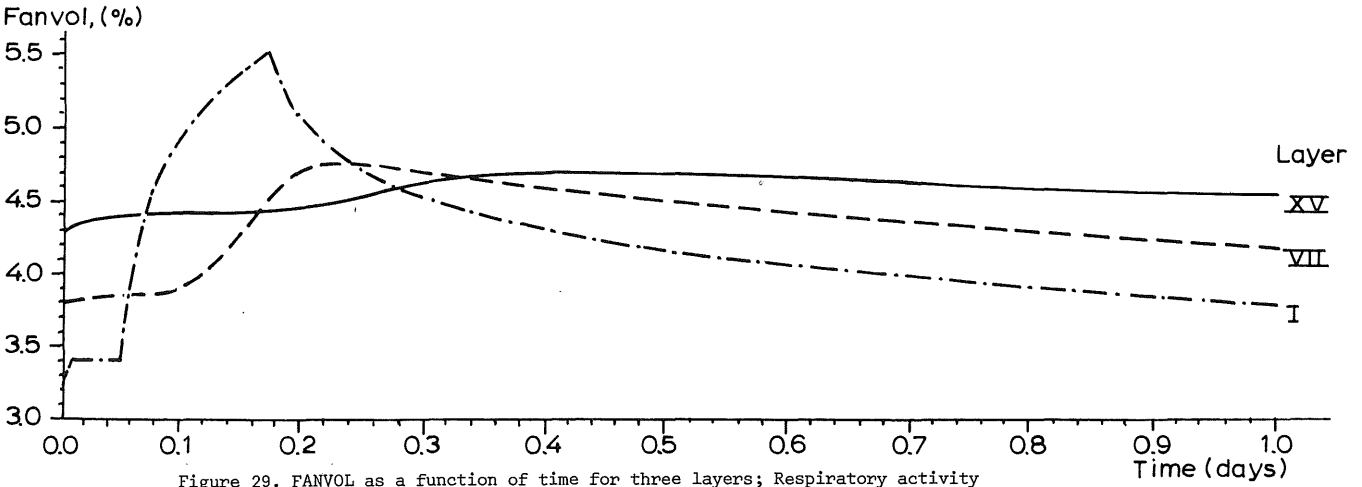

Figure 29. FANVOL as a function of time for three layers; Respiratory activity non-homogeneously distributed, run no. 12.

layers are presented; layer 1, 7, and 15. Layer 1 and 15 represent the two extremes of FANVOL in the soils, while layer 7 shows an intermediate situation. The results of the simulation runs no. 6 and no. 9 were within 0.5 and 2.5% of the results of the basic run. Therefore they are not presented in separate figures.

It is seen that at the onset of the simulations some time is needed to adjust FANVOL to its right initial value. This delay is somewhat longer for run no. 2, layer 7 and 15, where no two successive values of FANVOL are equal, indicating that probably equilibrium was not reached, when the calculations started. In view of this adaptation time, the shower always started after 0.05 day, that is after 500 integrations.

The abrupt increase of FANVOL in layer 1 under the different conditions indicates the onset of rain. Similarly, the abrubt decrease of FANVOL in this layer points to the end of the rain.

At the start and at the end of the simulation the values of FANVOL in layer 1 are found to be the lowest, followed by layer no. 7 and no. 15, except in run no. 4, where this sequence is 15, 1, and 7 at the end of the simulation. The initial value of FANVOL was not reached at the end of one day, except in simulation run no. 2, and no. 8 for layers 1 and 15. The same was the case with the relative water content of the soil layers.

All figures show soil layer no 1 to react stronger to the changing weather than the deeper soil layers; the total change in FANVOL as well as the maximum FANVOL reached are greater. This indicates that even the soil surface can easily be a potential place for denitrification, assuming that no other constraints prevail; anaerobic conditions are reached very quickly after the onset of a shower. The deeper soil layers lag behind in time as compared to the upper layer, as demonstrated by the fact that their maximum anaerobic volume is reached later. In fact, these maxima are reached after the rain has stopped. These deeper layers, however, are always partially anaerobic, even when it does not rain.

The increase in anaerobic soil volume after the onset of a shower proceeds faster than its decrease after rain has ceased. This is expressed by the skew curve around the maximum values of FANVOL reached in each case. It indicates that after a short rain there may be anaerobiosis in the soil profile for quite some time.

The maximum decrease in oxygen concentration in the simulations amounted to 1.106%, calculated for simulation run no 2, layer 15, at time 0.2 day. This result was expected because of the high air-filled porosity in the soil model.

5.2.2 Comparison of the results of the reruns with the results of the basic simulation run

Two categories of tested parameters can be distinguished in the schedule of reruns, (Table 6). There are four parameters influencing the moisture regime of the soil (GRWTAB, RAIN, KTB, CWT), and another four which influence the oxygen status of the soil (COT, CCO, DCSPH, DEFAC(1)). In the discussion these categories will be treated as two separate groups, though this is not the same sequence in which the results of the simulation runs are presented in the figures.

5.2.2.1 The influence of the moisture regime on FANVOL

The ground water level, GRWTAB, run no. 3, Fig. 22

Consider the Figs. 22 and 20. The initial anaerobic soil volume in all soil layers in Fig. 22 is higher than in Fig. 20. Even the top layer in Fig. 22, has an anaerobic volume of 1.33% at the onset of the simulation.
When rain starts the anaerobic soil volume in run 3 increases faster than in run no. 1; d(FANVOL)/dt being 27.49 and 14.55, respectively. The maximum value of FANVOL increases by factors of 2.65, 4.23, and 4.10 for the layers 1, 7, and 15, respectively. The relative water contents were 15, 31 and 32% higher.
A sharper decrease in FANVOL, after rain ceases is found in run no. 3, too; within one day the initial anaerobic conditions are reached again.

It may be concluded that when the depth of the ground water table is changed from one meter to 50 cm, anaerobiosis increases by more than their ratio. This implies for instance that in most of the Dutch grassland area, where high ground water tables prevail during the greater part of the year, anaerobic conditions may occur.

The rain intensity, duration and distribution, RAIN INT/DUR, runs no. 5, 10, and 11, Figs. 24, 27, and 28

Compare Figs. 24 and 20. The initial conditions in both cases are similar, of course. The rain duration was doubled in this simulation run to 6 hours, while its intensity remained the same (9 cm. d^{-1}). The rate of increase in FANVOL in the second half of these 6 hours is less than the first 3 hours; with d(FANVOL)/dt= 5.88 and 14.55, respectively. This is also expressed by the

maximum value of FANVOL reached in the different layers. Expressing these maxima as a fraction of run no. 1, as before, 1.44, 1.94, and 1.42 were calculated for the layers 1, 7, and 15, respectively.

Though rain duration in itself thus has a minor impact on the anaerobic soil volume as compared to for instance a higher groundwater table, it takes longer for the profile to return to its initial values of FANVOL, Fig. 24, at time 1.

The influence of a change in rain intensity from 9 to 4.5 cm. d^{-1} is shown in Figs. 27 and 24. As rain duration was doubled to 12 hours, the total precipitation equalled 2.25 cm in both cases.
The maximum value of FANVOL reached at a low rain intensity is less than that at a high rain intensity, 1.72 and 2.51%, respectively for layer 1. In fact, layer 1 of run 10 reaches about the same maximum FANVOL as layer 1 under a rain intensity of 9 cm. d^{-1}, which lasted only 3 hours, (Fig. 20). The maximum FANVOL of the deeper soil layers is affected more by a longer rain duration as compared to run no. 1, Fig. 20.

It is concluded that a higher rain intensity causes FANVOL to increase more than a longer rain duration, on the condition that total precipitation is equal. The total fractional anaerobic volume in the soil as a whole, however, does not change much. This is explained by the fact that in both simulation runs, the total amount of oxygen consumed in the course of a day, expressed as a percentage of the maximum oxygen consumption possible, COT, was 96.36 and 96.31% for simulation runs no. 10 and 5, respectively. These values denote that the average FANVOL during the day was 3.64 and 3.69%, respectively.

In simulation run no. 11 the rain intensity equalled 9 cm. d^{-1}, but it was given intermittently by alternating 2 hour periods of rain and dry weather, as shown in Eq. (78):

```
FUNCTION RAINTB = (0.,0.),(.05,0.),(.051,9.),(.1333,9.),(.1343,0.),
(.2176,0.),(.2186,9.),(.3009,9.),(.3019,0.),(.3852,0.),(.3873,9.),
(.4686,9.),(.4696,0.),(100.,0.)                                    (78)
```

The total amount of precipitation amounted to 2.25 cm as before in simulation run no. 5.
Figure 28 demonstrates that the conditions in the top soil layer follow the onset and the end of the showers exactly. In the deeper soil layers this effect is

smoothened out. In layers deeper than layer 7 there is no drop in FANVOL in the periods without rain, resulting in nearly the same maximum percentage of FANVOL for layer 15, e.g. 1.131 and 1.197% for simulation run no. 11 and 5, respectively.
The average value of FANVOL in the course of the day, however, amounted to 3.66%, which is just in between of the values given above.

The conductivity of the soil for water, KTB, run no. 4, Fig. 23.

In simulation run no. 4 the conductivity curve calculated according to Green & Corey (1971) was replaced by a conductivity curve given by Stroosnijder (1976), for the same sandy loam soil as used in this study. The values used were read from his Fig. 26i, page 87, and given below:

```
FUNCTION KTB = (.1933,.0001),(.2208,.0015),(.2625,.01),(.3,.037),
(.359,.15),(.4002,.82),(.4305,4.2),(.5165,16.5)                    (79)
```

This function was probably calculated by an empirical equation advanced by Rijtema (1969), yielding lower values for the hydraulic conductivity of the soil. Therefore, (Figs. 20 and 23) the average rate of increase in FANVOL over the rainy period is higher when compared to simulation run no. 1, for layer 1; d(FANVOL)/dt = 20.64 and 14.55, respectively.
On the other hand, due to this low water conductivity, FANVOL in layer 15 was not affected up to at least 20 hours after rain had ceased. Also the moisture content of this layer hardly changed in that period; there was only a slight decrease due to the water consumption by the roots, CWT.

The return of the anaerobic soil volume to its original value took longer in case of run no. 4, expressed by the higher percentage at the end of the day as compared to simulation run no. 1; 0.758, 0.798, and 0.050, 0.395 for layers 1 and 7, respectively.

It may be concluded that the moisture characteristics of the soil profile are important, but, as in the discussion about rain duration, it seems to have less influence on the anaerobic soil fraction than a changing ground water table. The spatial distribution of the water within the profile as a whole and within eventual aggregates in particular will be more important. This distribution will, however, be linked to soil conductivity for water. Some remarks about this subject will be made in the following chapter.

The water consumption by the roots, CWT, run no. 8, Fig. 26.

The consumption rate of water by roots was set at 0.9 cm. d^{-1} in run no. 8. This value is high for the Netherlands, but even than the influence of this consumption rate on FANVOL is only of minor importance, (Fig. 26). All values of the anaerobic soil volume are diminished slightly. In the long run, without precipitation, this factor could play a role, but that situation is rather unlikely.

In conclusion little attention seems necessary for this parameter. A deviation from the picture presented in Fig. 26, especially for the upper soil layers, would be introduced when soil-evaporation was to be included in the model.

5.2.2.2 The influence of the oxygen regime on FANVOL

The oxygen consumption rate, COT, run no. 2, Fig. 21.

Up till now the maximum anaerobic soil fraction reported did not rise above 4.6%. In simulation run no. 2, (Fig. 21), this maximum value is roughly quadrupled in case of layer 1.
Initially in the upper layer an anaerobic soil fraction of more than 10.9% is found, whereas the deeper soil layers no. 7 and 15 show values of about 12.1 and 13.3%, respectively. The average rate of increase of FANVOL during the rain amounts to 35.25, which value is nearly the same as in case of simulation run no. 7, where the diffusion coefficient of the aggregates was halved. The maximum FANVOL in run no. 2, expressed as a fraction of run no. 1, yields a factor 8.7, though only a 2.6-fold increase of the consumption rate was effectuated.

It may be concluded therefore that the model is very sensitive to changes in respiratory activity. Hence it is suggested, that much attention should be paid to this soil property.

The diffusion coefficient in an aggregate, DCSPH, run no. 7, Fig. 25.

The results of run no. 7, where the diffusion coefficient of the aggregates was halved, are very similar to those of run no. 2. This results might have been expected as both parameters appear in one and the same equation, (Eq. (41)).
The change in the value of the diffusion coefficient has been introduced because of the possibility of the presence of slickensides on the aggregates. These skins probably can seriously impair oxygen diffusion from the inter-aggregate

pores into the aggregates, as shown by the results of the model.
The initial anaerobic soil volume is somewhat lower than in simulation run no. 2, but there the oxygen consumption rate was higher by a factor 2.6 instead of a factor 2 as is the case here.

It is suggested that the diffusional processes through the surfaces of different structural units in soils should be subject to investigation because of the results presented in Fig. 25.

The distribution of the respiratory activity in the soil, run no. 12, Fig. 29.

Consider the Figs. 29 and 20. In simulation run no. 12 the total respiration is restricted to 50% of the aggregates and equalled again 10 l O_2. m^{-2}. DEPTHT^{-1}. d^{-1}. This condition was introduced by replacing Eqs. (36) and (44) in the basic model by:

```
CROCVS(I)=2.*CROC(I)*(VOLHEX/TOTVOL)/TCOM                    (80)
```

and

```
VOLAN1(I)=FVLAN1(I)*3.*V1                                    (81)

VOLAN2(I)=FVLAN2(I)*3.*V2                                    (82)

VOLAN3(I)=FVLAN3(I)*6.*V3                                    (83)
```

Initially an anaerobic soil fraction of about 3.4% is found in the upper layer, whereas in the deeper soil layers this value amounts to 3.8 and 4.9%, respectively.
The average rate of increase of FANVOL in layer 1 during the rain is calculated to be 17.68, which value is somewhat higher than was found in the basic run (14.55).
The maximum FANVOL, expressed as a fraction of run no. 1, equals 3.16. This value implies a strong non-linearity between FANVOL and total respiratory activity of the soil and it is concluded therefore that the spatial distribution of this soil property is of primary importance for the degree of anaerobiosis to be expected.

The critical oxygen concentration, CCO, run no. 6, and crustformation, DEFAC(1), run no. 9.

The critical oxygen concentration at which effective anaerobic conditions occur, is a property pertaining to microorganisms. Besides the value found in literature, which was used in most simulation runs, a value 10 times higher was used. The results of the simulation run with that high value of CCO, however, were so close to the one of run no. 1, that they are not presented.

From the point of view of anaerobiosis, the exact value of CCO seems unimportant therefore.

A surface crust could impair oxygen diffusion into the profile. Therefore, an empirical equation, introduced by Bakker & Hidding (1970) was included in simulation run no. 9, by replacing Eq. (65) by:

```
FLO=2.*DZERO*((PVOL-WC(1))**3)*(COUT-CO(1))/(.5*TCOM)          (84)
```

At an initial moisture content of 0.261883 $cm^3 . cm^{-3}$, and thus a gas-filled porosity of 0.3932, the diffusion coefficients in layer 1 can be calculated to be 2808.6 and 2374.3 $cm^2 . d^{-1}$ respectively, according to the method of Millington & Shearer (1971) (Eq. (16)) and the one of Bakker & Hidding (1970) (Eq. (84)). The results of the simulation run no. 12, with lower values of the macro diffusion coefficient for soil layer 1, were hardly different from the basic simulation run. This result is in accordance with the findings by van Bavel (1951), who stated that a relative shallow surface crust is not consequentional for the aeration status of the soil. At the other hand Bakker & Hidding (1970) concluded that the structure of the surface of the soil may become an extremely important factor for the aeration of soil.

It does not seem possible to draw any definite conclusions from the evidence at hand.

In the course of the work, it became evident that the relative water content probably could be correlated to the anaerobic soil fraction. This assumption was based on two indications. First, the maximum FANVOL reached in all reruns coincided with the maximum relative water contents in the layers. Secondly, the concentration of the oxygen in the profile never dropped by more than 1.106%. Figures 30 en 31 demonstrate that this correlation indeed exists. Except for

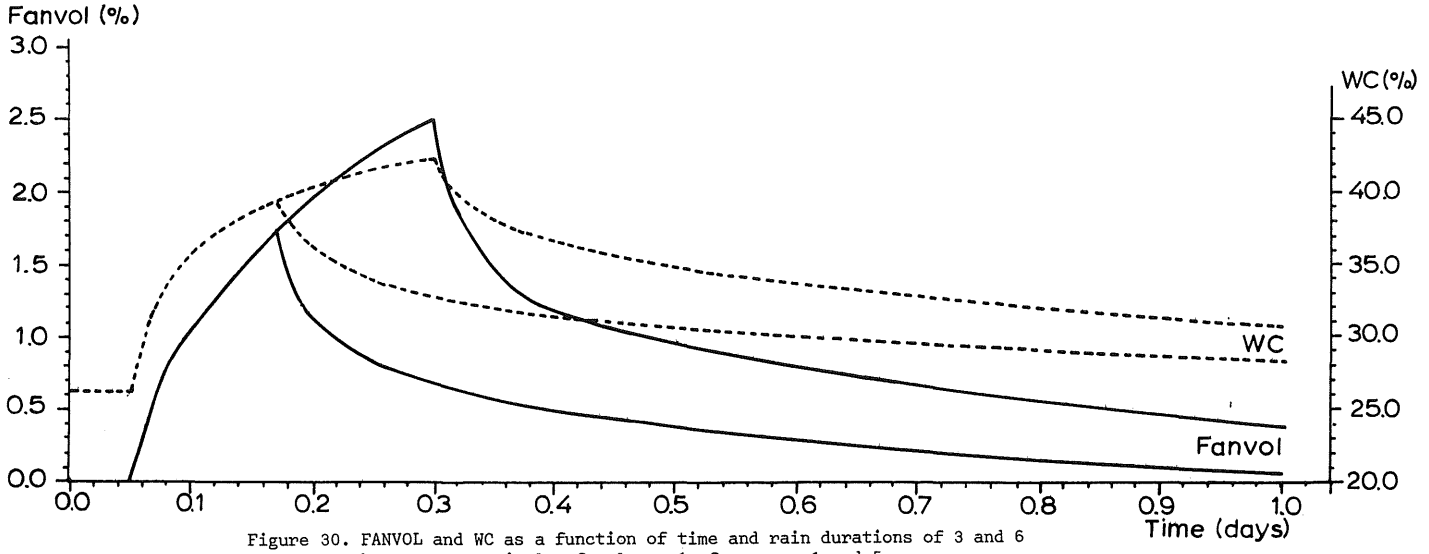

Figure 30. FANVOL and WC as a function of time and rain durations of 3 and 6 hours, respectively, for layer 1 of run no. 1 and 5.

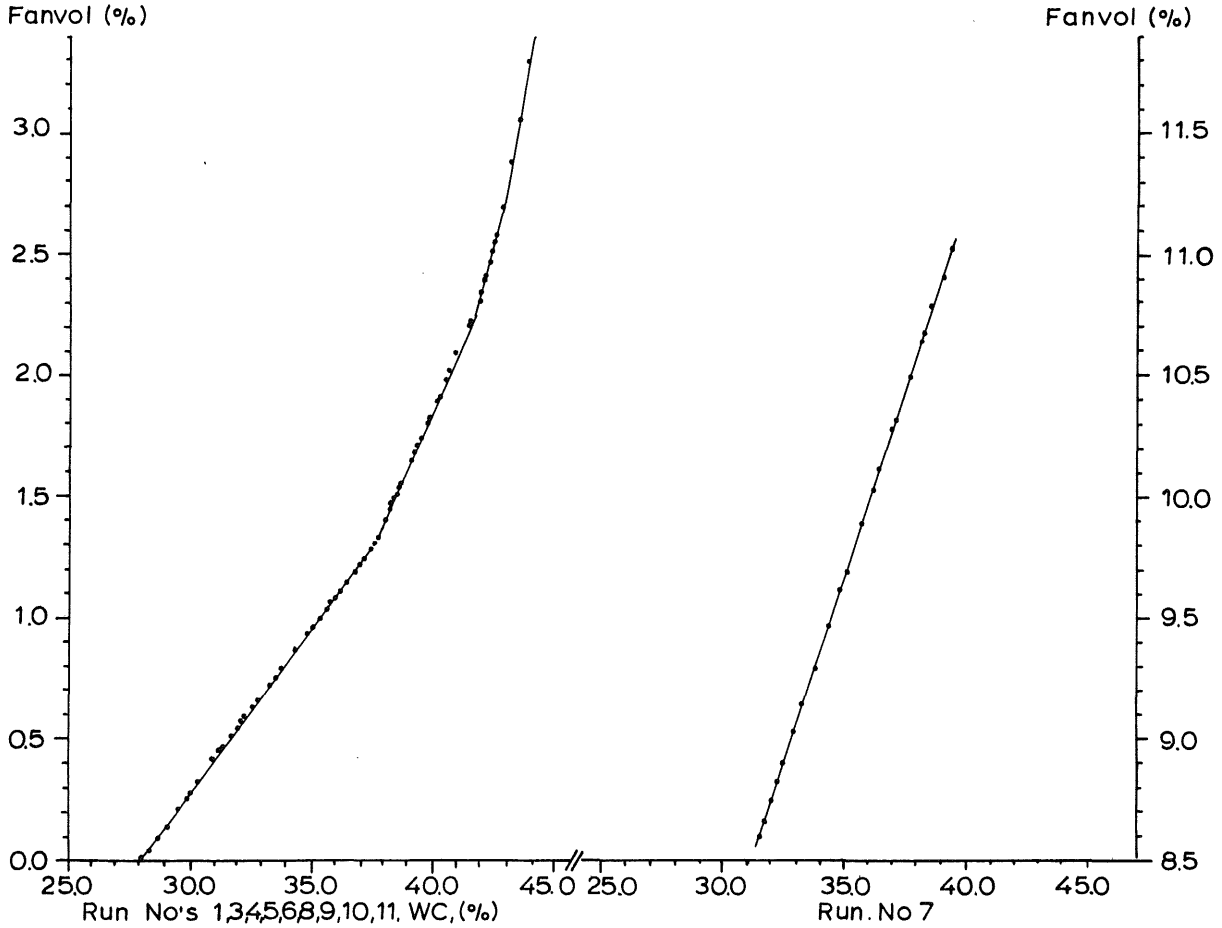

Figure 31. The relation between FANVOL and WC for different runs, layer 1.

run no. 7 and no. 2 all runs could be plotted in one figure, thus composing a line being discontinuous in the points of relative water content of 37.5, 41.8, and 43.0%.

To reduce computation time it might be worthwhile to investigate the possibility of replacing the sub-model, which calculates the anaerobic soil volume, by simple regression equations or a tabulated function. It should not lost sight of, however, that the sub-model, calculating the macro diffusion process, will be a limiting factor when it comes to the time constant of the model, see chapter 4.6.

The sensitivity of the anaerobic soil fraction with respect to the parameters in the model, can be summarized shortly, by expressing the results of each simulation rerun as a fraction of the results of the basic run, in the course of time. This has been done in Figs. 32 and 33 for layers no 1 and 7, respectively. Naturally, the conclusions so far advanced, do not change, but this way of presenting the results once more clarifies the degree of sensitivity of the model to the different parameters.
When a curve is decreasing, it denotes that FANVOL in that rerun does not increase as fast as FANVOL in simulation run no. 1. An increasing value of $FANVOL_i/FANVOL_1$, in the course of time points to the opposite situation.

Last but not least, a calculation of curves relating the anaerobic soil fraction to suction, is presented for three inter-aggregate oxygen concentrations e.g. 21, 19, and 17%, Fig. 34.
It is seen that for a soil, containing aggregates of 1 cm. diameter, the critical suction range is from zero to a suction of 100 mbar, the latter value corresponding to field capacity.
Figure 34 demonstrates that the influence of the oxygen percentage at a certain FANVOL at low suction is not pronounced. At lower percentages of the fractional anaerobic soil volume the influence of the outside oxygen concentration increases.
Both findings point to the possibility that at low suctions the diffusion of oxygen through the partially water-filled aggregates is hampered by the large equivalent radii, whereas at the higher suctions the outside oxygen concentration has an edge over the influence of the equivalent radii, in determining the anaerobic soil fraction.

The curves of Fig. 34 might be called "soil anaerobiosity characteristics", in analogy to the term soil moisture characteristic, which was proposed by Childs (1940).

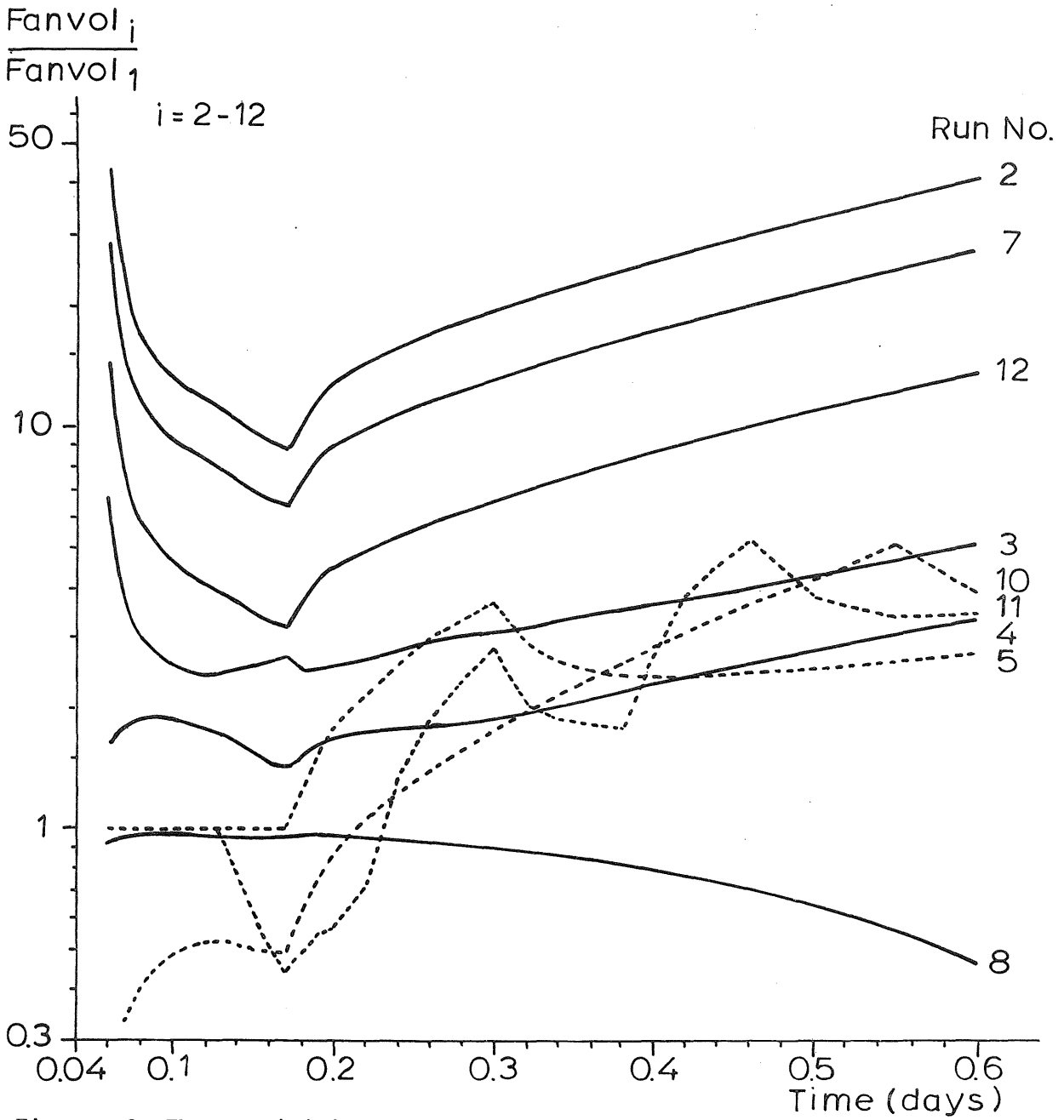

Figure 32. The sensitivity of FANVOL of run 2 to 12, expressed as fraction of run no. 1, in time, for layer 1.

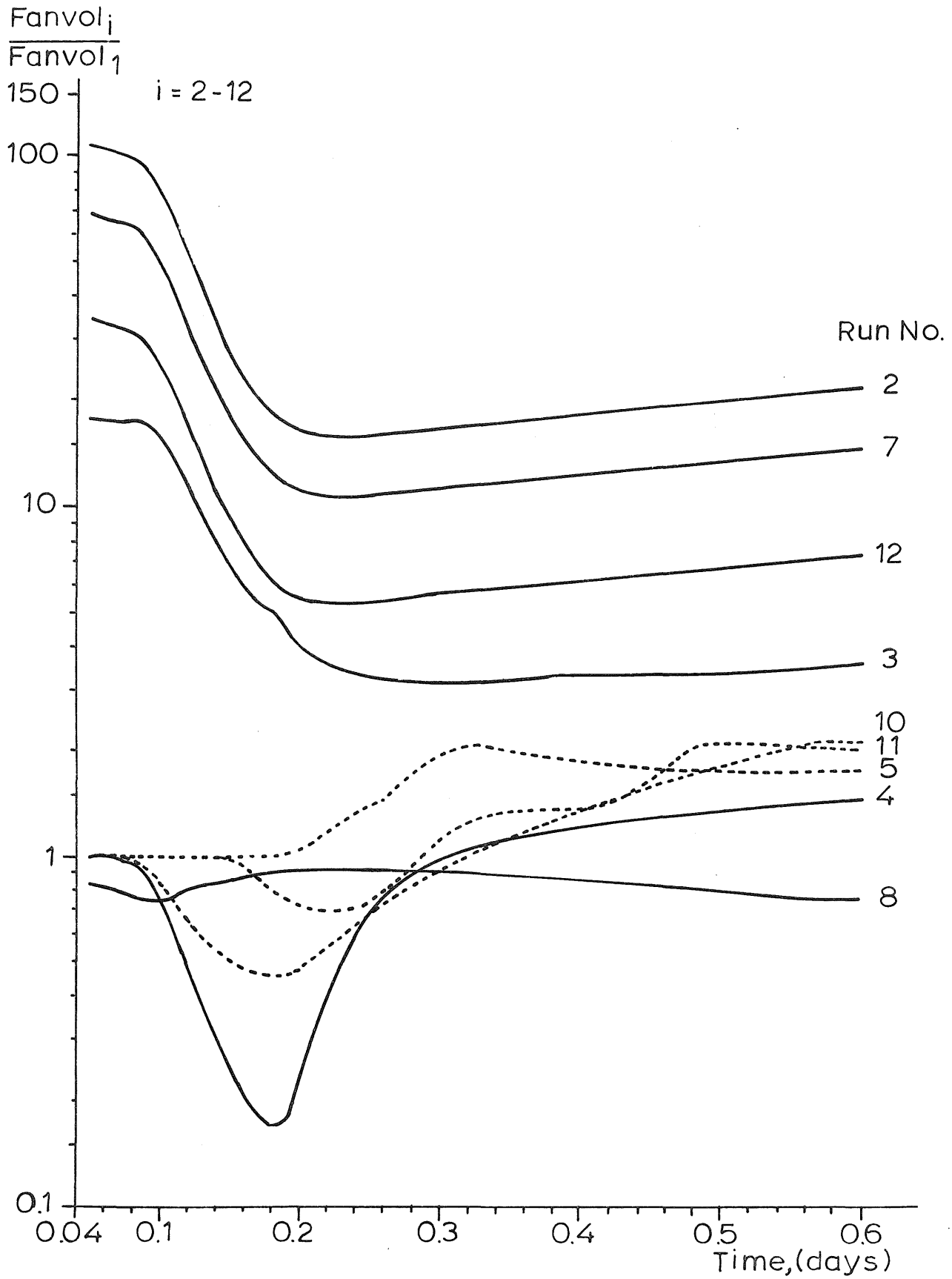

Figure 33. The sensitivity of FANVOL of run 2 to 12, expressed as a fraction of run no. 1, in time, for layer 7.

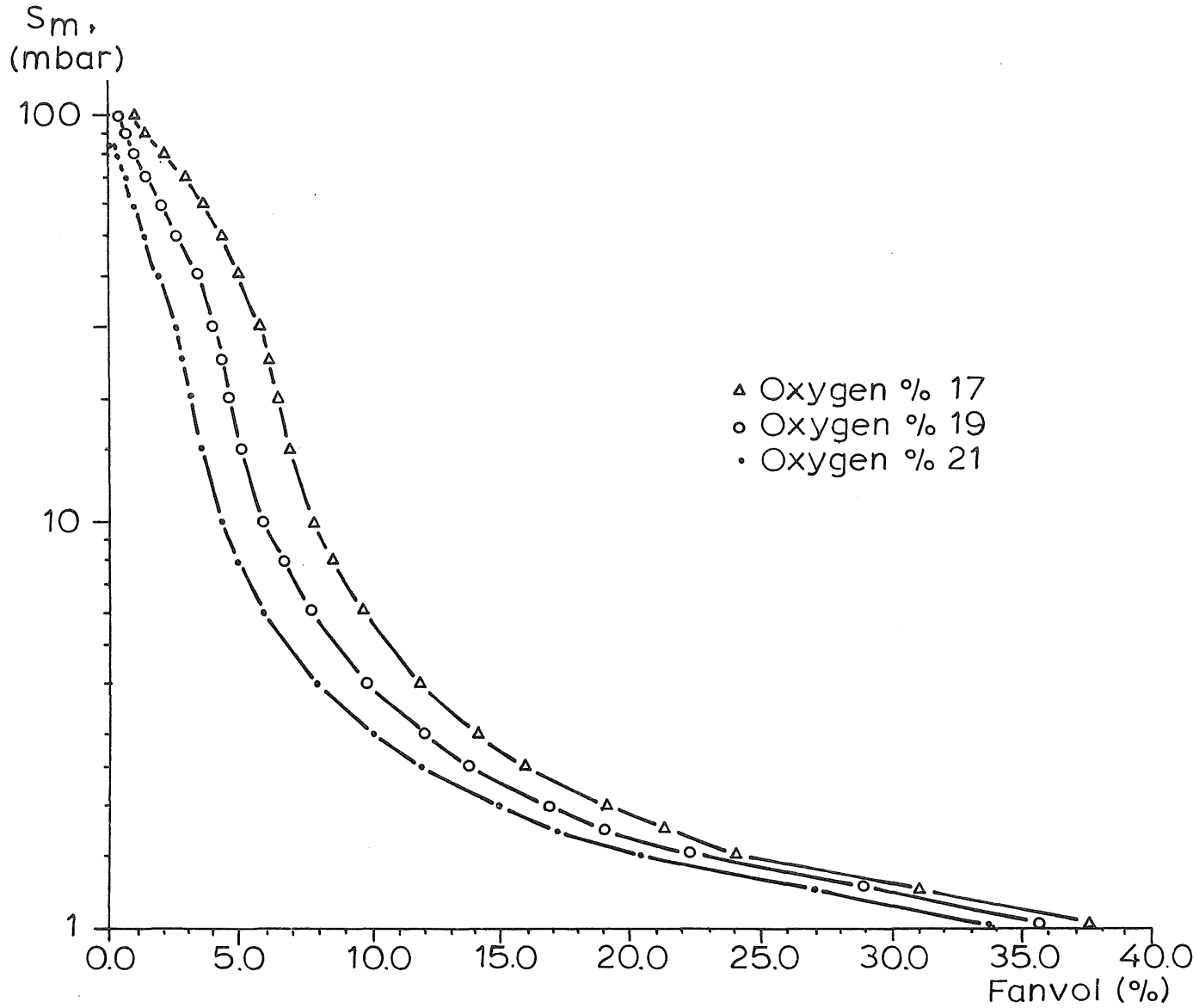

Figure 34. The relation between suction and FANVOL for three oxygen concentrations and aggregates of 1 cm diameter.

6. Some cautioning remarks

It seems unfeasible to criticize the work presented in the foregoing chapters in full detail, if only because of a sane self-conceit.
Attention should be paid to two basic problems, however: to what extent is it permitted to distinguish between inter- and intra-aggregate porosities?, and: what is the reliability of the soil moisture characteristic?

Pilot & Patrick (1972) investigated the effect of soil moisture tension on nitrate reduction in different soils. Soil samples were passed through a 2 mm. sieve before investigation, resulting in strongly disturbed soil structure. Air-filled porosities of less than 11 to 14 percent were found to induce denitrification, pointing to the onset of anaerobic conditions in the soil samples.
Possibly oxygen, entrapped by water-films between the soil particles was consumed, resulting in an anaerobic microsite, which points out that an entrapped air bubble in a soil void may act as an aggregate with a certain "equivalent radius".

On the other hand, soils having a well-developed structure, like clay soils, will be difficult to characterize with respect to this equivalent radius, too. Firstly, because of the possibility of swelling and shrinking, and secondly because larger structural elements may be composed of smaller units, which complicates the decision on aggregate size.

Obviously, it is of major importance to develop procedures to estimate an "equivalent radius" or rather a range of "equivalent radii" for different porous media, and in particular for field soils.

Usually when a soil is wetted, it will show at the same suction a lower moisture content than when water is extracted. This phenomenon is called hysteresis.
Usually a so-called boundary drying curve is determined, denoting that the soil moisture characteristic is determined by desaturating a previously completely saturated soil sample and weighing it at different know suctions.
The difference between a boundary drying curve and a boundary wetting curve can be appreciable, however, (Topp, 1969). This author worked on soil water hysteresis measured in a sandy loam soil. From his Fig. 2, it can be calculated that the maximum difference in moisture content between these two extremes, expressed

as a percentage of the boundary drying curve, amounts to 40%, at a suction of about 70 mbar.
The phenomenon of hysteresis implies that when rain is wetting a soil, the moisture content will be lower than would be calculated from the boundary drying curve, whereas the suctions are identical. The consequence for the anaerobic soil volume will be that it is smaller.
It also means that the soil moisture characteristic, which is considered very important, can not be determined very accurately, let alone the introduction of this phenomenon into the model.
Also the rhomboidal soil system was shown to posses hysteresis, Sewell & Watson (1965).

Emerson (1955) showed the process of water uptake by soil aggregates to be delayed quite some time. From his Fig. 2, it can be read that it takes about 6.6 and 17.2 days to absorb 90 and 97.5% of the total water taken up by a Grassland surface aggregate. Furthermore, from this Table 1 it can be calculated that the increase of the moisture content of these aggregates directly after applying a drop of water to initially dry samples, amounts to 63.6%, assuming a bulk density of 1.5 $g.cm^{-3}$. It may be argued that mainly the outer shell of an aggregate is directly wetted, possibly resulting in a closure of the pores for further oxygen diffusion. If this would be the case, it means that an air-bubble is enclosed, which possibly will vanish quickly, due to oxygen consumption within the aggregate, and that even at a lower water content of the aggregate anaerobiosis can prevail.

Obviously, the rate of water uptake by aggregates, as well as the distribution within the aggregates is of crucial importance to decide whether or not and to what extent anaerobiosis can occur.

7. Literature cited

Allison, F.E., J.N. Carter, and L.D. Sterling, 1960. The effect of partial pressure of oxygen on denitrification in soil. S.S.S.A. Proc., vol 24, no 4, pp. 283-285.

Azâroff, L.V., 1960. Introduction to solids. Mc.Graw-Hill Book Company Inc. New-York, Toronto, London. pp. 460.

Bakker, J.W., and A.P. Hidding, 1970. The influence of soil structure and air content on gas diffusion in soils. Neth. J. Agric. Sci., vol 18, pp. 37-48.

Bavel, C.H.M. van, 1951. A soil aeration theory based on diffusion. Soil Sci., vol 72, no. 1, pp. 33-46.

Bavel, C.H.M. van, 1952. A theory on the soil atmosphere in and around a hemisphere in which soil gases are used and released. S.S.S.A. Proc., vol 16, no. 2, pp. 150-153.

Bolt, G.H., A.R.P. Janse, and F.F.R. Koenings, 1970. Algemene bodemkunde, deel II, bodemnatuurkunde. Agric. Univ. Wageningen, the Netherlands, pp. 118.

Brakel, J. van, 1975. Capillary liquid transport in porous media. Ph. D. thesis. Univ. of Technology Delft. Pasmans - Den Haag, pp. 155.

Burington, R.S., 1973. Handbook of mathematical tables and formulas. McGraw - Hill Book Company. New York, pp. 500.

Carman, P.C., 1953. Properties of capillary-held liquids. J. Phys. Chem., vol 57, pp. 56-64.

Childs, E.C., 1940. The use of soil moisture characteristics in soil studies. Soil. Sci., vol 50, pp. 239-252.

Currie, J.A., 1960a. Gaseous diffusion in porous media. Part I. A non-steady state method. Brit. J. Appl. Phys., vol 11, pp. 314-317.

Currie, J.A., 1960b. Gaseous diffusion in porous media. Part II. Dry granular materials. Brit. J. Appl. Phys., vol 11, pp. 318-324.

Currie, J.A., 1961a. Gaseous diffusion in the aeration of aggregated soils. Soil Sci., vol 92, no. 1, pp. 40-45.

Currie, J.A., 1961b. Gaseous diffusion in porous media. Part III. Wet granular materials. Brit. J. Appl. Phys., vol 12, pp. 275-281.

Currie, J.A., 1965. Diffusion within soil microstructure, a structural parameter for soils. J. of Soil Sci., vol 16, no. 2, pp. 279-289.

Emerson, W.W., 1955. The rate of water uptake of soil crumbs at low suctions. J. of Soil Sci., vol 6, no. 1, pp. 147-159.

Emerson, W.W., 1959. The structure of soil crumbs. J. of Soil Sci., vol 10, no. 2, pp. 235-244.

Emerson, W.W., and M.G. Dettmann, 1959. The effect of organic matter on crumb structure. J. of Soil Sci., vol 10, no. 2, pp. 227-234.

Fisher, R.A., 1926. On the capillary forces in an ideal soil; correction of formulae given by W.B. Haines. J. Agric. Sci., vol 16, no. 3, pp. 492-505.

Flühler, H., M.S. Ardakani, T.E. Szuszkiewicz, and L.H. Stolzy, 1976a. Field--measured nitrous oxide concentrations, redox potentials, oxygen diffusion rates, and oxygen partial pressures in relation to denitrification. Soil Sci., vol 122, no. 2, pp. 107-114.

Flühler, H., L.H. Stolzy, and M.S. Ardakani, 1976b. A statistical approach to define soil aeration in respect to denitrification. Soil Sci., vol 122, no. 2, pp. 115-123.

Focht, D.D., 1974. The effect of temperature, pH, and aeration on the production of nitrous oxide and gaseous nitrogen - a zero-order kinetic model. Soil Sci., vol 118, no. 3, pp. 173-179.

Gardner, W.R., 1956. Representation of soil aggregate-size distribution by a logarithmic-normal distribution. S.S.S.A. Proc., vol 20, no. 2, pp. 151-153.

Garity, J.W. Mc., 1961. Denitrification studies on some south Australian soils. Plant and Soil, vol 14, no. 1, pp. 1-21.

Grable, A.R., 1966. Soil aeration. Adv. Agron., vol 18, pp. 57-106.

Greenwood, D.J., 1961. The effect of oxygen concentration on the decomposition of organic materials in soil. Plant and Soil, vol 14, no. 4, pp. 360-376.

Green, R.E., and J.C. Corey, 1971. Calculation of hydraulic conductivity: A further evaluation of some predictive methods. S.S.S.A. Proc., vol 35, no. 1, pp. 3-7.

Hagin, J., and A. Amberger, 1974. Contribution of fertilizers and manures to the N- and P-load of waters. A computer simulation. Final Rept. to the Deutsche Forschungs Gemeinschaft from Technion, Israel, pp. 123.

Haines, W.B., 1925a. Studies in the physical properties of soils. II. A note on the cohesion developed by capillary forces in an ideal soil. J. of Agric. Sci., vol 15, no. 4, pp. 529-535.

Haines, W.B., 1925b. Studies in the physical properties of soils. III. Observations on the electrical conductivity of soils. J. of Agric. Sci., vol 15, no. 4, pp. 536-543.

Haines, W.B., 1927. Studies in the physical properties of soils. IV. A further contribution to the theory of capillary phenomena in soil. J. of Agric. Sci., vol 27, no. 2, pp. 264-290.

Haines, W.B., 1930. Studies in the physical properties of soils. V. The hysteresis effect in capillary properties, and the modes of moisture distribution associated therewith. J. of Agric. Sci., vol 20, no. 1, pp. 97-116.

Keen, B.A., 1924. On the moisture relationships in an ideal soil. J. of Agric. Sci., vol 14, no. 2, pp. 170-177.

Keulen, H. van, 1974. Evaluation of models. Proc. of the first Int. Congress Ecology, the Hague, the Netherlands.

Keulen, H. van, and C.G.E.M. van Beek, 1971. Water movement in layered soils. Neth. J. Agric. Sci., vol 19, pp. 138-153.

Kessel, J.F. van, 1976. Factors affecting the denitrification rate in two water--sediment systems. Agric. Res. Rep. 858, Wageningen, the Netherlands, pp. 104.

Kruyer, S., 1958. The penetration of mercury and capillary condensation in packed spheres. Trans. Far. Soc., vol 54, pp. 1758-1767.

Lemon, E.R., 1977. Nitrous oxide (N_2O) exchange at the land surface. Report to the Kearney Foundation Workshop, Lake Arrowhead, Cal., U.S.A., pp. 28.

Lemon, E.R., and C.L. Wiegand, 1962. Soil aeration and plant root relations II. Root respiration. Agron. J., vol 54, pp. 171-175.

Marshall, T.J., 1958. A relation between permeability and size distribution of pores. J. of Soil Sci., vol 9, no. 1, pp. 1-8.

Millington, R.J., and R.C. Shearer, 1971. Diffusion in aggregated porous media. Soil Sci., vol 111, no. 6, pp. 372-378.

Pilot, L., and W.H. Patrick Jr., 1972. Nitrate reduction in soils: effect of soil moisture tension. Soil Sci., vol 114, pp. 312-316.

Rao, P.S.C., R.E. Green, L.R. Ahuja, and J.M. Davidson, 1976. Evaluation of a capillary bundle model for describing solute dispersion in aggregated soils. S.S.S.A. Proc., vol 40, no. 6, pp. 815-820.

Redlich, G.C., 1940. Determination of soil structure by microscopical investigation. Soil Sci., vol 50, pp. 3-13.

Rijtema, P.E., 1969. Soil moisture forecasting. Nota 513. I.C.W., Wageningen, the Netherlands.

Sewell, E.C., and E.W. Watson, 1965. Hysteresis in the moisture characteristics of ideal bodies. Bulletin R.I.L.E.M. (Reunion Internationale des Laboratoires d'Essais et de recherches sur les Materiaux et les constructions), vol 29, pp. 125-131.

Slichter, C.S., 1899. Theoretical investigation of the motion of ground waters. 19 th. Annual report U.S. Geol. Survey, part II, pp. 295-328.

Smith, K.A., 1977. Soil aeration. Soil Sci., vol 123, no. 5, pp. 284-291.

Smith, W.O., P.D. Foote, and P.F. Busang, 1931. Capillary rize in sands of uniform spherical grains. Physics, vol 1, pp. 18-26.

Stanford, G., R.A. van der Pol, and S. Dzienia, 1975a. Denitrification rates in relation to total and extractable soil carbon. S.S.S.A. Proc., vol 39, no. 2, pp. 284-289.

Stanford, G., S. Dzienia, and R.A. van der Pol, 1975b. Effect of temperature on denitrification rate in soils. S.S.S.A. Proc., vol 39, no. 5, pp. 867-870.

Stroosnijder, L., 1976. Infiltratie en herverdeling van water in grond. Pudoc, Wageningen, the Netherlands, pp. 213.

Tanji, K.K., and S.K. Gupta, 1977. Computer simulation modeling for nitrogen in irrigated croplands. Report to the Kearney Foundation Workshop, Lake Arrowhead. Cal., U.S.A., pp. 53.

Taylor, S.A., 1949. Oxygen diffusion in porous media as a measure of soil aeration. S.S.S.A. Proc., vol 14, no. 1, pp. 55-61.

Topp, G.C., 1969. Soil water hysteresis measured in a sandy loam and compared with the hysteresis domain model. S.S.S.A. Proc., vol 33, no. 5, pp. 645-651.

Veen, H. van, 1977. The behaviour of nitrogen in soil - a simulation study. Ph. D. thesis. Vrije Univ. Amsterdam, pp. 164.

Walker, T.H., 1956. Fate of labeled nitrate and ammonium nitrogen when applied to grass and clover grown separately and together. Soil Sci., vol 81, pp. 339-351.

Wilsdon, B.H., 1921. Studies in soil moisture, part I. Memoirs of the department of agriculture in India. Chemical Series, vol VI, no. 3, pp. 155-186.

Wit, C.T. de, and J. Goudriaan, 1974. Simulation of ecological processes. Pudoc, Wageningen, the Netherlands, pp. 159.

Wit, C.T. de, and H. van Keulen, 1975. Simulation of transport processes in soils. Pudoc, Wageningen, the Netherlands, pp. 100.

Woldendorp, J.W., 1963. The influence of living plants on denitrification. Ph. D. thesis, Wageningen, the Netherlands, pp. 100.

APPENDIX I

A. The cone volume

The volume V_c of the cone equals, (Burington, 1973):

$$V_c = \frac{1}{3} \pi (h_B + h_T) (R_B^2 + R_T^2 + R_B R_T) \quad (1)$$

where $R_B = \sqrt{R^2 - (R - h_B)^2}$

$R_t = \sqrt{R_x^2 - (R_x - h_T)^2}$

$h_B = R (1 - \cos \gamma)$

$h_T = R_x (1 - \cos \alpha)$

$h_B + h_T = (R + R_x) - R_x \cos \alpha - R \cos \gamma = R_x(1 - \cos \alpha) + R (1 + \cos(\alpha+\beta))$

R_B^2, R_T^2 and $R_B R_T$ can be derived now:

$R_B^2 = R^2 - (R - R (1 - \cos \gamma))^2 = R^2 - R^2 \cos^2 \gamma =$

$= R^2 (1 - \cos^2 \gamma) = R^2 \sin^2 \gamma = R^2 \sin^2 (\alpha + \beta)$

$R_T^2 = R_x^2 \sin^2 \alpha.$

$R_B R_T = R \sin (\alpha + \beta) \; R_x \sin \alpha$

and $V_c = \frac{1}{3} \pi(R_x(1-\cos\alpha) + R (1+\cos(\alpha+\beta)))(R^2\sin^2(\alpha+\beta) + R_x^2 \sin^2\alpha+R_x\sin\alpha \; R\sin(\alpha+\beta))$

(2)

B. The spherical segment for the R_x spheres

The volume V_{R_x} of a spherical segment is given by Burington (1973) as:

$$V_{R_x} = \pi (R_x h_T^2 - \frac{h_T^3}{3}) \quad (3)$$

and using the above symbols:

$$V_{R_x} = \pi (R_x R_x^2(1 - \cos\alpha)^2 - \frac{1}{3} R_x^3 (1 - \cos\alpha)^3)$$

$$= \pi \; R_x^3 ((1 - \cos\alpha)^2 - \frac{1}{3} (1 - \cos\alpha)^3)$$

$$= \pi R_x^3(1 + \cos^2\alpha - 2\cos\alpha - \tfrac{1}{3}(1 - \cos^3\alpha - 3\cos\alpha + 3\cos^2\alpha))$$

$$= \frac{\pi}{12} R_x^3 (8 - 9\cos\alpha + \cos 3\alpha) \qquad (4)$$

Substituting the proper symbols, V_R is obtained easily as:

$$V_R = \frac{\pi}{12} R^3(8 + 9\cos(\alpha + \beta) - \cos 3(\alpha + \beta)) \qquad (5)$$

C. The volume of the fraction of the torus

Consider Fig. 35 The volume of the napkin ring can be described as, (Goudriaan, pers. comm.)

$$V_t = 2\pi \int_{-y_1}^{+y_1} (x + \xi\cos\delta - y\sin\delta)d\xi\, dy =$$

$$= 2\pi \left(x y + \xi\cos\delta\, y - \tfrac{1}{2} y^2 \sin\delta \right)_{-y_1}^{+y_1} d\xi$$

$$= 2\pi (2 x y_1 + 2\xi y_1 \cos\delta)\, d\xi = 4\pi (x + \xi\cos\delta)\, y_1\, d\xi$$

where $y_1 = r\sin\Delta$

$$\xi = r(1 - \cos\Delta) \rightarrow d\xi = r\sin\Delta\, d\Delta$$

$$V_t = 4\pi \int_0^{\frac{1}{2}\beta} (x + r(1 - \cos\Delta)\cos\delta)\, r^2 \sin^2\Delta\, d\Delta$$

$$= 4\pi x r^2 \int_0^{\frac{1}{2}\beta} \sin^2\Delta\, d\Delta + 4\pi\cos\delta\, r^3 \int_0^{\frac{1}{2}\beta} \sin^2\Delta\, d\Delta -$$

$$4\pi r^3 \cos\delta \int_0^{\frac{1}{2}\beta} \cos\Delta \sin^2\Delta\, d\Delta$$

$$= 4\pi (x r^2 + r^3\cos\delta) \int_0^{\frac{1}{2}\beta} \sin^2\Delta\, d\Delta - 4\pi r^3 \cos\delta \int_0^{\frac{1}{2}\beta} \cos\Delta \sin^2\Delta\, d\Delta$$

$$V_t = 4\pi (x r^2 + r^3\cos\delta)(\tfrac{1}{2}\Delta - \tfrac{1}{2}\sin\Delta\cos\Delta)_0^{\frac{1}{2}\beta} - \frac{4}{3}\pi r^3 \cos\delta(\sin^3\Delta)_0^{\frac{1}{2}\beta}$$

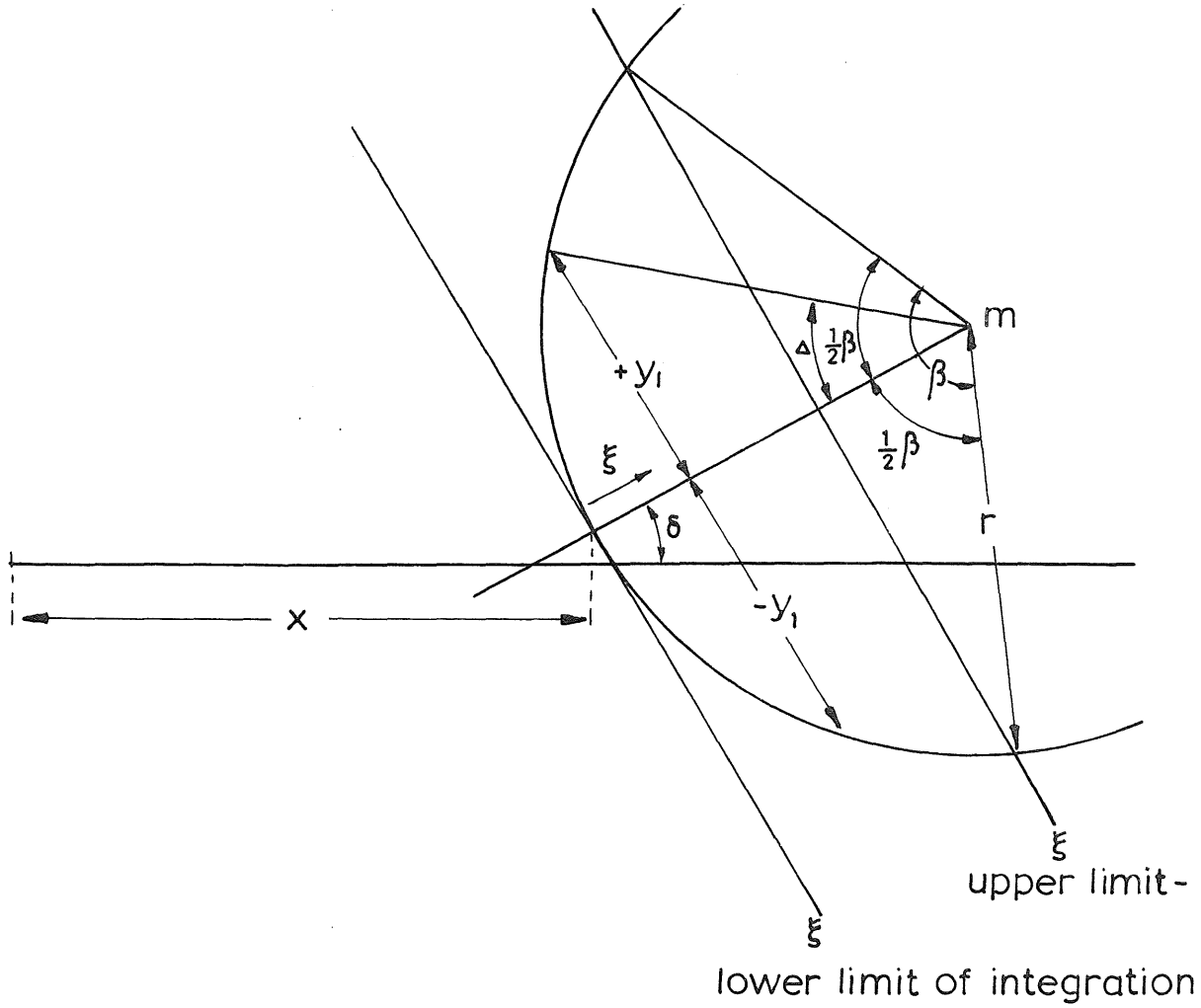

Figure 35. Coordinate design to calculate the volume of the napkin ring.

$$= 4\pi (x r^2 + r^3 \cos\delta)(\tfrac{1}{4}\beta - \tfrac{1}{2}\sin\tfrac{1}{2}\beta\cos\tfrac{1}{2}\beta) - \tfrac{4}{3}\pi r^3 \cos\delta \sin^3\tfrac{1}{2}\beta$$

where $x = (R_x + r)\sin\alpha - r\cos\delta$

$$\delta = \alpha + \tfrac{1}{2}\beta - 90$$

α and β are derived from the law of cosines,

$$\cos\alpha = \frac{R_x (R_x + R) + r (R_x - R)}{(R_x + R)\ (R_x + r)}$$

$$\cos\beta = \frac{r (r + R + R_x) - R R_x}{(R_x + r)(R + r)}$$

and substituting x and δ yields:

$$V_t = 4\pi (r^3 \sin\alpha + r^2 R_x \sin\alpha - r^3 \cos(\alpha + \tfrac{1}{2}\beta - \tfrac{1}{2}\pi) + r^3 \cos(\alpha + \tfrac{1}{2}\beta - \tfrac{1}{2}\pi))$$

$$(\tfrac{1}{4}\beta - \tfrac{1}{2}\sin\tfrac{1}{2}\beta\cos\tfrac{1}{2}\beta) - \tfrac{4}{3}\pi r^3 \cos\delta \sin^3\tfrac{1}{2}\beta$$

which equation is simplified to:

$$V_t = 4\pi (r^2 \sin\alpha(R_x + r))\ (\tfrac{1}{4}(\beta - \sin\beta)) - (\tfrac{4}{3}\pi r^3 \cos(\alpha + \tfrac{1}{2}\beta - \tfrac{1}{2}\pi)\sin^3\tfrac{1}{2}\beta)$$

expressing all angles in degrees yields Eq. (5).

APPENDIX II

The radius of the cylinder which just can pass a window, (Eq. 7, page 19)

Consider Fig. 36

$$A = \sqrt{2 R_x R + R_x^2} \tag{1}$$

(R, y) is given by solution of the following set of equations:

$$R^2 + y^2 = (R + r)^2 \rightarrow y^2 = (R + r)^2 - R^2 \rightarrow y^2 = 2 R r + r^2 \tag{2}$$

$$(A - y)^2 = (R_x + r)^2 \rightarrow y = A - R_x - r \tag{3}$$

Substituting Eq. (2) in (3) yields:

$$A^2 + R_x^2 + r^2 - 2 A r - 2 A R_x + 2 R_x r = 2 R r + r^2$$

from which r is solved as

$$r = \frac{A^2 + R_x^2 - 2 A R_x}{2 (A + R - R_x)} = \frac{(A - R_x)^2}{2 (A - R_x) + 2 R}$$

or

$$r = \frac{(R + R_x - A)}{(R - R_x + A)} R_x$$

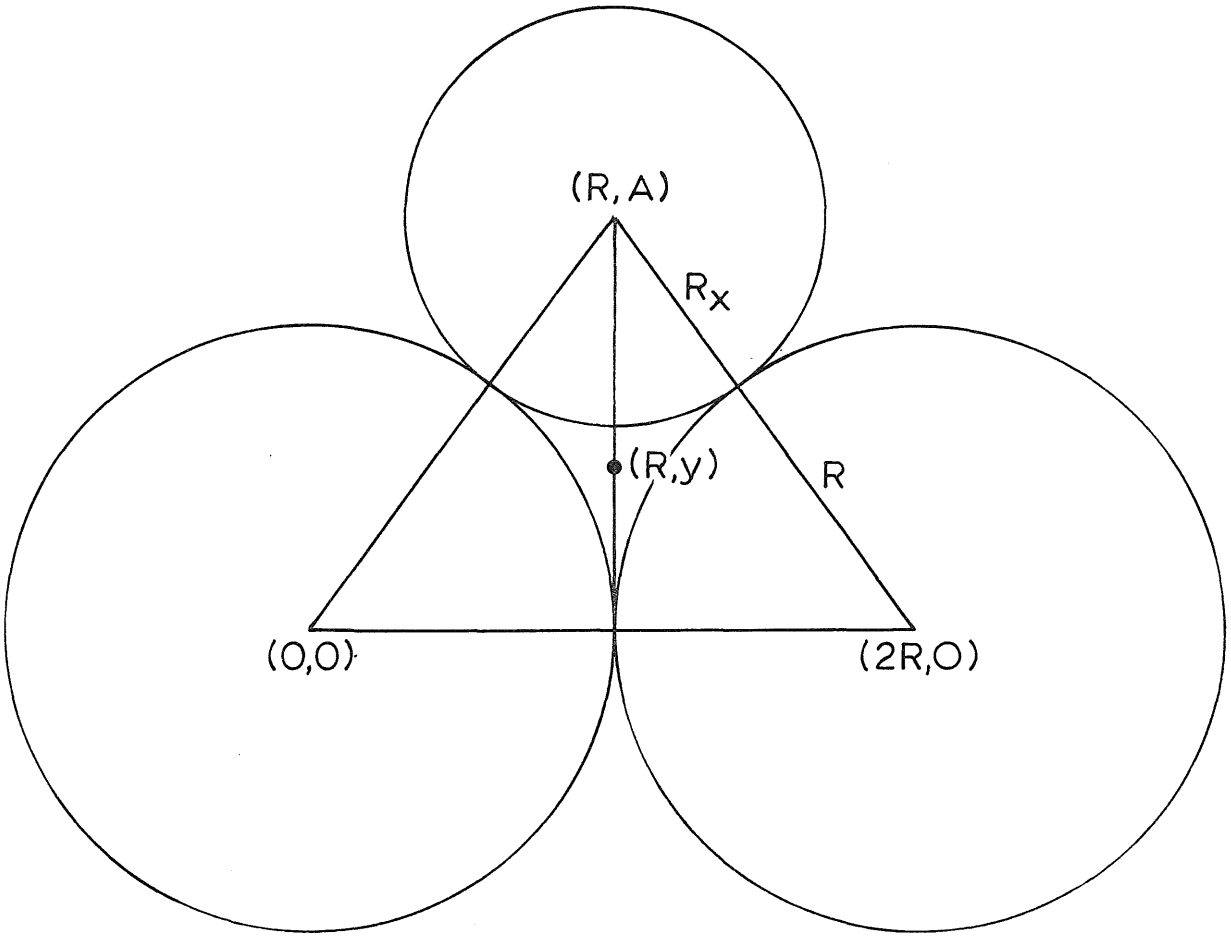

Figure 36. Coordinate design to calculate the radius of the cylinder which just can pass a window.

APPENDIX III

The air-exposed area A.E.A.

The air-exposed area is obtained by calculating the water covered area of a sphere and subtracting this area from the whole sphere surface. Compare Fig. 11 for the symbols.

$$a = \text{area covered by a pendular ring} = 2\,\pi\,R_x h_T \tag{1}$$

where

$$h_T = R_x(1 - \cos\alpha) \tag{2}$$

$$\cos\alpha = \frac{R_x^2 + R\,R_x + R_x\,r - R\,r}{(R + R_x)\,(R_x + r)} \tag{3}$$

Substituting Eqs. (2) and (3) in (1) gives:

$$a = 2\,\pi\,R^2\left(1 - \frac{(R_x\,(R + R_x) + r\,(R_x - R))}{(R + R_x)\,(R_x + r)}\right) \tag{4}$$

Expressing Eq. (4) as a fraction of the total sphere surface and taking C points of contact yields Eq. (14):

$$\text{A.E.A. (\%)} = \left(1 - \frac{C}{2}\left(1 - \frac{(R_x\,(R_x + R) + r\,(R_x - R))}{(R_x + R)\,(R_x + r)}\right)\right) 100$$

APPENDIX IV

Calculation of hydraulic conductivity as a function of moisture content.

A. The moisture characteristic is divided into 20 steps of 0.0135 each, with respect to θ_v. It is supposed that beyond a suction of 200 mbar, the pores do not contribute to flow.

Sm	θ_v	$\overline{Sm}$	class, i
0.0	0.465		
5.8210	0.4515	2.9105	1
13.6521	0.4380	9.7366	2
25.9785	0.4245	19.8153	3
34.4718	0.4110	30.2252	4
40.3303	0.3975	37.4011	5
46.1887	0.3840	43.2595	6
52.0472	0.3705	49.1188	7
57.9057	0.3570	54.9765	8
63.7641	0.3435	60.8349	9
69.6226	0.3300	66.6934	10
75.4811	0.3165	72.5519	11
81.3396	0.3030	78.4104	12
87.1981	0.2895	84.2689	13
93.0566	0.2760	90.1274	14
98.9155	0.2625	95.9859	15
116.9231	0.2490	107.9191	16
137.6923	0.2355	127.3077	17
158.4615	0.2220	148.0769	18
179.2308	0.2085	168.8462	19
200.0	0.1950	189.6154	20

Suction Sm was obtained by linear interpolation of the curve no. 9 from Rijtema, for the different values θ_v. The average suction, $\overline{Sm}$, belonging to each class i, was calculated by averaging Sm in its turn.

The formula used is:

$$K = 270 \cdot \frac{(0.465)^2}{(20)^2} \cdot \left((\overline{Sm})^{-2} + 3\,(\overline{Sm})^{-2} + \ldots 2\,(n-1)(\overline{Sm})^{-2} \right) \qquad (1)$$

where 0.465 is the porosity of the sandy loam soil taken from Rijtema. In the following table $(\overline{Sm})^{-2}$, and the multiplication is presented to obtain the calculated saturated conductivity.

i	$(\overline{Sm})^{-2}$	multiplication factor	Product
1	$1.1805.10^{-1}$	1	$1.1805.10^{-1}$
2	$1.0548.10^{-2}$	3	$3.1645.10^{-2}$
3	$2.5468.10^{-3}$	5	$1.2734.10^{-2}$
4	$1.0946.10^{-3}$	7	$7.6623.10^{-3}$
5	$7.1488.10^{-4}$	9	$6.4339.10^{-3}$
6	$5.3436.10^{-4}$	11	$5.8780.10^{-3}$
7	$4.1448.10^{-4}$	13	$5.3883.10^{-3}$
8	$3.3086.10^{-4}$	15	$4.9629.10^{-3}$
9	$2.7021.10^{-4}$	17	$4.5935.10^{-3}$
10	$2.2482.10^{-4}$	19	$4.2716.10^{-3}$
11	$1.8998.10^{-4}$	21	$3.9895.10^{-3}$
12	$1.6265.10^{-4}$	23	$3.7409.10^{-3}$
13	$1.4082.10^{-4}$	25	$3.5205.10^{-3}$
14	$1.2311.10^{-4}$	27	$3.3239.10^{-3}$
15	$1.0854.10^{-4}$	29	$3.1476.10^{-3}$
16	$8.5862.10^{-5}$	31	$2.6617.10^{-3}$
17	$6.1701.10^{-5}$	33	$2.0361.10^{-3}$
18	$4.5606.10^{-5}$	35	$1.5962.10^{-3}$
19	$3.5077.10^{-5}$	37	$1.2978.10^{-3}$
20	$2.7813.10^{-5}$	39	$1.0847.10^{-3}$
			Σ Products = $2.2802.10^{-1}$

Subsequently, the matching factor was calculated as

$$\frac{K_s}{K_{sc}} = \frac{16.5 \quad (86400)^{-1}}{2.2802\ 10^{-1}\ 270\ \frac{(0.465)^2}{(20)^2}} = 5.7383\ 10^{-3}$$

where the factor 86400 converts days into seconds.

Now K can be calculated f.i. for $\theta = 0.222$, then $K = 270 \frac{(0.222)^2}{(2)^2}$ 86400 $5.7383\ 10^{-3}$ $(3.5077\ 10^{-5} + (2.7813\ 10^{-5})\ 3) = 1.9551\ 10^{-1}$ $cm.d^{-1}$.

In this way the following table was calculated and the θ_v corrected for the water held in the inter-aggregate pores. From this table Fig. 18 was constructed.

K	Σ Products	$\varepsilon^2.n^{-2}$	K $cm.d^{-1}$	θ_v
1 - 20	$2.2802.10^{-1}$	$5.4056.10^{-4}$	16.5	0.5165
2 - 20	$7.4648.10^{-2}$	$5.6469.10^{-4}$	5.6427	0.4562
3 - 20	$4.9875.10^{-2}$	$5.9211.10^{-4}$	3.9532	0.4390
5 - 20	$3.0161.10^{-2}$	$6.5985.10^{-4}$	2.6641	0.4112
7 - 20	$1.8957.10^{-2}$	$7.5233.10^{-4}$	1.9092	0.3841
9 - 20	$1.1645.10^{-2}$	$8.8506.10^{-4}$	1.3799	0.3571
12 - 20	$5.0038.10^{-3}$	$1.2367.10^{-3}$	$8.285.10^{-1}$	0.3165
15 - 20	$1.6155.10^{-3}$	$2.1160.10^{-3}$	$4.577.10^{-1}$	0.2760
18 - 20	$2.8990.10^{-4}$	$6.1623.10^{-3}$	$2.392.10^{-1}$	0.2355
19 - 20	$1.1852.10^{-4}$	$1.2321.10^{-2}$	$1.955.10^{-1}$	0.2220
20	$2.7813.10^{-5}$	$4.3472.10^{-2}$	$1.6188.10^{-1}$	0.2085

where $\varepsilon^2.\ n^{-2}$ is the water-filled porosity divided by the n pore classes contributing to flow. K was calculated by Eq. (1) and the conversionfactor for seconds to days.

APPENDIX V: Listing of the computer program

```
TITLE ANAEROBIC SOIL VOLUME
**********BOUNDARY CONDITIONS MODEL **************************
*****************************************************************
* DIMENSIONS GRAM  CENTIMETER  DAY TEMP=25 C
* FLOW DIRECTION OF WATER AND OXYGEN DOWNWARD POSITIVE
* 100 PERCENT OF ROOTS HOMOGENEOUSLY DISTRIBUTED IN LAYER 0-25CM
* GROUNDWATER TABLE 100 CM BELOW SOIL SURFACE
* TOTAL CONSUMPTION OXYGEN 10 LITER/M**2/25CM DEPTH/DAY
* MODEL VALUBLE BETWEEN S =1.0171 AND 2180 MBAR
* SANDY LOAM SOIL RYTEMA NO9, MODIFIED WITH HYPOTETICAL MODEL
* RAIN DURATION 3 HOURS INTENSITY 9 CM/DAY
**********INITIAL PART OF PROGRAM**********************************
*****************************************************************
INITIAL
STORAGE RWC(16),WC(16),ST(16),S(16),AVK(16),K(16),FLW(16)
STORAGE DEPTH(16),FVLAN1(16),FVLAN2(16),FVLAN3(16)
STORAGE CO(16),CROC(16),CROCVS(16),CROS1(16),CROS2(16),CROS3(16)
STORAGE AEAR1(16),AEAR2(16),AEAR3(16),DCALC1(16),DCALC2(16),DCALC3(16)
STORAGE RCRIT1(16),RCRIT2(16),RCRIT3(16),REQ(16)
STORAGE RATIO1(16),RATIO2(16),RATIO3(16),NFLO(16)
STORAGE VOLAN1(16),VOLAN2(16),VOLAN3(16),FANVOL(16),CRO(16),CRW(16)
STORAGE DEFAC(16),DEF(16),ADEF(16),DFLO(16),CRWC(16)
**********DEFINITIONS*****************************************
* AMWI=AMOUNT WATER INITIAL, AMW=AMOUNT WATER,NFLW=NET FLOW RATE WATER
* WC=WATER CONTENT, S=SUCTION, ST=SUCTION TOTAL,K=CONDUCTIVITY WATER
* AVK=AVERAGE CONDUCTIVITY WATER, FLW=FLOW RATE WATER
* RWC=RELATIVE WATER CONTENT
* AMOI=AMOUNT OXYGEN INITIAL, AMO=AMOUNT OXYGEN
* NFLO=NET FLOW RATE OXYGEN, FLO=FLOW RATE OXYGEN
* N=NUMBER OF COMPARTMENTS, TCOM=THICKNESS COMPARTMENT
* PVOL=POROSITY BY VOLUME, R1=RADIUS SPHERE1, V1=VOLUME SPHERE1
* TOTVOL=TOTAL VOLUME OF SPHERES IN HEXAGONAL, VOLHEX=VOLUME HEXAGONAL
* COT=CONSUMPTION OXYGEN TOTAL (GRAM O2/CM**2/DEPTHT/DAY)
* COR=CONSUMPTION OXYGEN ROOTS
* COM=CONSUMPTION OXYGEN MICROORGANISMS
**********DEFINITION OF GEOMETRY*******************************
R2=.4142*R1
R3=.2247*R1
TCOM=3.266*R1
V1=4.1888*R1**3
V2=4.1888*R2**3
V3=4.1888*R3**3
TOTVOL=25.1327*(R1**3+R2**3+2.*R3**3)
VOLHEX=33.9411*R1**3
**********CALCULATION OF PARAMETERS****************************
COM=COT/3.
COR=2.*COT/3.
PARAM N=15,PVOL=.6551,R1=.5
TABLE RWC(1-15)=.261883,.265648,.269414,.27318,.276945,.280711,...
.284476,.288242,.292007,.295773,.299539,.303304,.30707,.310835,...
.314601
FIXED N,I
NOSORT
* CALCULATE WATER CONTENT (G/LAYER)
      DO 1 I=1,N
      AMWI(I)=RWC(I)*TCOM
  1   CONTINUE
* CALCULATE OXYGEN CONTENT (G/LAYER)
      DO 2 I=1,N
      AMOI(I)=.21*1.3099E-3*(PVOL-RWC(I))*TCOM
```

```
  2    CONTINUE
* CALCULATE DATA HALFWAY TCOM
       DEPTH(1)=.5*TCOM
       DO 3 I=2,N
       DEPTH(I)=DEPTH(I-1)+TCOM
  3    CONTINUE
       DO 5 I=1,N
* FVLAN=FRACTIONAL VOLUME ANAEROBIC PER SPHERE
       FANVOL(I)=0.
       FVLAN1(I)=0.
       FVLAN2(I)=0.
       FVLAN3(I)=0.
  5    CONTINUE
       OFLO(16)=0.
DYNAMIC
NOSORT
* SECTION TO CALCULATE ANAEROBIC SOIL VOLUME
**********************************************************************
**********************DEFINITIONS*************************************
* CROC=CONSUMPTION RATE OXYGEN CALCULATED PER LAYER
* CROCVS=CONSUMPTION RATE OXYGEN CALCULATED PER UNIT VOLUME OF SPHERES
* FRT=FRACTION ROOTS
* CRO=CONSUMPTION RATE OXYGEN
* AEAR1=AIR EXPOSED AREA SPHERE CLASS ONE (FRACTION)
* DCALC=DIFFUSION COEFFICIENT OXYGEN CALCULATED
* DCSPH=DIFFUSION COEFFICIENT OXYGEN IN WATER-FILLED PART OF SPHERE
* CROS1(I)=CONSUMPTION RATE OXYGEN PER SPHERE CLASS 1
* FVLAN=FRACTION OF VOLUME ANAEROBIC OF A SPHERE
* RCRIT=CRITICAL RADIUS ABOVE WHICH ANAEROBY OCCURS
* CCO=CRITICAL CONCENTRATION OXYGEN FOR EFFECTIVE ANAEROBIC CONDITION
* SOLO=SOLUBILITY OXYGEN IN WATER ((G/CM**3 H2O)/(G/CM**3AIR))
* REQ=EQUIVALENT RADIUS WHEN WATER CONCENTRATED IN SPHERE CENTER
* VOLAN1(I)=VOLUME ANAEROBIC SPHERE CLASS ONE (CM**3)
* VOLANT=VOLUME ANAEROBIC TABULATED (FRACTION)
* FANVOL=FRACTIONAL ANAEROBIC VOLUME PER SOIL LAYER
* CALCULATE WATER CONTENT (G/CM**3.) AND CONCENTRATION OXYGEN (G/CM**3.)
       DO 6 I=1,N
       WC(I)=AMW(I)/TCOM
       CO(I)=AMO(I)/(TCOM*(PVOL-WC(I)))
  6    CONTINUE
* CALCULATE OXYGEN CONSUMPTION PER SPHERE (G/CM**3SPHERE/DAY)
       DO 7 I=1,N
       CROC(I)=FRT*(COP+CON)
       CROCVS(I)=CROC(I)*(VOLPEX/TOTVOL)/TCOM
       CRO(I)=CROC(I)*(1.-FANVOL(I))
* CALCULATE AIR EXPOSED AREA PER SPHERE
       AEAR1(I)=AFGEN(AEAR1T,WC(I))
       AEAR2(I)=AFGEN(AEAR2T,WC(I))
       AEAR3(I)=AFGEN(AEAR3T,WC(I))
* CALCULATE DIFFUSION COEFFICIENT IN SPHERE (CM**2/DAY)
       DCALC1(I)=DCSPH*AEAR1(I)
       DCALC2(I)=DCSPH*AEAR2(I)
       DCALC3(I)=DCSPH*AEAR3(I)
* CALCULATE CONSUMPTION RATE OXYGEN PER SPHERE
       CROS1(I)=CROCVS(I)*V1*(1.-FVLAN1(I))
       CROS2(I)=CROCVS(I)*V2*(1.-FVLAN2(I))
       CROS3(I)=CROCVS(I)*V3*(1.-FVLAN3(I))
* CALCULATE CRITICAL RADIUS OF SPHERES (CM)
       RCRIT1(I)=SQRT(6.*DCALC1(I)*(CO(I)-CCO)*SOLO/CROS1(I))
       RCRIT2(I)=SQRT(6.*DCALC2(I)*(CO(I)-CCO)*SOLO/CROS2(I))
```

```
      RCRIT3(I)=SQRT(6.*DCALC3(I)*(CO(I)-CCO)*SOLO/CROS3(I))
   7  CONTINUE
*  CALCULATE EQUIVALENT RADIUS (REQ)
      DO 8 I=1,N
      REQ(I)=AFGEN(REQT,VC(I))
*  CALCULATE RADIUS RELATIVE TO CRITICAL RADIUS
      RATIO1(I)=REQ(I)*P1/RCRIT1(I)
      RATIO2(I)=REQ(I)*P2/RCRIT2(I)
      RATIO3(I)=REQ(I)*P3/RCRIT3(I)
   8  CONTINUE
*  CALCULATE FRACTIONAL ANAEROBIC VOLUME PER SPHERE CLASS
      DO 9 I=1,N
      FVLAN1(I)=AFGEN(VOLANT,RATIO1(I))
      FVLAN2(I)=AFGEN(VOLANT,RATIO2(I))
      FVLAN3(I)=AFGEN(VOLANT,RATIO3(I))
      VOLAN1(I)=FVLAN1(I)*6.*V1
      VOLAN2(I)=FVLAN2(I)*6.*V2
      VOLAN3(I)=FVLAN3(I)*12.*V3
      FANVOL(I)=(VOLAN1(I)+VOLAN2(I)+VOLAN3(I))/VOLHEX
   9  CONTINUE
PARAM COT=1.3089E-3
PARAM FRT=6.6667E-2
PARAM DCSPH=1.2715E-1
PARAM CCO=2.24E-8
PARAM SOLO=2.9796E-2
FUNCTION AEAR1T=.015,.9999,.061,.9999,.092,.9995,.142,.9973,...
.195,.9933,.26,.9867,.3262,.9815,.4101,.963,.4192,.9584,.4283,.9445,...
.4351,.926,.1393,.9075,.4438,.8735,.4541,.8156,.4634,.7245,.4712,...
.6341,.4730,.5866,.4790,.5446,.4871,.4559,.4958,.3679,.5165,.1778
FUNCTION AEAR2T=.015,.9999,.061,.9999,.092,.9994,.142,.997,.195,...
.9926,.26,.9853,.3262,.9796,.4101,.9594,.4192,.9545,.4283,.9394,...
.4351,.9196,.4393,.9,.4438,.8695,.4541,.8046,.4634,.7135,.4712,...
.6264,.4730,.5818,.4790,.543,.4871,.4632,.4958,.3867,.5165,.2296
FUNCTION AEAR3T=.015,.9999,.061,.9999,.092,.9991,.142,.9958,...
.195,.9896,.26,.9795,.3262,.9715,.4101,.9439,.4192,.9372,.4283,...
.917,.4351,.8907,.4393,.865,.4438,.8258,.4541,.745,.4634,.6371,...
.4712,.5396,.4730,.4917,.4790,.451,.4871,.3702,.4958,.2963,.5165,.1547
FUNCTION REQT=.015,.3183,.061,.5081,.092,.5827,.142,.6734,.195,...
.7485,.26,.8238,.3262,.8885,.4101,.9588,.4192,.9659,.4283,.9726,...
.4351,.9776,.4393,.9805,.4438,.9832,.4541,.9893,.4634,.9932,...
.4712,.995,.4730,.9957,.4790,.9962,.4871,.9969,.4958,.9975,.5165,.9982
FUNCTION VOLANT=0.,0.,1.,0.,1.1,.0175,1.25,.0675,1.5,.1574,1.75,...
.2375,2.,.3057,2.5,.4125,3.,.5,3.5,.561,4.,.61,4.5,.65,5.,.6805,5.5,...
.707,6.,.73,6.5,.7495,7.,.766,7.5,.7825,8.,.795,8.5,.807,9.,.816,9.5,...
.826,10.,.8335,14.1421,.8809,18.2574,.9072,31.6228,.946,100.,.9999,...
101.,.9999
*  WATER FLOW SECTION
************************************************************************
**********DEFINITIONS*************************************************
*  GRWTAB=GROUNDWATER TABLE, REPRESENTS GRAVITY POTENTIAL
*  DEPTHT=DEPTH TOTAL
*  THWL=THICKNESS WATER LAYER, REPRESENTS HYDROSTATIC PRESSURE
*  SSURF=MATRIC SUCTION AT SOIL SURFACE WHEN WATER IS STANDING ON PROFIL
*  STSURF=TOTAL SUCTION AT SOIL SURFACE
*  MAXINF=MAXIMUM INFILTRATION RATE WATER (CM/DAY)
*  KSAT=CONDUCTIVITY AT SATURATION
*  CWT=CONSUMPTION WATER TOTAL(GRAM H2O/CM**2/DEPTHT/DAY)
*  CALCULATE MATRIC SUCTION AND CONDUCTIVITY OF SOIL (CM/DAY)
      DO 10 I=1,N
      S(I)=-1.*AFGEN(SUTB,WC(I))
```

```
      K(I)=AFGEN(KTB,WC(I))
   10 CONTINUE
*  CALCULATE AVERAGE CONDUCTIVITY (CM/DAY) AND SUCTION TOTAL (MBAR)
      DO 11 I=2,N
      AVK(I)=(K(I-1)+K(I))*.5
      ST(I)=S(I)+(GRWTAB-DEPTH(I))
   11 CONTINUE
*  CALCULATE FLOW RATE OF WATER
      DO 12 I=2,N
      FLW(I)=AVK(I)*(ST(I-1)-ST(I))/TCOM
   12 CONTINUE
*  CALCULATE MAXINF AND RAIN (CM/DAY)
      STSURF=SSURF+GRWTAB+THWL
      ST(1)=S(1)+(GRWTAB-DEPTH(1))
      MAXINF=(K(1)+KSAT)*.5*(STSURF-ST(1))/(.5*TCOM)
      RAIN=AFGEN(RAINTB,TIME)
*  CALCULATE RESTRICTION INFILTRATION OF WATER IN SOIL
      FLW(1)=FCNSW(THWL,AMIN1(MAXINF,RAIN),AMIN1(MAXINF,RAIN),...
                   AMIN1(MAXINF,RAIN+THWL/DELT))
*  CALCULATE FLOW THROUGH LOWER BOUNDARY
      FLW(16)=(K(15)+KSAT)*.5*ST(15)/(GRWTAB-DEPTHT)
*  CALCULATE CONSUMPTION RATE WATER
      DO 13 I=1,N
      CRWC(I)=FRT*CWT
      CRW(I)=CRWC(I)*(1.-FANVOL(I))
*  CALCULATE NET FLOW RATE OF WATER
      NFLW(I)=FLW(I)-FLW(I+1)-CRW(I)
   13 CONTINUE
PARAM GRWTAB=100.,DEPTHT=24.495
PARAM SSURF=0.
PARAM KSAT=16.5
PARAM CWT=.3
FUNCTION SUTB=.015,1000000.,.061,16000.,.092,2500.,.142,500.,.195,...
200.,.26,100.,.3262,71.2916,.4101,34.9418,.4192,31.,.4283,22.9236,...
.4351,16.9525,.4393,13.3892,.4438,10.,.4541,6.3393,.4634,4.0322,...
.4712,2.895,.4730,2.5,.4790,2.2208,.4871,1.7762,.4958,1.4615,.5165,...
1.0174
FUNCTION KTB=.015,.011,.1,.035,.2085,.1619,.222,.1955,.2355,.2392,...
.276,.4577,.3165,.8285,.357,1.3799,.384,1.9092,.4112,2.6641,.439,...
3.9532,.4562,5.6427,.5165,16.5
FUNCTION RAINTB=0.,0.,.05,0.,.051,9.,.175,9.,.176,0.,100.,0.
*  OXYGEN FLOW SECTION MACRO
**********************************************************************
*********************DEFINITIONS**************************************
*  DEF=EFFECTIVE DIFFUSION COEFFICIENT IN SOIL SYSTEM
*  DZERO=DIFFUSION OF OXYGEN IN FREE AIR, ADEF=AVERAGE DEF
*  DEFAC=DIFFUSION EFFICIENCY FACTOR=DEF/DZERO
*  DFLO=DIFFUSIVE FLOW OF OXYGEN
*  COUT=CONCENTRATION OF OXYGEN IN FREE AIR
*  R=RESTRICTED ,DZW=DIFFUSION COEFFICIENT IN FREE WATER
*  MFLO=MASS FLOW OXYGEN DUE TO AIR DISPLACEMENT BY WATER INFILTRATION
*  CALCULATION OF DIFFUSION COEFFICIENT IN SOIL (CM**2./DAY)
      DO 14 I=1,N
      DEFAC(I)=AFGEN(DEFACT,(PVOL-WC(I)))
      DEF(I)=DZERO*DEFAC(I)
   14 CONTINUE
*  CALCULATE AVERAGE EFFECTIVE DIFFUSION COEFFICIENT
      DO 15 I=2,N
      ADEF(I)=(DEF(I)+DEF(I-1))*.5
      DFLO(I)=ADEF(I)*(CO(I-1)-CO(I))/TCOM
```

```
  15  CONTINUE
* CALCULATE DFLO FOR BOUNDARIES
      FLO=DEF(1)*(COUT-CO(1))/(.5*TCOM)
      RDFLO=DZW*(COUT-CO(1))/(THWL+NOT(THWL))
      DFLO(1)=FCNSW(THWL,FLO,FLO,RDFLO)
* CALCULATE NET FLOW OF OXYGEN (DIFFUSIVE+ MASS FLOW)
      DO 16 I=1,N
      MFLO(I)=WFLW(I)*CO(I)
      NFLO(I)=DFLO(I)-DFLO(I+1)-CRO(I)-MFLO(I)
  16  CONTINUE
PARAM DZERO=1.9526E4
PARAM COUT=2.7487E-4
PARAM DZW=2.2464
FUNCTION DEFACT=.1386,.0411,.1593,.0669,.168,.0781,.1761,.089,.1839,...
.0975,.201,.1165,.2113,.1206,.2157,.122,.2268,.1231,.245,.1242,...
.3289,.1316,.3951,.1442,.4601,.1579,.5131,.167,.5631,.1734,.5941,...
.1764,.6401,.1798
**********INTEGRALS**********
**********DEFINITIONS**********
* CUMINF=CUMULATIVE WATER INFILTRATION
* CUMOUT=CUMULATIVE OUTFLOW WATER
* CUMCOX=CUMULATIVE OXYGEN CONSUMPTION
      AMW=INTGRL(AMWI,NFLW,15)
      CUMINF=INTGRL(0.,FLW(1))
      CUMOUT=INTGRL(0.,FLW(16))
      AMO=INTGRL(AMOI,NFLO,15)
      CUMCOX=INTGRL(0.,DFLO(1))
      THWL=INTGRL(0.,RAIN-FLW(1))
* OUTPUT SECTION
**********
      A=IMPULS(0.,PRDEL)
      IF(A*KEEP.LT.0.5)GO TO 99
      WRITE(6,100)(FANVOL(I),I=1,15)
  100 FORMAT(/1H ,13HFANVOL(1-15)=//8E10.4/8E10.4/)
      WRITE(6,101)(WC(I),I=1,15)
  101 FORMAT(/1H ,9HWC(1-15)=//8E10.4/8E10.4/)
      WRITE(6,102)(CO(I),I=1,15)
  102 FORMAT(/1H ,9HCO(1-15)=//8E10.4/8E10.4/)
      WRITE(6,103)(VOLAN1(I),I=1,15)
  103 FORMAT(/1H ,13HVOLAN1(1-15)=//8E10.4/8E10.4/)
      WRITE(6,104)(RATIO1(I),I=1,15)
  104 FORMAT(/1H ,13HRATIO1(1-15)=//8E10.4/8E10.4/)
      WRITE(6,105)(CRW(I),I=1,15)
  105 FORMAT(/1H ,10HCRW(1-15)=//8E10.4/8E10.4/)
      WRITE(6,106)(CRO(I),I=1,15)
  106 FORMAT(/1H ,10HCRO(1-15)=//8E10.4/8E10.4/)
      WRITE(6,107)(MFLO(I),I=1,15)
  107 FORMAT(/1H ,11HMFLO(1-15)=//5E12.4/5E12.4/5E12.4/)
      WRITE(6,108)(S(I),I=1,15)
  108 FORMAT(/1H,8HS(1-15)=//5E12.4/5E12.4/5E12.4/)
PRINT THWL,CUMINF,CUMCOX,CUMOUT
      COONE=CO(1)
FINISH COONE=2.241E-4
  99  CONTINUE
METHOD RECT
TIMER FINTIM=1.00,PRDEL=.01,DELT=.0001
END
STOP
ENDJOB
```